F.M. Verhage

Design and Functional Assessment of a Versatile Gripper for a Care-Robot

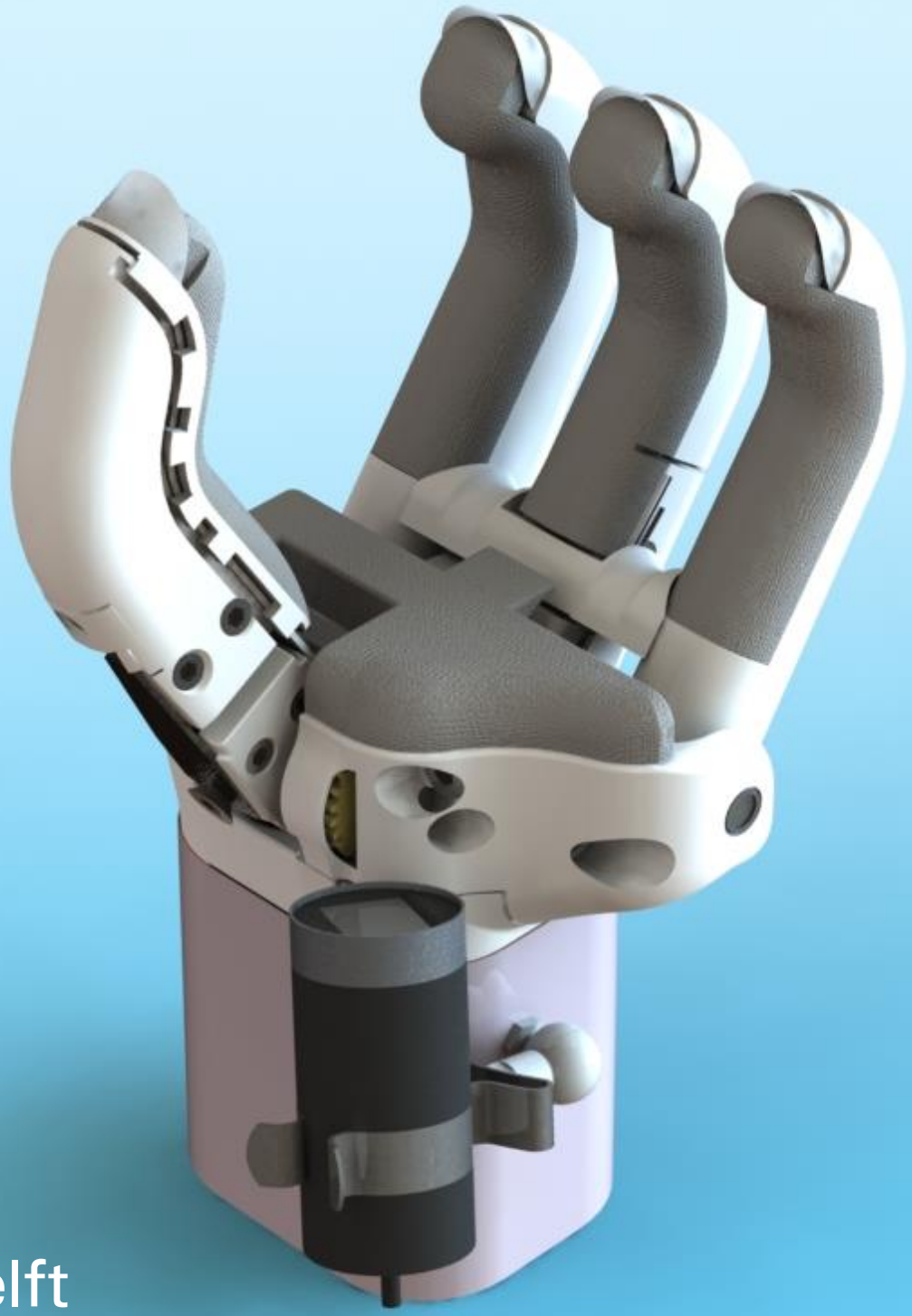

TU Delft

Design and Functional Assessment of a Versatile Gripper for a Care-Robot

By

F.M. Verhage

in partial fulfilment of the requirements for the degree of

Master of Science
in Mechanical Engineering

at the Delft University of Technology,
to be defended publicly on Thursday August 26, 2021 at 14:30.

Supervisors:	Dr. ir. G. Smit	TU Delft
	Dr. ir. C.J.M. Heemskerk	HiT
	J.J. Peres, MSc	HiT
Thesis committee:	Dr. ir. G. Smit	TU Delft
	Dr. ir. T. Horeman	TU Delft
	Dr. D. Farhadi Machekposhti	TU Delft

An electronic version of this thesis is available at http://repository.tudelft.nl/.

TU Delft

Design and Functional Assessment of a Versatile Gripper for a Care-Robot

Fabian Matthias Verhage
4591801
ME51035 TU Delft
(Dated: August 12, 2021)

The Netherlands has a severe shortage of care workers. The shortage is expected to increase in the coming years. Care-robots could provide a solution, by taking work out of the hands of the care workers. The potential utility of the care-robot is dependent on the functionality of the gripper. The goal of this study was to design and develop a new gripper for a care-robot, applicable in a care environment. Furthermore, the functional performance of the gripper was to be assessed and evaluated. The new gripper needed to outperform the previous gripper of the robot, named the RPG, in terms of functionality. A new gripper was designed in this study, named the 4FH. The 4FH has four fingers, resembling a human thumb, index, middle and ring finger. Sideways rotation of the thumb allows for two grasping modes, namely a pinch mode and a power grip mode. The 4FH has three DOFs in total. A glove is fitted around the gripper for hygiene. An improvement was made to the 4FH by modifying the shape of the thumb. The improved version is named the 4FH-i. A set of three assessments was drawn up for measuring functional performance of a gripper for a care-robot. The set consists of the the EIT, modified SHAP and modified AHAP. The SHAP and AHAP were modified in this study to make them representative for applications of a care-robot. Both the 4FH and 4FH-i outperformed the RPG on the modified SHAP and on the modified AHAP. All grippers passed the EIT. The results showed a significant increase in grasp stability, comparing the 4FH and 4FH-i to the RPG. The higher scores on the assessments indicated that the 4FH and 4FH-i have improved functional performance compared to the RPG.

1. INTRODUCTION

In the Netherlands, a severe shortage of care workers has been identified [1]. Population ageing is the main cause for the shortage. In 2020, a total of 1.4 million people were active in the care sector in the Netherlands [2]. It is estimated that in 2040, over 2 million care workers will be needed [3]. It is a huge challenge to fill the gap in the coming years, while there is already a shortage of approximately 150 thousand care workers in 2020 [4]. The Dutch minister of Public Health has acknowledged that trying to gain more care workers is not the complete answer [3]. He argued that the care sector needs more innovation and a different approach on providing care. Care-robots could be the innovation needed. Care-robots can be used to take work out of the hands of care workers [5]. This way, the required amount of care workers will be lowered. Also, the cost for the care sector will be lowered, as the long term costs of care-robots are lower than those of care workers.

FIG. 1: Robot used by HiT to create care-robot Rose [6]

Heemskerk Innovative Technology (HiT) is a company in the Netherlands, currently developing a care-robot named Rose. The care-robot can be seen in Figure 1. Rose is intended to support care workers, by performing various tasks. Rose can talk to the clients, for example to give them information about appointments or ask for their needs. Other tasks involve for example cleaning a nightstand, unloading a dishwasher or put away groceries. Picking up and handing objects to the client is also an important task of Rose. The robot is not intended for physical contact with the clients. HiT focuses

on making the robot perform tasks autonomously. In case autonomy does not suffice, the robot can be controlled via tele-operation. Rose features a robot arm with seven Degrees of Freedom (DOFs). A force-torque (F/T) sensor is integrated between the end-effector and the robot arm, to allow for force-feedback.

During the intended use of the robot, various kinds of objects need to be grasped. Grasping is realized by using an end-effector, also called a gripper. Consequently, the gripper is an essential part of the robot to be able to perform its tasks. In other words, the potential utility of the robot is dependent on the functionality of the gripper [7]. Industrial grippers in general are designed for repetitive tasks with one specific type of object [8]. Consequently, such grippers are strongly limited in grasping objects of various shapes, sizes, weights and stiffness [7]. The tasks of Rose include handling a great variety of objects. Therefore, a versatile gripper is essential to allow for grasping as many types of objects as possible [8].

Previous projects at HiT have been designated to design a versatile gripper for Rose. The final result was a parallel gripper, which can be seen in Figure 2. The gripper is called the Rose Parallel Gripper (RPG). The RPG has two opposing fingers. A four-bar mechanism in both fingers results in parallel movement of the fingertips. The RPG, however, was not designed for application in a care environment. The RPG has sharp points and edges, exposed electrical wires and an exposed actuator which could heat up to harmful temperatures. Furthermore, the RPG is not disinfectable or water resistant. It was concluded that the RPG does not allow for the safety needed in a care environment. Also, low grasp stability was identified for several types of objects during use on the robot. Therefore, the need for a new gripper was identified. The new gripper must be applicable in a care environment and must have improved functional performance. This project is the study of this paper.

In literature, different kinds of versatile grippers have been presented. Most argue that shape adaptivity is needed to handle a great variety of objects. A common approach to allow for shape adaptivity, but limit the number of actuators and control complexity, is using rigid-body under-actuation [7]. Furthermore, versatile grippers using compliant mechanisms, soft robotics or tendons for shape adaptivity have been presented [9]. No gripper designs, however, have been presented specifically for care-robots. Consequently, no grippers have been found in literature, readily meeting the demands of the gripper of this study.

Robotic grippers and prosthetic hands have various similarities [10]. For example, both aim at high functional performance and durability. Furthermore, low weight and low cost are desired. The specific case of the gripper for care-robot Rose shares even more desired features. The gripper of this study must contain all its functional components inside, similar to prosthetic hands. Furthermore, both the gripper and prosthetic hands are aimed at allowing for grasping a great variety of objects and performing various tasks, normally done with the human hand. Other examples of shared requirements are disinfectability, being safe to use with humans nearby and being waterproof. Because of all these similarities, literature covering upper-limb prostheses has been included in this study as well. For example, requirements, design considerations and assessments for upper-limb prostheses have been evaluated. During previous projects for developing a new gripper for Rose, care workers and clients have given feedback on the gripper designs. The feedback of the previous projects was used in the current study. This way, insight was gained in wishes and needs for a care-robot gripper.

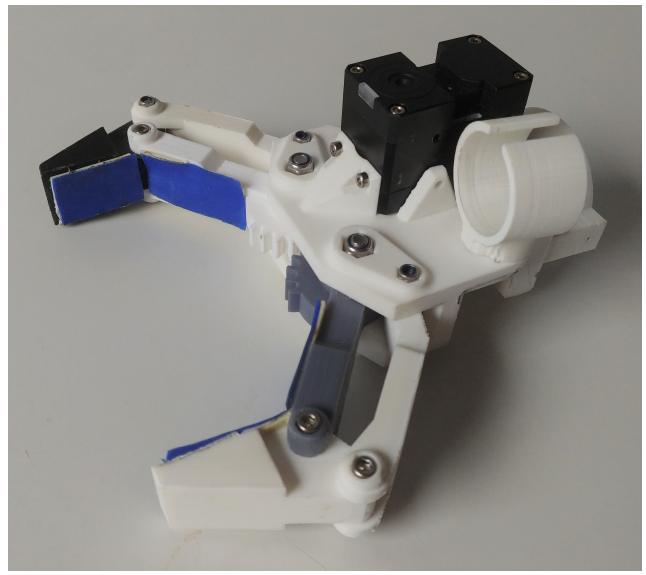

FIG. 2: The previous gripper of robot Rose, named the RPG

Goal

The goal of this study was to design, develop and assess a versatile gripper for a care-robot. The gripper should be applicable in a care environment, in terms of hygiene, safety and aesthetics. Regarding functional performance, the gripper should outperform the gripper previously used on the robot. A set of assessments is to be set up for measuring functional performance, covering the span of real world applications of the care-robot and gripper.

2. DESIGN METHODS, CHOICES AND TEST METHODS

2.1. Design methods

2.1.1. Requirements

To guide the design process of the gripper, a list of requirements was drawn up. This list was generated by the use of three methods. First of all, a literature search was conducted to find requirements set to versatile robotic grippers and upper limb prostheses. How the literature search was performed is described in Appendix A. All requirements found in literature were structured and evaluated for relevancy to the gripper of this study, and duplicates were removed.

Secondly, a list of requirements defined by the company during previous designs of the gripper was carefully reviewed. Some criteria were scrapped or rewritten, as they presented a certain design solution instead of posing the underlying requirement. For example, under-actuation and having two fingers were required in previous projects, but other solutions can be applied as well. Quantitative requirements were compared to the related values used in literature. This also led to various modifications of the requirements.

Thirdly, the complete list of requirements, containing criteria from literature and from previous design projects for Rose, was critically reviewed. Missing requirements were added to fill gaps identified during the evaluation, such as requirements on functional performance and temperature. Duplicate requirements were removed.

The complete list of requirements can be found in Appendix B. The list can be structured in seven types of requirements, namely general, mechanical, functional, actuation and control, safety, build up and casing, and interface. Each category will be briefly discussed below. Related values and details are specified in Appendix B.

Overall requirements
The general requirements are related to the overall design of the gripper. They consist of three design criteria, concerning the affordability, weight and size. The maximum weight is based on requirements for prosthetic hands in literature. Various weight limits are presented, but for a robotic gripper the weight is of less importance than for prostheses. Therefore, one of the higher weight limits often presented for prostheses is used, namely 500 g [11–13]. It needs to be noted, however, that increased gripper weight results in a decreased net pay-load of the robot arm.

Mechanical requirements
The gripper needs to achieve a minimum pinch force of 30 N to allow for a broad range of activities [14, 15], and must be able to hold a 2 kg item. The stroke width of the gripper needs to be larger than 85 mm. The allowed time needed for fully closing the gripper from open position is limited to 0.7 s. This time limit was chosen to equal the closing time of the RPG. Literature also suggests that for prosthetic hands, a closing time of 0.8 s is regarded sufficient [11]. Furthermore, a robust gripper design and high repeatability of the opening and closing cycle of the gripper are required.

Functional requirements
The gripper needs to have sufficient functional performance. Three requirements are set to the functional performance, by the use of three assessments. In order to be a useful gripper design, the gripper at least needs to be able to pick up a number of the most essential items for application in the care environment. This is measured in the Essential Items Test (EIT). Secondly, the new gripper is required to achieve a higher overall score on a modified version of the Southampton Hand Assessment Procedure (SHAP) than the RPG. The modified SHAP was generated in this study, as not all items of the original SHAP are relevant for the gripper of this study. The modified SHAP assesses ability to manipulate objects of various shapes, sizes and rigidity, and to perform various Activities of Daily Living (ADLs). Thirdly, the new gripper is required to score higher on a modified version of the Anthropomorphic Hand Assessment Procedure (AHAP) than the RPG. As for the SHAP, the original AHAP is not completely relevant for the new gripper. Therefore, a modification was made in this study. The modified AHAP aims at evaluating grasp stability. For a more elaborate description of the three assessments, see Section 2.3.1.

Actuation and control requirements
The actuation of the gripper needs to be electrically powered, to comply with the power source in the robot. The actuation system may not to overheat when using the gripper. Simplicity of the control system is desired, to reduce costs and increase reliability and load carrying capacity [16–18]. An optimum always needs to be found, however, between simplicity and functionality. Therefore, in this study a critical evaluation was made regarding which sensors could be useful for the gripper, covering advantages and disadvantages. See Appendix D for the complete sensor evaluation. For the best balance between simplicity and functionality, force sensing only was concluded to be beneficial. Consequently, to

enable controlling the gripper with force feedback, one or multiple force sensors need to be integrated in the design.

Safety requirements
As the gripper will be applied in a care environment, the gripper needs to be safe to use with people nearby. To avoid harming persons upon contact, the outer surface of the gripper may not contain sharp points or edges. Also, the outer surface is not allowed to heat up to unsafe temperatures. Some parts of the gripper are more likely to be touched than others, such as the fingers and palm of the gripper. Although the gripper is not intended for physical contact with humans, the safest threshold for temperatures was chosen for the fingers and palm. This level allows these parts to be held for 8 h continuously without causing harm. The thresholds are taken from the ECMA Standard for Safety of Electronic Equipment [19]. The rest of the gripper has a lower chance of being touched, and the touch duration is most likely shorter than 1 s. As the gripper will be applied in the care environment, however, one level safer was chosen. The chosen level allows for a contact period up to 10 s without causing harm.

Build up and casing requirements
The gripper must be easy and quick to manufacture and assemble. Once assembled, the design needs to allow for quick maintenance and replacement of parts. Furthermore, the design should be modular, containing all its functional components inside the gripper. A camera must be fitted for visual inspection. Additionally, the gripper is required to function in wet and dirty environments. This means that the gripper has to be water resistant and that the outer surface materials may not be prone to corrosion. Also, dirt may not be able to accumulate anywhere in the gripper, for example in holes or cavities. The gripper must be completely disinfectable.

Interface requirements
For mounting the gripper on the robot arm, a bayonet-fitting needs to be integrated in the design. Additionally, it is required that the bayonet-fitting is detachable, such that other interfaces can be mounted when needed. Bolting was the preferred attachment method.

2.1.2. Design methodology

A structural design methodology is needed to make well-funded decisions in the design process. To this end, a morphological chart was used in combination with the ACRREx method. The ACRREx method is designed to enhance creativity and find voids in a set of knowledge based design solutions [20]. ACRREx stands for Abstracting, Categorizing, Reflecting, Reformulating and Extending. In this study, the ACCREx method has been applied to find and fill voids in the morphological chart, by evaluating and combining two of the sub-functions of the morphological chart. See Figure 3 for the application of the ACRREx method to the sub-functions 'amount of fingers' and 'finger orientation'. Note that the ACRREx method has been applied to more of the sub-functions, although these are not presented to save space. In Appendix E, more detailed information can be found.

The morphological chart consists of 12 sub-functions, being the amount of fingers, finger relative orientation, finger movement, finger DOFs, actuation, shape adaptivity, hygiene, enhancing grip, actuator heat dissipation, transmission, production and force measuring. It can be noted that the working principle of gripping was not included as a sub-function. Various gripping principles exist, such as using suction, shape grip, friction grip, magnetic forces, electrostatic forces, or adhesion to grasp items [20]. The gripper of this study, however, must allow for grasping a wide variety of objects. Suction, magnetic forces, electrostatic forces and adhesion can only be applied to objects with specific characteristics. It was concluded that the gripper would need to use the principle of shape or friction grip for the highest level of versatility. Therefore, the gripping principle was not included as a sub-function in the morphological chart. In total, 67 solutions have been identified and are presented in the morphological chart. The complete morphological chart can be found in Figure 4. In Appendix E, elaborate descriptions of each sub-function can be found, and notes including advantages and disadvantages of various solutions are presented.

In addition to the morphological overview and ACRREx method, quick prototyping was applied for the structural design process. Various design solutions and concepts were made into rough physical prototypes. This way, an early feel on the practical characteristics and potential functional performance was created. The prototypes were assembled using LEGO® Technic™.

With the notes presented in Appendix E in mind, solutions of each sub-function of the morphological overview were combined to generate four promising gripper concepts. The combination of solutions applied in each of the four concepts is presented in Table I. For each concept it was chosen to limit the amount of actuators to one, to limit weight, volume, cost and control complexity. Design solutions applied in the RPG are included in the last column of the table.

Figure 5 presents rough sketches of the four concepts, as well as the design of the RPG. Note that the sketches

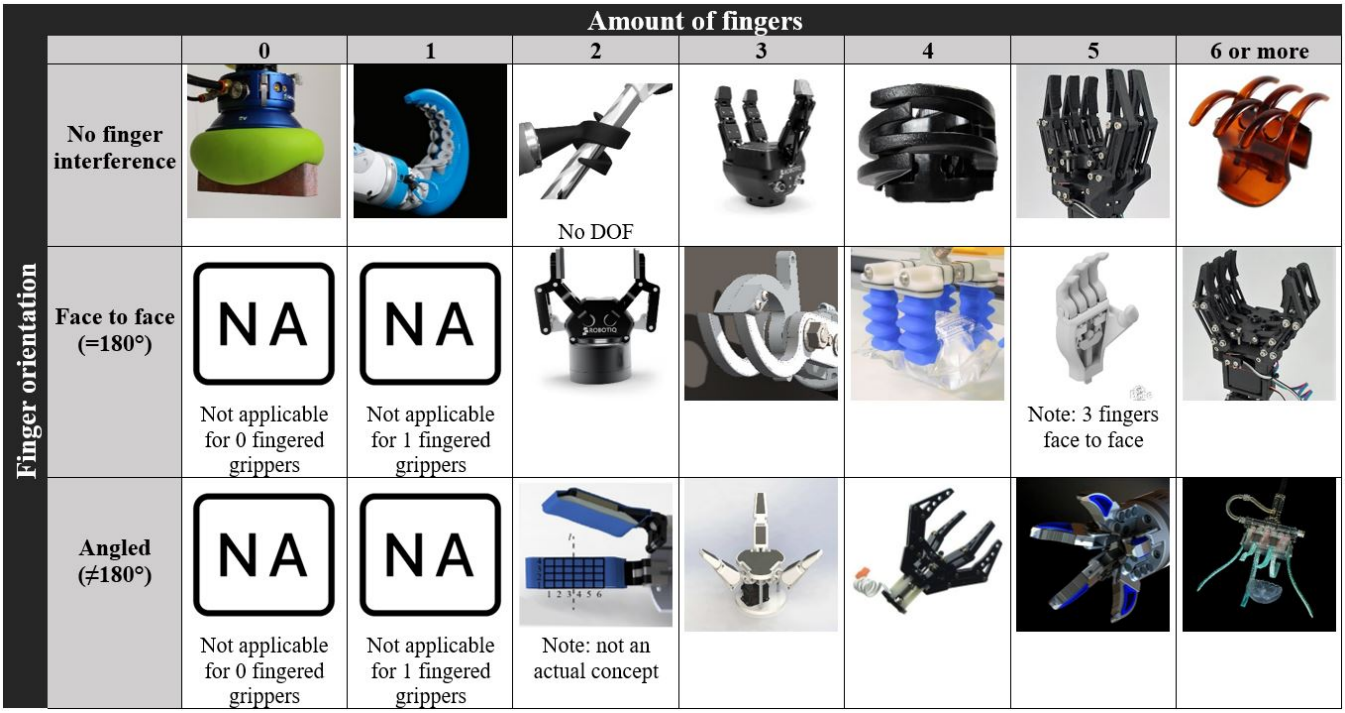

FIG. 3: ACRREx method applied to two sub-functions of the gripper design: amount of fingers and finger orientation

are for forming an initial idea of the concepts. They do not aim to visualise all information presented in Table I, or to provide exact relative dimensions and scaling. A short description of each concept can be found below.

Concept A - Whippletree Hand (WTH): The gripper design of the WTH is presented in Figure 5a. The design consists of five fingers. The thumb has zero DOFs, the remaining four fingers have one DOF each. The DOFs of the fingers is the rotation at the base of the fingers. The four fingers can rotate quasi-independently, resulting in a total of four DOFs in the gripper. The quasi-independent movements are made possible by the use of a whippletree mechanism, which distributes the input force approximately equally over the four outputs. The WTH is based on a prosthesis concept, presented by Cuellar et al. (2019), aimed at designing a non-assembly 3D-printed hand prosthesis [21]. In contrast to the prosthesis concept, the WTH is not completely 3D-printed, but makes use of off-the-shelf metal parts as well. The WTH is actuated by a stepper motor combined with a spindle transmission, pulling the base bar of the whippletree mechanism. As the gripper has the shape of a human hand, an off-the-shelf cleanable glove can be used for hygiene.

Concept B - Under-Actuated Linkage Gripper (UALG): A sketch of the UALG can be found in Figure 5b. This concept consists of four linkage under-actuated fingers, two on each side of the finger. Each finger has two DOFs: rotation around the base of the finger, and rotation of the second phalanx of the finger relative to the first phalanx. The actuation of the four fingers is coupled, meaning that four DOFs are coupled. Therefore, the gripper has a total of five independent DOFs. The high amount of DOFs allow for a high level of shape adaptivity. For hygiene, a self-produced glove should be applied, as the gripper does not have a shape similar to the human hand.

Concept C: Four Fingered Hand (4FH): Figure 5c shows the design of the 4FH. This gripper has four fingers, as the name suggests. It resembles a human hand, without the little finger. Each finger is rigid and can rotate only around the base of the finger. The rotation of the thumb and outer two opposing fingers are coupled. A rotary spring couples the middle finger of the 4FH to the other fingers, providing quasi-independent movement to the middle finger. Additionally, the thumb can rotate sideways, for a short angular distance. The rotation is bi-stable at the positions where the tip of the thumb opposes the tip of the index or middle finger. The thumb rotation allows for two grasp modes, one mainly suitable for precision grasp patterns, the other mainly for power grasp patterns. The rotation of the thumb is not actuated. Therefore, in total the 4FH has one actuated independent DOF, and two non-actuated independent DOFs.

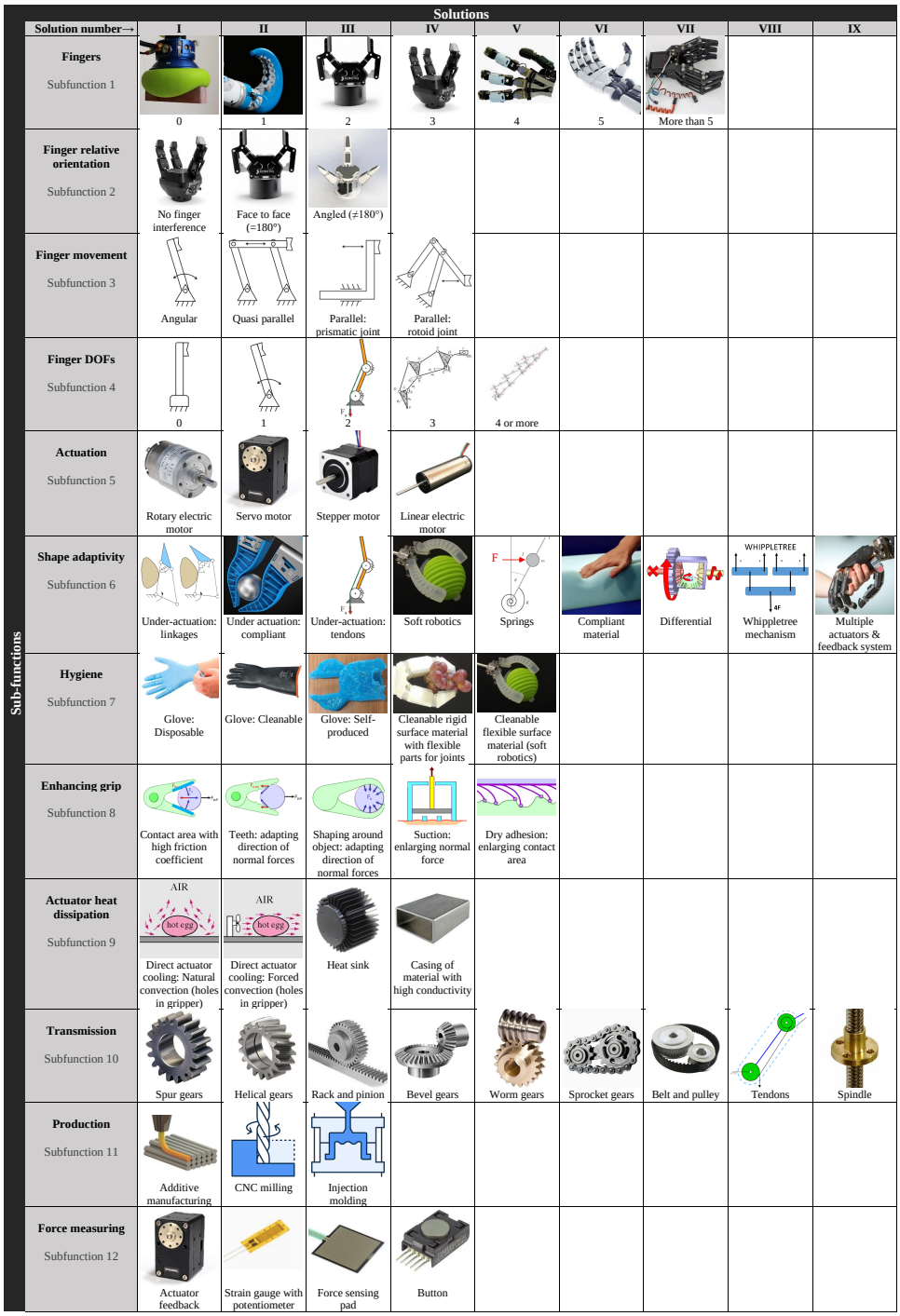

FIG. 4: Morphological chart for structurally generating a new gripper design

The shape of the 4FH is to some degree similar to a human hand, so disposable gloves can be used for hygiene.

Concept D - Split Hook Gripper (SHG): The design of the SHG is based on prosthetic split hooks, and is presented in Figure 5d. Despite the simple design, a prosthetic split hook can be used to perform various tasks and grasp a wide range of objects [22]. On the other hand, the simple design offers high repeatability,

TABLE I: Presentation of the four most promising new gripper concepts, and the previous gripper applied to robot Rose. The left column represents the 12 sub-functions in the morphological overview, the roman numerals represent the related sub-solutions.

↓ **Sub-functions**	**Concept A** ***Whippletree Hand (WTH)***	**Concept B** ***Under-Actuated Linkage Gripper (UALG)***	**Concept C** ***Four Fingered Hand (4FH)***	**Concept D** ***Split Hook Gripper (SPG)***	**Previous gripper** ***Rose Parallel Gripper (RPG)***
1. Fingers	VI: 5	V: 4	V: 4	III: 2	III: 2
2. Finger relative orientation	I&II: No interference & Face to face	II: Face to face	I&II: No interference & Face to face	II: Face to face	II: Face to face
3. Finger movement	I: Angular	I: Angular	I: Angular	I: Angular	II: Quasi-parallel
4. Finger DOFs	I&II: 0&1 (Total: 4)	II: 2 (Total: 5)	II&III: 1&2 (Total: 3)	I&II: 0&1 (Total: 1)	II: 1 (Total: 1)
5. Actuation	III: Stepper motor	II: Servo motor	II: Servo motor	II: Servo motor	II: Servo motor
6. Shape adaptivity	VI&VIII: Compliant material & Whipple-tree mechanism	I&VI: Under-actuation: linkages & Compliant material	V&VI: Springs & Compliant material	N.A.	N.A.
7. Hygiene	II: Glove: Cleanable	III: Glove: Self-produced	I: Glove: Disposable	IV: Cleanable rigid plus flexible surface	N.A.
8. Enhancing grip	I&III: High friction coefficient & Shaping around object	I&III: High friction coefficient & Shaping around object	I&III: High friction coefficient & Shaping around object	I: High friction coefficient	I: High friction coefficient
9. Actuator heat dissipation	III: Heat sink	IV: Casing of material with high conductivity	IV: Casing of material with high conductivity	IV: Casing of material with high conductivity	I: Natural convection
10. Transmission	XI: Spindle	V: Worm gears	V: Worm gears	I: Spur gears	I: Spur gears
11. Production	I: Additive manufacturing	I: Additive manufacturing	I: Additive manufacturing	I&II: Additive manufacturing & CNC/metalworking	I: Additive manufacturing
12. Force measuring	III: Force sensing pad	I&III: Actuator feedback & Force sensing pad	I&III: Actuator feedback & Force sensing pad	I&II: Actuator feedback & Strain gauge with potentiometer	I: Actuator feedback

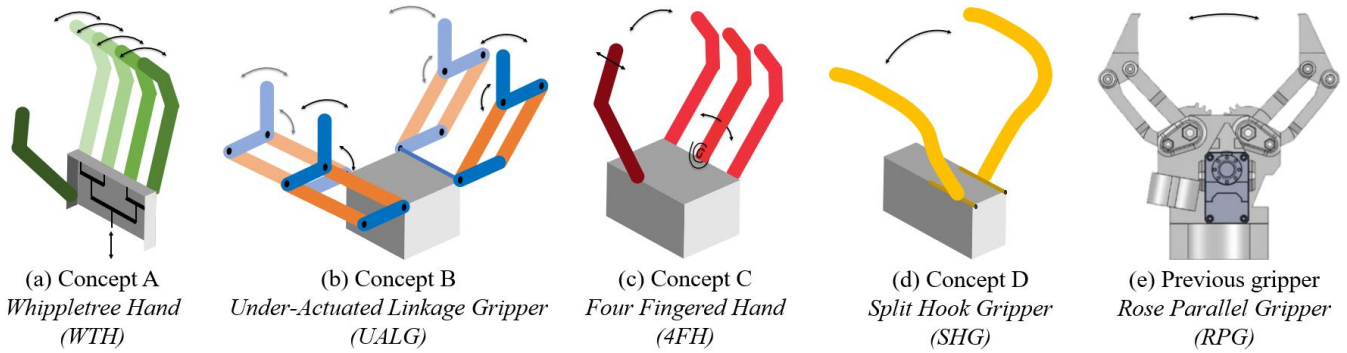

FIG. 5: Rough sketches of the four promising gripper concepts, as presented in Table I, and the design of the previous gripper. Arrows indicate DOFs.

reliability and robustness. Similar to prosthetic split hooks, the SHG has two opposing rigid fingers. One finger is stationary, and the other can rotate around the base of the finger. Therefore, the gripper has one DOF. Both fingers are shaped as a hook, with specific curves, allowing for specific grasp patterns. The material of the fingers is metal to allow for slender finger designs, compared to 3-D printed fingers. A desinfectable metal needs to be chosen for the fingers. At the joint of the rotating finger, a flexible cover needs to be applied for hygiene.

Previous gripper - Rose Parallel Gripper (RPG): Figure 2 and Figure 5e show the design of the RPG. This gripper consists of two opposing fingers. The finger movement of both fingers is quasi-parallel, as a result of two four-bar mechanisms. The movement of the fingers is coupled, resulting in one independent DOF in the gripper. The design is not suitable for disinfection or fitting a glove. Furthermore, the design does not include force transducers, but torque feedback of the actuator could be used for rough force measurement.

TABLE II: Harris Profile for the systematic selection of the most promising gripper concept

	Concept A WTH				**Concept B UALG**				**Concept C 4FH**				**Concept D SPG**				**Previous gripper RPG**			
	-2	-1	+1	+2	-2	-1	+1	+2	-2	-1	+1	+2	-2	-1	+1	+2	-2	-1	+1	+2
Overall properties																				
Low cost																				
Small size																				
Low weight																				
Mechanical properties																				
Repeatability																				
Robustness																				
Functional properties																				
Shape adaptivity																				
Precision grasp patterns																				
Power grasp patterns																				
Grasp stability																				
Orientation independence																				
Actuation and control																				
Control simplicity																				
Build up and casing																				
Production simplicity																				
Ease of disinfection																				
Non-industrial look																				

Concept selection

Using a Harris Profile, the five concepts were evaluated and compared in a systematic manner. Each design was rated on 14 characteristics, being cost, size, weight, repeatablility, robustness, shape adaptivity, precision grasp patterns, power grasp patterns, grasp stability, orientation independence, control simplicity, production simplicity, ease of disinfection and aesthetics. The designs were rated with -2, -1, 1 or 2 points on each characteristic, with the notes presented in Appendix E in mind. Each criteria and design was rated by the author twice, with a day in between, to increase the reliability of the outcomes. The Harris profile is presented in Table II. A detailed discussion can be found in Appendix F. From the Harris profile, it was concluded that the 4FH was the most promising design. The Harris Profile showed that this design fits all aspects of the design problem sufficiently, and does not require significant concessions. It provides a nice balance between simplicity and functional properties, scoring positively on almost all characteristics. In contrast, the WTH and the UALG can be considered too complex to score well on several characteristics. On the other hand, the SHG and the RPG were shown to lack in several functional properties due to simplicity. Consequently, the 4FH was chosen to continue the design process with.

2.2. Design choices

The concept of the 4FH was transformed into a detailed design. Possibilities were thoroughly compared, and supported by calculations and 3D-modelling in Solidworks. The final CAD model of the 4FH is presented in Figure 6. Each component of the design is globally described below. Calculations and deeper evaluations can be found in Appendix G.

Actuation

A servo motor was chosen to actuate the 4FH, to comply with the requirement that the gripper must be electrically powered and easy to control. Another benefit of using a servo is its ability to detect and control the actuator force, orientation and velocity. This benefit was identified in Appendix D. A servo was chosen with 4.1 Nm stall torque, more than sufficient to comply with the minimum required pinch force of 30 N. In Appendix G 1, the related equations and calculations can be found.

Transmission

A worm gear set was applied as transmission between the actuator and the fingers. The transmission system is shown in Figure 7. In the gripper design, two worm gears are positioned on opposite sides of a worm. This way, equal rotation but in opposite direction is obtained

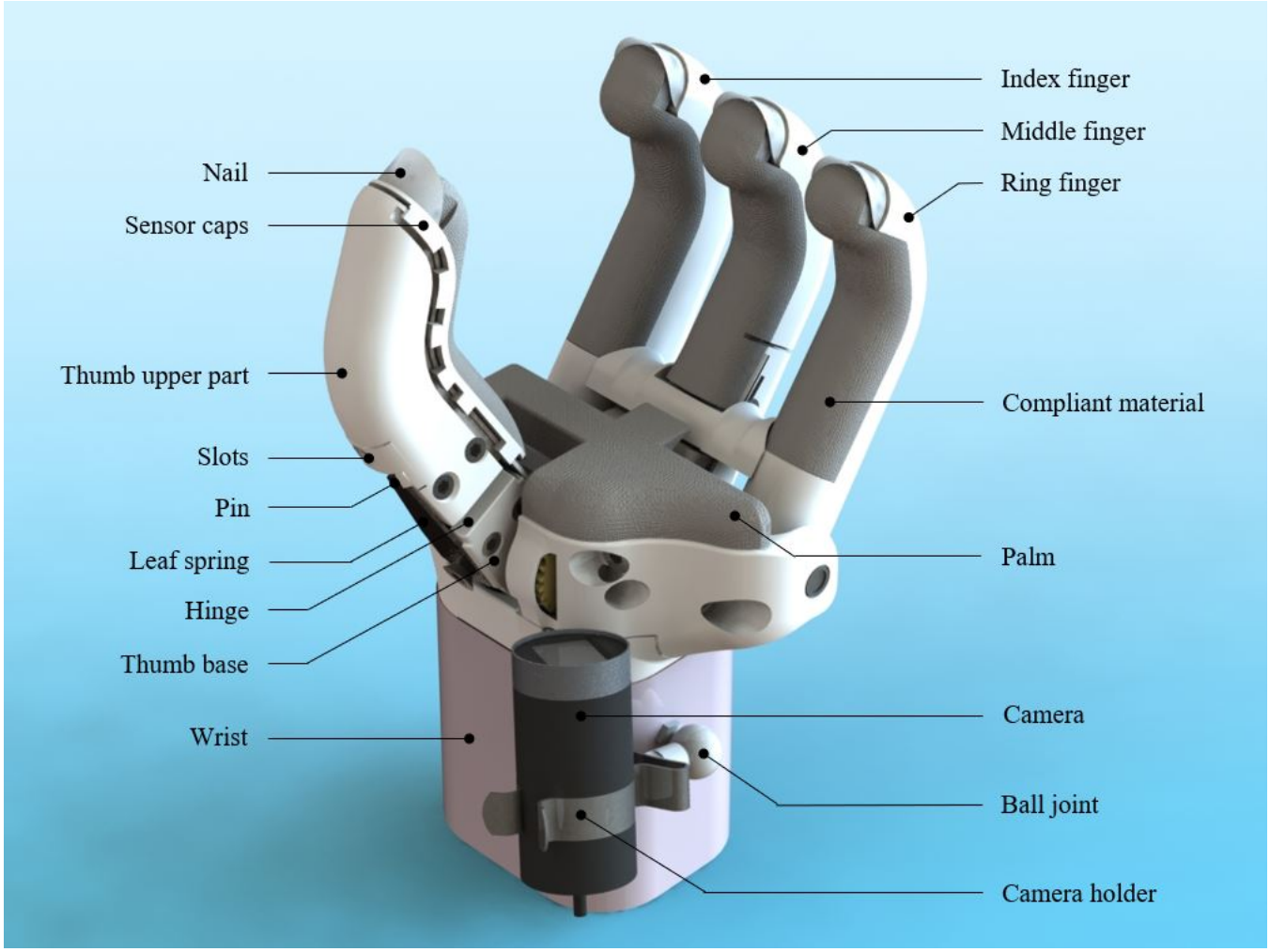

FIG. 6: CAD model of the detailed design of the 4FH without glove

for the worm gears driving the fingers. The benefit of using a worm gear set as transmission mechanism, is that it has low backdrivability. Therefore, an object can be held secure without actively needing to maintain the full grip force with the actuator. As a result, the gripper can have a lower power consumption and lower heat generation, compared to most other transmission systems. A transmission with a ratio of 4.5:1 was chosen, to comply with the required gripper closing time of 0.7 s and the required minimum pinch force of 30 N. In theory, the transmission in combination with the actuator would allow for a pinch force of 82 N and a closing time of 0.46 s for a stroke width of 85 mm. See Appendix G 2 for the underlying equations and further evaluation.

Driving shafts

Three driving shafts are present in the gripper, as can be seen in Figure 7. One goes trough the worm, and is directly connected to the actuator. Another drive shaft goes through one of the worm gears, and is connected to the thumb. The last goes through the other worm gear, and is connected to the index, middle and ring finger. Each driving shaft is supported at two points by synthetic sliding bearings. For the driving shafts, the material silver steel was chosen. This tool steel has a high carbon and chromium content, which gives the steel high strength and high wear resistance [23]. Silver steel also has an extremely fine surface finish, which is beneficial for use with sliding bearings.

A requirement set to the driving shafts, is that they may not plastically deform under the maximum torque of the actuator. A diameter of 6 mm was chosen for each driving shaft, such that the maximum stress in the shafts stays below the yield point. The maximum angle of twist, caused by the maximum torque load by the actuator, is equal to 2.9°. The maximum angle of twist can be found in the driving shaft of the index, middle and ring finger.

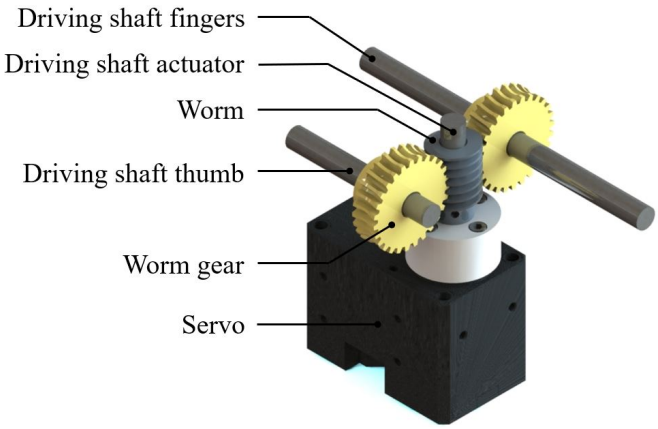

FIG. 7: CAD model of the actuation and transmission system of the 4FH

The maximum twist can be translated to the maximum displacement of the finger tips, being 4.5 mm. The underlying equations, calculations and detailed reasoning concerning the driving shafts can be found in Appendix G 3. It needs to be kept in mind that the maximum torque will very rarely occur, as the maximum actuator torque generates a grasp force much higher than required.

The fingers and gears are secured on the driving shafts using set screws, pushing on flattened parts of the shafts. A thread-locking adhesive was applied to prevent self-loosening. Threading in the 3D-printed fingers was obtained using brass inserts.

Glove

As stated in Section 2.1.1, the gripper must be disinfectable. Hygiene of the gripper was obtained by fitting a disposable glove around the whole gripper. After use, the glove can be replaced for a clean glove. Additionally, the glove makes the gripper water and dirt proof, as required. In general, disposable gloves of four materials are available on the market, namely latex, nitrile, vinyl and polyethylene [24]. For the gripper of this study, nitrile gloves are most promising. The glove is the outer surface of the complete gripper, so a material with a high coefficient of friction was desired for gripping performance. The importance of friction for functional performance is highlighted in literature [21, 25]. Under dry conditions, nitrile is shown to have a significantly higher coefficient of friction compared to latex on various types of surfaces [26]. Another benefit of nitrile gloves can be found in the fact that they are more resistant to wear down and friction, compared to other gloves of similar thickness [24]. Compared to vinyl and polyethylene, nitrile has significantly higher elasticity and adaptability. In contrast to latex, nitrile can not cause allergic reactions. Additionally, due to inner surface treatment, nitrile gloves are easier to put on than latex gloves.

Further choices were made regarding the size and thickness of the glove. In multiple studies, it has been shown that a larger size of artificial hand is beneficial for its functionality [27, 28]. Therefore, the largest commercially available size was chosen, being size XL. Regarding thickness, the thinner the glove, the better the functionality of the nails on top of the fingers. Additional benefits for thin gloves are the reduced weight and increased shape adaptability, making it easier to put it on the gripper. Thicker gloves, however, have higher resistance to wear down and have the potential to be used for prolonged periods. For the purpose of the gripper, high functionality was deemed of highest importance. Consequently, thin gloves were chosen, with 0.08 mm thickness at the fingers and palm and 0.05 mm thickness at the wrist.

The colour of the glove determines the colour of the complete gripper. The aesthetics of the gripper should not frighten the clients, so the colour should be reassuring. Common colours for gloves are blue, green, pink, white and black. Blue and green gloves are commonly used for the food industry and medical applications. Mainly the association with medical applications, hospitals and surgery was to be avoided, as this might frighten clients. Using pink gloves may cause the gripper to enter the uncanny valley, so this colour was avoided as well. Black and white both are neutral colours, with little association to negative emotions. The colour scheme of the care-robot is white, orange and black. Consequently, one of these colours is preferred for fitting aesthetics. Considering heat dissipation through radiation, black is beneficial for increased emissivity. Therefore, black gloves were chosen for the gripper. The importance of heat dissipation will be explained later.

Fingers

The gripper has four fingers, which resemble the thumb, index, middle and ring finger of a human hand. No little finger is present in the 4FH. This design choice was based on literature, in which findings are presented that the little finger does not contribute much to the functional performance of the human hand [29]. Other literature states that four fingers are sufficient to pick up any 3D-item [30]. Therefore, benefits of adding a little finger to the gripper did not weigh up to the drawbacks, being added weight, size and complexity.

All fingers are rigid and can rotate only around the centreline of its driving shaft. Therefore, the finger movement can be classified as angular movement, according to classifications presented in literature [31]. Consequently, the amount of DOF of each finger is limited to one. This choice was based on literature, arguing that the least

amount of DOF should be used with which the gripper can fit its purposes [32], and that single DOF prostheses can outperform multiple DOF prostheses on functional performance [33].

The thumb is driven by the thumb driving shaft, the index, middle and ring finger are driven by the finger driving shaft. The two driving shafts rotate in opposite directions, as a result of the worm wheel transmission. Therefore, the rotations of all fingers are coupled. The movements of the index and ring finger are identical, as they are fastened on the same driving shaft. This design choice was based on research, which presented a high correlation coefficient between movements of the index and ring finger in human hands while performing tasks [34]. The movement of the middle finger, however, does not need to be identical to the movement of the outer two fingers, as the middle finger is connected to its driving shaft via a torsion spring. Therefore, the movement of the middle finger will or will not be identical to the movement of the outer two fingers, depending on whether or not a counteracting force is applied to the middle finger. From rest position the middle finger can only rotate backwards, due to integration of a mechanical stop. The adaptive middle finger allows for shape adaptivity around 3D objects. It also provides a way to carefully pick up light and fragile objects between the thumb and middle finger, without the need for precise actuator control.

Torsion spring

The rotational stiffness of the middle finger needed to be high enough high enough to enable grasping of light and fragile objects, but low enough to allow for shape adaptivity. A torsion spring with a stiffness of 0.54 Nmm^2 was chosen, pretensioned in the gripper with 195°. The torsion spring has a base torque of 127 Nmm with angular displacement. This results in a needed force of 2.58 N on the fingertip to displace the middle finger. The middle finger can rotate backwards for approximately 40°. The required force to push the finger to this orientation is 2.82 N, which is only 0.24 N higher than the minimum force to displace the middle finger. So, when pinching an object between the thumb and middle finger using orientation control of the actuator, the operator can be sure that the force applied on the object is between 2.58 N and 2.82 N. This is low enough to not damage most fragile objects, and high enough to stably grasp lightweight objects.

Finger geometry

The shape of the fingers was designed to resemble a human hand. The index, middle and ring finger have three phalanxes, like human fingers, but with a fixed relative angle. The angle between the phalanxes is 45°. This was chosen for a high functional versatility and for resembling a human hand grasping a cylindrical object. The length of the phalanxes was based on the the length ratio's in human hands. For the human index, middle and ring finger, the ratio between the distal phalanx, medial phalanx and proximal phalanx is on average 1:1.5:2.5 [35]. The phalanx length ratio for the gripper fingers is 1:1.5:3. The relatively longer proximal phalanx was chosen as the rotation point of the gripper finger is further down the palm than for human fingers. A longer proximal phalanx also benefits the stroke width of the gripper. The gripper thumb has two phalanxes, like the human thumb, but again with a fixed angle of 45°. An increased length of proximal phalanx has also been applied for the thumb, with the same reasoning.

The length and the cross-sectional area of the fingers was designed to fit the disposable glove. This means that the thickness of each finger is different, like human fingers. Also, the cross-sectional area of each finger decreases towards the finger tip. The length of the fingers up to the palm of the 4FH is approximately equal to the length of the fingers of the glove up to its palm. The gripper being designed to fit the glove has an additional benefit. The glove is designed to have the shape of a human hand, so the gripper resembles the human hand as well. Therefore, the gripper will not look too industrial or alien-like, which could scare clients in the care home.

Bistable mechanism

The thumb of the gripper consists of two parts, namely the thumb base connected to the driving shaft, and the upper part of the thumb. Relative to the thumb base, the upper part of thumb can rotate sideways, in which it has two stable orientations. In one stable orientation, the tip of the thumb is opposing the tip of the index finger, in the other stable orientation it is opposing the tip of the middle finger. The orientations can be seen as modes of the gripper, named the pinch mode and power grip mode. The pinch mode mainly allows for pinching, the power grip mode mainly for cylindrical grasping. The pinch mode of the gripper can be seen in Figure 8a, the power grip mode in Figure 8b. The orientation of the thumb can be changed by applying an external load on the upper part of the thumb. This can be done by pushing the thumb against a rigid part of the environment using movement of the robot arm.

The bistable mechanism consists of a butt hinge, two slots and a pin. See Figure 6 for the placement of the parts in the gripper design. The hinge is positioned between the two parts of the thumb, enabling the sideways rotation. The two slots are positioned on the upper part

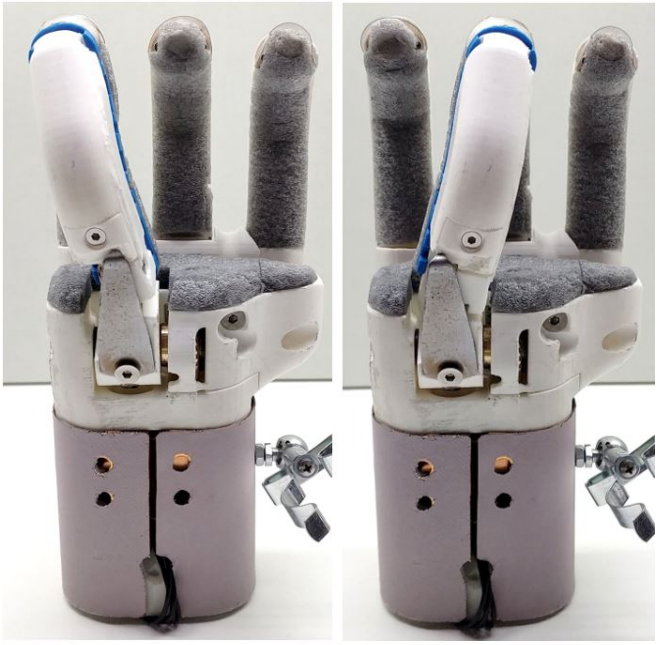

(a)
Pinch mode: Thumb opposing index finger

(b)
Power grip mode: Thumb opposing middle finger

FIG. 8: Presentation of the gripper in the grip and pinch mode, and the related orientation of the thumb

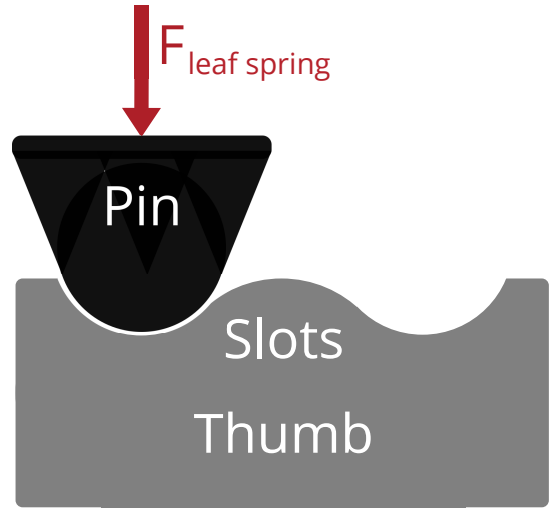

FIG. 9: Simplified visualisation of the bistable mechanism in the thumb, shown as a cross-section. $F_{leaf\ spring}$ is the force exerted on the pin by the leaf spring. The two slots are the stable positions of the pin.

of the thumb, with the exact relative angle to generate the required sideways displacement of the thumb tip. A pin is connected to the base of the thumb, and is passively pressed into one of the slots. For a simplified visualisation of the pin and slots, see Figure 9. When the thumb tip is rotated sideways, the pin moves out of the slot and into the other slot. As the part between the two slots is raised, the pin does not only travel sideways but also needs to travel upwards. The pin is connected to the thumb base by a leaf spring, due to which the pin is pressed into the slots. Therefore, the needed upwards movement of the pin traveling between two slots results in added potential energy in the leaf spring, causing an unstable position. When the pin is positioned in one of the slots, the minimum amount of energy is stored in the leaf spring, resulting in two stable orientations of the thumb tip.

Grasping forces result in a torque and shear force at the hinge, causing the thumb tip to be pressed backwards. Therefore, it was chosen to position the pin and spring leaf on the backside of the thumb base. This way, the upper part of the thumb, and thus the slots, will be pressed extra against the pin while grasping. Therefore, the risk of unwanted sideways rotation of the thumb during use is decreased. The leaf spring was produced from a steel plate with 1 mm thickness, resulting in a leaf spring with significant stiffness. High stiffness is needed, because a small backwards deformation should cause a significant change in force. The leaf spring is fastened on the thumb base using a bolt. The bolt can be tightened, up to the desired resistance against sideways rotation.

The slots in the upper part of the thumb needed iteration in precise relative angles for exact alignment with the opposing fingers. The slots are prone to wear as the steel pin is pressing and sliding along the 3D printed PLA slots. The slots are 3D-printed, to allow for quick prototyping. Easy replacing of the slots was therefore required. This was obtained by having the slots in a small separate part, which could be reprinted in a short time, and which is bolted on the upper part of the thumb.

The choice for a conventional butt hinge instead of a compliant mechanism was based on several points. A compliant mechanism with the correct bistable properties, without having a rigid part around the thumb to connect leaf springs to, is very complex. Having a compliant mechanism without the bistable properties, so only replacing the hinge, is much more realistic. Compliant hinges, however, have a stiffness against rotation, which would counteract the desired stable orientations of the thumb. If the stiffness is low, the counteracting torque would not impose a problem. A low stiffness, however, needs to be obtained using thinner leaf springs, disregarding high complexity compliant mechanisms. Thinner leaf springs, as well as high complexity compliant mechanisms, can easily be damaged or plastically deformed, due to buckling, overbending or clamping issues. This decreases the robustness of the thumb.

TABLE III: Properties and settings used for the 3D-printed parts of the gripper

3D-Printing properties	
Material	PLA
Filament thickness	2.85 mm
Nozzle	0.4 mm
Layer height	0.1 mm
Wall thickness	1.05 mm
Infill density	10%
Infill pattern	Grid

Robustness is an important aspect of the gripper design. A conventional butt hinge, however, can deal with high loads without being damaged. On the other hand, a disadvantage is that conventional hinges introduce backlash to the system, as it consists of separate parts with clearance in between. This disadvantage, however, is not present in the gripper thumb, as the pin presses against the upper part of the thumb and thus removes the backlash.

Manufacturing method

The fingers, palm and bayonet-fitting were manufactured using additive manufacturing, more specifically using Fused Filament Fabrication technology (FFF). This method allows for manufacturing complex shapes, while complying to the requirements of low cost and quick manufacturing. It has to be noted, however, that this project was aimed at designing one prototype. When a larger number of grippers need to be manufactured, other methods are likely to be less expensive, quicker and of higher durability.

The printer settings used for manufacturing the 4FH can be found in Table III. The low infill density was chosen to minimize weight and manufacturing duration. At some areas in the printed parts, however, higher strength was needed. At these points the parts were printed solidly. This was the case at the base of all fingers, for high strength around the brass inserts for secure connection to the driving shafts. Also, parts of the palm and bayonet-fitting were printed solidly, around inserts and around the functional part of the bayonet-fitting.

Literature was taken as guideline for strength of 3D-printed parts [36]. During the manufacturing process of the gripper, it was taken into account that prints have relatively low strength in the build direction, compared to lateral direction. Orientations for printing parts were chosen accordingly.

Nails

Each finger of the gripper is fitted with a nail, positioned similarly as human nails. The nails allow for high precision grasping, especially grasping flat items from a flat surface. For example, the nails allow for picking up coins or a credit card from a table. The nails were laser cut from a thin sheet of plastic. The flattened nail has the shape of half a circle. The nail is bent over the complete width for 180 degrees, as can be seen in Figure 10. The straight side of the nail, or the backside, presses against the finger when a load is applied to the nail. The curve of the nail improves the stiffness of the nail in specific directions, and increases the possible force in the direction of the finger before buckling.

FIG. 10: One of the fingers of the 4FH, including the nail (transparent) at the finger tip and the compliant material (grey) on the inside of the finger

For the nail applies, the thinner the nail is, the better the theoretical functionality for grasping extremely flat items. On the other hand, the nails needed to have sufficient thickness to handle the grasping forces without being damaged. Plastic sheet with high flexibility was chosen as the material of the nail. The thickness of the sheet is 0.16 mm, chosen by iterating three different thicknesses and evaluating their functionality. The high flexibility has various benefits. First, the flexibility allows the nail to adapt its shape to the surface it is pressed on. In the case of a table, the nail will flatten at the part where it is pressed on the table. This creates a larger potential contact edge between the nail and the flat object to grasp. Also, the shape adaptivity results in a lower needed precision to position the nail exactly on the flat surface. The nail creates a low stiffness contact with the flat surface, which is beneficial for the force feedback control. Another advantage of flexible nails is its safety. As the nails are extremely flat, the nails could potentially harm people upon contact. With flexible nails, however, the nails can bend away upon contact, so the risk of harming people is minimized. Please note

that the nails are positioned on the fingers, so the glove covers the nails. This increases the functional thickness of the nail, but also increases the safety and cleanability of the gripper.

Compliant material

Literature shows that prosthetic hands with low compliance in the hand-object contact area's score lower on functional performance [37]. Therefore, hand-object contact area's were fitted with complaint material. The concerning area's are the fingertips, the inside of the fingers and the palm between the fingers. Figure 10 shows the positioning of the dark grey compliant material on one of the fingers.

The soft material offers shape adaptivity around objects. Loads applied to the objects are spread out over a larger area, reducing the stress applied on the object and thus reducing the risk of damage or unwanted deformations. A spread out contact area also prevents unwanted rotations of grasped items. A larger contact area namely results in a larger potential torque load normal to the plane of the contact area. Additionally, for rubber-like material, such as the glove, it holds that a larger contact area results in a larger potential friction force, increasing the pay-load of the gripper.

Low stiffness contact as a result of the compliant material is also beneficial for the force feedback control of the robot arm. For example, opening drawers was identified as a difficult task with the RPG. The rigid fingers of the gripper needed to pull a rigid handle of the drawer, which created resonance in the force feedback control. Low stiffness contact can prevent this, as the change between no contact and applying force to the handle is gradual.

Polyethylene (PE) was chosen for the compliant material. PE has a closed cell structure. It was chosen for its mechanical properties, namely its high shock absorbing properties and its ability to regain original shape after loading.

Sensor

The addition of a force sensor in the gripper is beneficial for grasping fragile objects. Following the evaluation and reasoning of Appendix D, noting advantages and disadvantages of various types of force transducers, it was concluded that a pad force transducer was the best choice for the gripper design. More specifically, a flexible pad with the shape of the gripper finger was needed, so an oblong Force Sensing Resistor (FSR) was integrated in the design. A FSR can measure the total force applied on its sensing area, irrespective of the position, contact area or amount of contact points. The FSR strip is positioned in the thumb, as shown in Figure 11. The thumb is opposing the other three fingers. Therefore, all force applied on a grasped object is also applied on the thumb, following Newton's third law. Accordingly, a single FSR placed in the thumb can measure all force applied on an object.

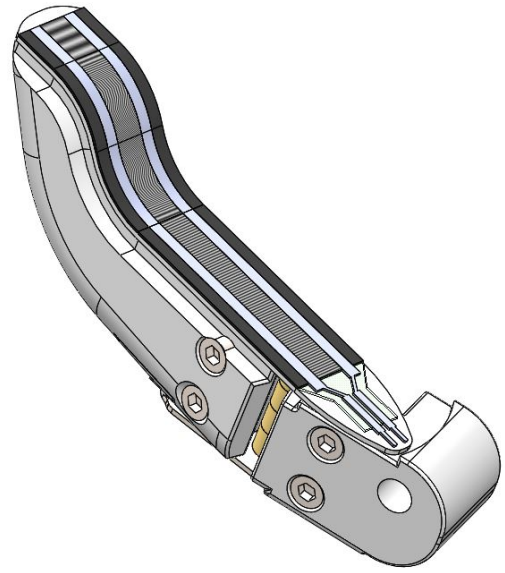

FIG. 11: CAD model of the FSR positioned on the 3D-printed structure of the thumb. On top of the FSR, sensor caps and compliant material are positioned, but are hidden in the figure for visibility of the FSR.

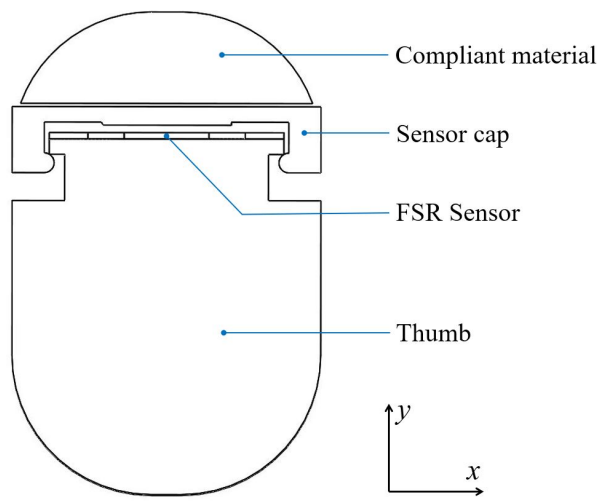

FIG. 12: Cross-section of the gripper thumb, showing how the FSR is positioned in the thumb design.

The FSR chosen is the FSR UX 408 developed by Interlink Electronics. This FSR strip has a force sensing range of 0.5 N - 150 N, with a force repeatability for a single part of ±2% [38]. Furthermore, the FSR is flexible and may be bent, and can be cut to the desired length. The FSR is 15.3 mm wide, but the active sensing area is only 5.1 mm wide. It is of importance

that the forces applied by the object on the thumb go through the active sensing area only, otherwise the force measurement is inaccurate. To this end, sensor caps were designed, which are visualised in Figure 12. The sensor caps are located in between the FSR and the compliant material covering the thumb. The sensor cap has an elevation in the middle, corresponding to the width of the active sensing area. Due to the elevation, all grasping forces in the thumb go through the active sensing area of the FSR. The sensor cap is kept in place by hooks on both sides, clicked around the 3D-printed structure of the thumb. The hooks provide free motion in y-direction, meaning that forces in y-direction do not run through the hooks but through the FSR to the thumb structure. The hooks constrain movement in the x-direction, making sure the sensor caps are kept in place. This means that forces in x-direction do flow through the hooks. This is not an issue, as grasping forces are normal to the fingers, and thus in y-direction. The FSR is covered by four sensor caps in total.

Heat dissipation

Heat generated by the actuation of the gripper must be dissipated, to prevent the actuator from overheating and to keep the gripper surface within safe temperature ranges, as required. Overheating of the actuator during operations is likely to result in failed tasks, due to a decrease or complete loss of actuator torque. The amount of heat that must be dissipated depends on the duty cycle and actuator torque. The duty cycle can be divided in sections of non-grasping, grasping and maintaining grasp. The ratio between the three sections is highly task dependent. The worst case scenario was evaluated, being a task in which the gripper needs to grasp an object with high force and maintain the grasp for a long period. Quantitatively speaking, a duty cycle of 0% non-grasping, 25% grasping and 75% maintaining grasp was taken as the worst case scenario. Most tasks, however, would consist of higher ratios of non-grasping or maintaining grasp, relative to grasping. During grasping and maintaining grasp, the actuator is in stall, so all electrical power is converted to heat. While maintaining grasp, the actuator torque can be lower than while grasping, without a decrease in grip or pinch force. This is a result of the worm gear set as transmission, which has low backdrivability. The lower required actuator torque correlates to lower power and thus lower heat dissipation. In Appendix G 4, the fraction of the initial grasping torque that is needed to maintain the grip or pinch force is determined. Theoretically, the grasping torque could be lowered to 42% for maintaining the grasp force. The force considered for the worst case scenario is the 30 N pinch force, based on the requirements. Combining the duty cycle and the force, the average amount of power consumed by the actuator could be determined, as done in Appendix G 4. The amount of electrical power, converted to heat and to be dissipated by the gripper, for the worst case scenario, is equal to 6.81 W.

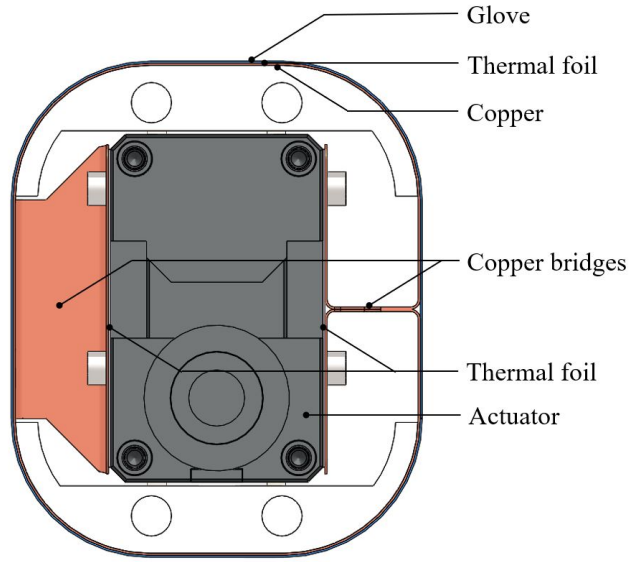

FIG. 13: Cross-section of the wrist design of the gripper

The actuator is located in the wrist of the gripper, so the wrist needs to allow for high heat dissipation. From inside to outside, the wrist consists of the actuator, thermal foil, copper bridges, copper sheet, thermal foil and the glove. The wrist design can be seen in Figure 13. The thermal foil between the actuator and copper bridges was applied to ensure high thermal conductivity. The copper bridges ensure high heat transfer between the inside of the wrist where the actuator is positioned, and the outside of the wrist where the heat needs to be dissipated. The copper bridges are connected to the copper sheet surrounding the wrist. The copper sheet is needed to distribute the heat from the bridges to the whole circumference of the wrist. The glove is the outer layer of the wrist to allow for disinfection, as required. The thermal foil between the glove and the copper creates a layer of non-metal material around the copper, allowing for a higher surface temperature, according to the ECMA Standard for Safety of Electronic Equipment [19].

Appendix G 4 gives a more detailed overview of the wrist design and considerations, and evaluates its maximum heat dissipation capacity, substantiated with equations and the assumptions made. The theoretical heat dissipation capacity of the wrist was found to be 7.72 W. Therefore it can be concluded that the wrist can dissipate all heat generated by the actuator, even in the worst case scenario.

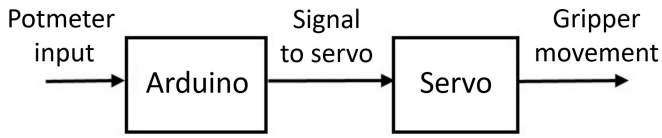

FIG. 14: Block scheme of the open loop control, used for testing the RPG, 4FH and 4FH-i

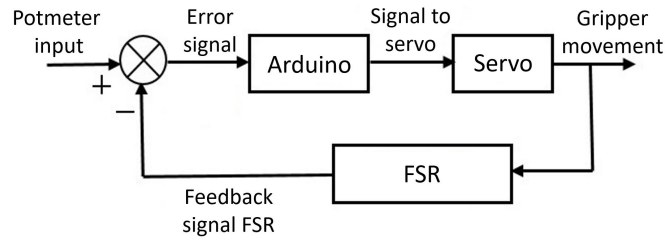

FIG. 15: Block scheme of the closed loop control, used for proof of concept of the FSR in the 4FH and 4FH-i

Camera

Camera integration in the gripper design was required to allow for visual inspection during grasping tasks. In the design, a camera with a diameter of 28 mm is held by a galvanised steel clamp. The clamp is mounted on a galvanised steel ball joint, which in turn is mounted on the wrist. Both the clamp and ball joint are disinfectable and are not prone to corrosion, due to the galvanisation. The ball joint allows for optimizing the view orientation of the camera by hand. The positioning of the camera enables viewing all finger tips of the gripper. In case a new camera will be applied, a different holder can be attached. The holder can easily be taken of, as the holder is bolted to the gripper.

Control

Two control loops were designed for the 4FH, one open loop and one closed loop. The block scheme of the open loop control is presented in Figure 14. The open loop control is fairly simple, using a potentiometer, servo, Arduino and Arduino shield. The Arduino shield is needed for communication between the Arduino and the servo in the gripper. The open loop control works as follows. The potentiometer can be rotated by the operator. The output of the potentiometer, related to its angular position, is read, scaled and written as servo output. In other words, turning the potentiometer directly results in turning of the servo, and thus moving of the fingers. This way, the gripper is not just limited to an open or closed state. The fingers can be controlled to any desired state between fully open or fully closed. Furthermore, the opening and closing speed can be controlled, by rotating the potentiometer with the desired angular velocity. Naturally, the maximum speed is limited, due to specifications of the servo in combination with the transmission. With the open loop control, opening and closing of the gripper can be manually adapted to the object to grasp. For example, a low pace and more precise angular positioning can be applied for fragile objects. The current was limited to 75/1193 units, which translates to approximately 0.2 A.

Additionally, a closed loop control was designed. Figure 15 shows the block scheme for the closed loop control. This control loop makes use of the same items as the open loop control, in combination with the FSR sensor in the thumb as described previously. In this loop, the potentiometer is not used for controlling the orientation of the fingers, but for controlling the desired amount of force applied on the object to grasp. The output of the potentiometer is read and scaled. The output of the FSR sensor, directly related to the amount of force applied on the FSR and thus on the object, is read and scaled as well. The values of the potentiometer and FSR are continuously being compared. When the value of the FSR is higher than that of the potentiometer, it means that the applied force is higher than desired. Then, the applied force is automatically decreased. When the value of the FSR is lower than that of the potentiometer, the applied force is lower than desired and is automatically increased. When the two values are equal, with a certain tolerance, the applied force is as desired. Increasing and decreasing of applied force was done by tiny steps of opening or closing of the gripper. Due to spring-like behaviour of the compliant material on the fingers, the applied force is directly related to the compression of the compliant material. The closed loop control shows potential for intuitive grasping using haptic master gripper devices, or even fully automated grasping.

The open loop control was used for the testing procedure of the 4FH, as this control method was the most robust and ready to use. The closed loop-control was used as a proof of concept, to show the potential and usefulness of the FSR integrated in the gripper. The electrical circuits for both control schemes can be found in Appendix H.

2.3. Test methods

2.3.1. *Assessments functional performance*

For the research and development of any technological device, it is crucial to have reliable and valid quantified results of their performance. Only then, different designs can be objectively compared, and well-founded conclusions can be drawn regarding design considerations

FIG. 16: Set of nine objects used for the Essential Items Test (EIT)

and potential improvements [34, 39]. This is the basis for technological advancement. Therefore, the gripper of this study was subjected to various tests to evaluate functional performance on different levels.

A gap of standardised and validated assessments for robotic hands and grippers was identified in literature, see the literature study of Appendix C. Robotic hands, and the gripper of this study in particular, have many similarities with upper limb prostheses, as described in the introduction and in literature [10]. Therefore, relevant functional performance assessments for upper limb prostheses were used. Furthermore, a new assessment was drawn up, specifically aimed at the application field of the 4FH. Three separate tests were used for the assessment of functional performance. For evaluation, the results of the 4FH were compared to results obtained by the RPG. Each of the three tests is described below.

EIT

The first test is the Essential Items Test (EIT). The EIT is a test generated in this study. The EIT is meant as a baseline test, to verify whether or not the gripper can be useful for the care environment. The test consists of picking up some of the most essential objects in a care environment, from two different heights. The objects in question are a pill box, credit card, keys, wallet, cloth, empty mug, filled 0.5 L plastic bottle, TV-remote and a bowl. The set of objects for the EIT are shown in Figure 16. The objects were chosen in collaboration with the company and using indirect feedback from care workers. The set consists of everyday items, so a similar or closely resembling set can easily be reproduced.

Objects need to be picked up by the gripper from two different heights, namely from the floor and from a table. It can be argued that differing the height is mainly a test for the (robot) arm, but assessing at different heights is of importance for assessing the gripper design as well. Due to limitations in the range of motion of the arm, the possible gripper orientation relative to objects is limited as well. Therefore, assessing at different heights aims at assessing the grippers potential to grasp objects in various orientations, mainly being from the side and from above.

The scoring of the EIT is based only on whether or not the gripper can pick up all items at the specified heights. If the gripper fails at one or more items, the gripper fails the test. In that case, the gripper should be improved until the EIT can be performed, before continuing to the next tests. The time needed to pick up objects does not play a role in the EIT.

For each item, the object must be positioned directly in front of the arm in the conventional non-supported orientation of the object. Each item must be picked up from the floor and table. After picking up, the object must be held in the air for at least three seconds, without dropping the object. The height for lifting up the object is not important, as long as the object is free of contact with the surrounding environment.

Further detailing of the EIT can be found in Appendix I 1, including the prescribed object orientations and the table height. The sizes and weights of the test objects are presented here as well, to allow for reproducing the test set.

Modified AHAP

The second test is a modified version of the Anthropomorphic Hand Assessment Protocol (AHAP). The original AHAP was designed in 2019 [25]. The AHAP consists of 26 tasks, covering the eight most used human grip types. The test is aimed at measuring grasp stability under motion and human-like execution or anthropomorphism. Assessing grasp stability is very useful for the assessment of the gripper of this study. Grasp stability contributes to the functional performance and reliability of a gripper. Anthropomorphism, however, is not required for the gripper of the care-robot. Therefore, a modified version of the AHAP was generated in this study.

In the modified AHAP, the scoring part for measuring anthropomorphism is disregarded. Consequently, the scoring in the modified AHAP is purely based on per-

FIG. 17: Performing one of the tasks of the modified AHAP. The object must be rotated 180° and back for three times. Score is based on whether the object is dropped or shows motion with respect to the gripper.

formance under motion. This performance is measured according to the protocol of the original AHAP. Each object must be handed to the gripper under assessment in the correct orientation. The gripper needs to hold the object for three seconds. Then, the gripper should be rotated 180° in a smooth manner. After three seconds, the gripper should be rotated back. This sequence needs to be repeated three times, after which the object can be released. In Figure 17 the execution of the modified AHAP is visualised.

During this procedure, 1 point is scored if the object does not visibly move with respect to the gripper during the rotation sequence. When the object moves with respect to the gripper, but is not dropped, 0.5 points are achieved. If the object is dropped, no points are scored. This scoring method is identical to that of the original AHAP.

In the original AHAP, two of the 26 tasks are only scored based on human-like execution. Therefore, these two tasks are not relevant for this study and thus not included in the modified AHAP. Although using the correct grip type is not part of the modified AHAP, each item was grasped in a way that approximates the prescribed grasp in the original AHAP. This way, it

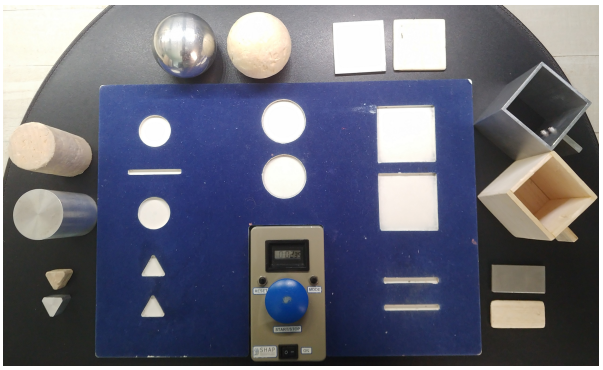

FIG. 18: The form board used for the SHAP and modified SHAP, including the 12 abstract items

was tried to preserve the variety of the test set. In Appendix I 2, a detailed list of objects used for the modified AHAP can be found, including weights and sizes. Additionally, pictures are presented of the grippers performing the tasks of the modified AHAP.

Modified SHAP

The third test of the set is a modified version of the Southampton Hand Assessment Procedure (SHAP). The SHAP was presented in 2002, and aims at measuring functional performance of human hands and upper limb prostheses [40]. The SHAP consists of 12 abstract tasks and 14 Activities of Daily Living (ADLs). The abstract items and form board for the abstract tasks is shown in Figure 18. See the literature study in Appendix C for a more detailed description of the SHAP, as well as reasoning why the SHAP is recommended as gripper assessment.

Not all tasks of the SHAP are relevant for robotic hands, or specifically for the gripper of this study. Therefore, a modified version of the SHAP was generated in this study. The modified SHAP aims at evaluating functional performance of grippers for care-robots. The modified SHAP is very similar to the original SHAP. The only difference is that six tasks of the original SHAP are disregarded in the modified SHAP, and six new tasks are added. The disregarded tasks are the ADLs opening a jar, lifting a tray, cutting food, turning pages, unbuttoning and using a screwdriver. The first two are disregarded as they are bi-manual tasks. Care-robot Rose is equipped with one arm and one gripper only, so these two tasks can not be performed according to protocol. The last four ADLs were regarded non-relevant for the care-robot, either for safety reasons or unnecessity. Six new tasks representative of real-life tasks of the care-robot were added. The added tasks are to pick and place a credit card, shallow plate, cloth, and mug, and to open and close a drawer and carry a grocery bag. The tasks are

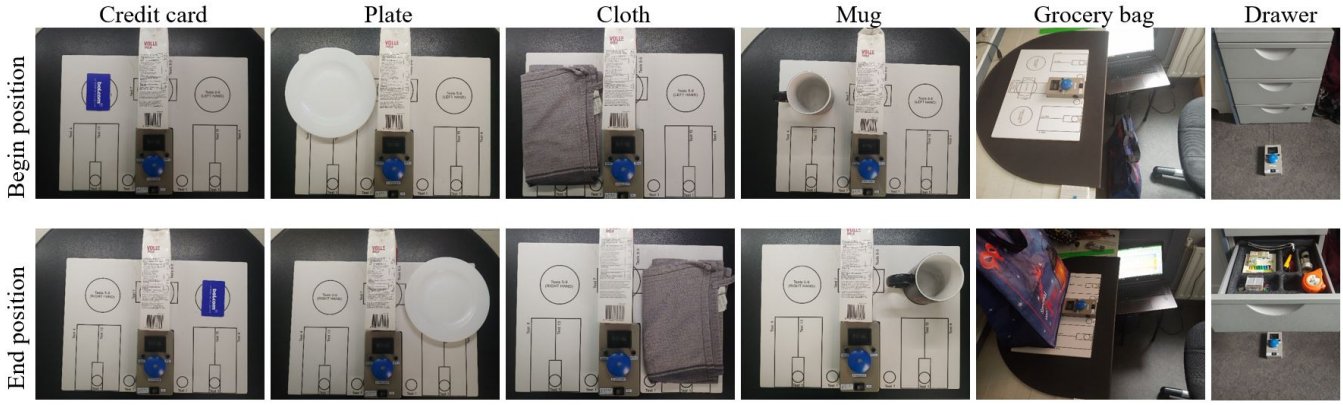

FIG. 19: Visualisation of the six tasks added to the original SHAP to form the modified SHAP

visualised in Figure 19. As for the EIT, the items needed for the modified SHAP are everyday items. Therefore, a comparable set can easily be reproduced.

Rest of the SHAP, being 20 tasks, was kept identical in the modified SHAP. Furthermore, the test protocol was kept exactly the same. This means that the test needs to be performed while seated directly in front of the form board. The form board is positioned on a table at elbow height, and at 8 cm from the front edge of the table. The scoring of the modified SHAP is also identical to that of the original SHAP. The scoring is entirely based on task completion times.

The original scoring computations of the SHAP are criticized in literature, as they are not published [41]. Therefore, the scoring method can not be checked for errors, while it is suspected to induce bias. Furthermore, the non-published computation forces SHAP users to purchase an expensive software license to generate scores. For these reasons, Burgerhof et al. generated and published alternative score computations for the SHAP in 2017 [41]. These score computations provide alternatives for both the overall score and sub-scores of the SHAP. In the alternative method, the overall score is called W-LIF and the sub-scores LIFPP. Research has shown very high correlations between both scoring methods, validating the use of the alternative computation. To this end, the alternative scoring method was used in this study. It needs to be noted, however, that research identified a three point difference with a standard deviation of three between W-LIF and IOF scores.

Only minor adaptions were made to the computations of the W-LIF and LIFPP in this study, to account for the disregarded and added tasks. The choice was made to not distribute the added tasks over the existing sub-groups for the LIFPP, which are based on prehensile patterns. Instead, an extra sub-score was generated for the extra tasks, in the same way the LIFPP scores are computed. This was done in order to maintain the reliability of the original LIFPP scores, not spoiled by extra non-validated tasks. Also, the performance on the extra tasks can be evaluated more easily this way. Appendix I 3 presents detailed protocols for the execution of the added tasks, as well as the weights and sizes of the related objects for reproducing the set. Furthermore, determination of normative completion times and the score computations used for the modified SHAP are presented.

SHAP

The three described assessments, the EIT, modified SHAP and modified AHAP, were used as a direct measure of functional performance of the grippers. In addition, one test was performed which was not a direct measure of functional performance, being the original SHAP. The original SHAP was added to the set of assessments to be able to present functional performance outcomes of the grippers on a well-known, validated and reliable assessment. This way, the grippers can more easily be compared to other grippers and prostheses in literature. Only the RPG and the final version of the 4FH were assessed with the SHAP.

Most of the tasks of the SHAP were already performed for the modified SHAP, so these outcomes were copied. Only six tasks of the original SHAP were not yet tested in the modified SHAP. According to the original protocol, some of these tasks can be or need to be bi-manual. These tasks are using button board, opening a jar, lifting a tray and using a screwdriver. For this study, the non-dominant hand of the participant was used as the assisting hand.

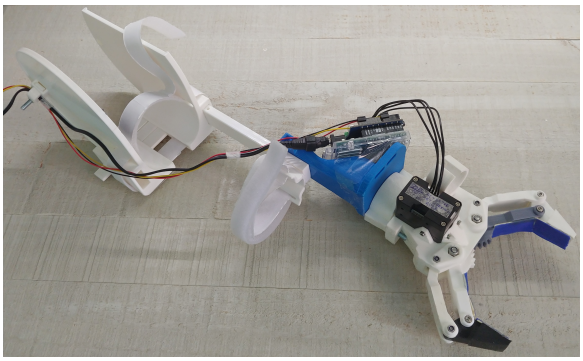

FIG. 20: The RPG gripper attached to the prosthesis simulator 'Delft Pro Simulator'

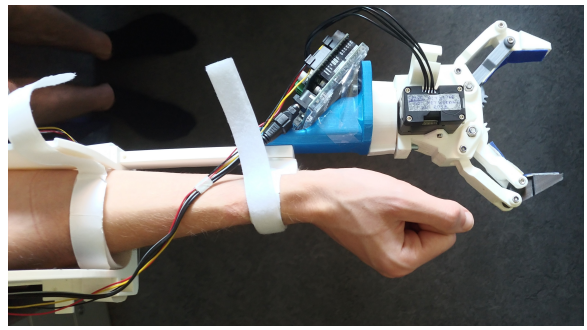

FIG. 21: The Delft Pro Simulator attached to the arm for testing the gripper

2.3.2. *Assessment execution*

Equipment

Initially, the plan was to test the gripper conform the way it will be used in the care environment. That is, with the gripper attached to the robot arm, and controlling the robot arm and gripper using tele-operation. Due to issues with the robot arm, however, the tests could not be performed using the robot. Therefore, an alternative was chosen, namely using a prosthesis simulator. A prosthesis simulator is a device for attaching hand prostheses directly to the forearm of people with intact arms, in order to allow for functional testing. The prosthesis simulator used in this study is the Delft Pro Simulator, which was designed to be accessible and 3D-printable [42]. This prosthesis simulator allows for flexion and extension of the elbow, but constrains pro-and supination of the forearm, to simulate transradial limb absence. The Delft Pro Simulator is presented in Figure 20 and 21. Only a minor modification was made to the Delft Pro Simulator in this studies, to allow for attachment of the RPG and the 4FH. The modified part can be seen in the figures in blue. During the modification, special attention was paid such that the pinching fingers of both grippers are at identical height relatively to the prosthesis simulator.

The prosthesis simulator was considered a good alternative for testing functionality, for multiple reasons. First of all, this study is aimed at evaluating relative performance between the previous and newly developed gripper. This means that the most important aspect is that both grippers are tested in an identical manner, to be sure that the difference in scoring is not caused by external factors. Following this reasoning, using the prosthesis simulator instead of the robot arm does not affect the relative functional performance of both grippers, as they were assessed in an identical manner. Secondly, the prosthesis simulator is designed to test functional performance of below-elbow prosthesis, meaning that it is designed to take functionality of the human hand out of the loop. This is beneficial for unbiased testing. The high level of dexterity and sensation of human hands, namely, is likely to influence the test results when the gripper would be attached to the hand or hand-held. Also, the prosthesis simulator makes sure that both grippers are attached to the arm in exactly the same manner. Thirdly, the robot arm resembles the human arm in terms of force-feedback. When the gripper on the robot comes into contact with the environment, namely, the force is fed back to the operator due to a F/T sensor in the wrist of the robot arm.

Significantly higher test scores can be expected for the prosthesis simulator compared to the robot arm. Using the prosthesis simulator, the gripper is moved through space using the human arm. A human is very skilled in manipulating his or her arm. Due to proprioception, the human has an internal model of where the hand is located at all times, allowing for fast control and manipulation of the hand, or in this case, gripper. Controlling the robot arm, however, is much less intuitive. The exact position of the robot arm must be checked using visual inspection, because the human brain can not generate a natural model of the exact robot arm position as for the human arm. Therefore, significantly higher task completion times can be expected when testing with the robot. Another difference can be found in the DOFs of the arms. The human arm naturally has seven DOF, three in the shoulder, one in the elbow, one in the forearm and two in the wrist. When using the prosthesis simulator, the gripper is attached to the forearm, eliminating the DOFs of the wrist. Also, the pro-and supination of the forearm is constrained. Therefore, the DOFs of the arm with the prosthesis simulator is limited to four. The robot arm has seven DOFs as well, which are identical to those of a human arm. Comparing the two arms, it can be found that the amount of DOFs is significantly lower for the prosthesis simulator than for the robot arm. The limited amount of DOFs using the prosthesis simulator resulted

in awkward positioning of the gripper for certain tasks of the SHAP. It can be expected that the robot arm is less limited in positioning the gripper in the orientations required. This could be beneficial for scores of some of the SHAP tasks. Due to the named differences, it is important to note that absolute scores for the presented tests obtained in following studies, using the robot arm, can not directly be compared to the results of this study.

The prosthesis simulator was used for the EIT, modified SHAP and SHAP. The prosthesis simulator was not needed for the AHAP. The protocol of the AHAP only requires grasping and rotation of the hand, so the control of the arm is not important. In this study, the AHAP was executed by holding and rotating the gripper by hand.

Subject

The three tests were performed by one subject, being the author. The choice for limiting the study to one subject was made to reduce the influence of the operator on the comparative scoring, as also described in literature [43–45]. By limiting the amount of subjects to one, as much as possible variables between testing the RPG and 4FH are kept identical. Therefore, the scores obtained highlight the differences in functional performance of the two gripper designs, without being influenced by inter-subject variations. Another benefit of using one subject, is that the grippers can be assessed with more repetitions over a span of more days, than would be practical and ethical with a group of subjects.

The subject had no experience in using a prosthesis or prosthesis simulator. The subject is male, aged 23, and is right handed. The dominant hand was chosen for all assessments, as the subject is most experienced in manipulating that arm. Differences between scores due to awkward arm movement is therefore likely to be reduced.

Protocol

Scoring of the modified SHAP is completely based on task completion times. Consequently, the scores are dependent on skill in performing the tasks and manipulating the gripper. Therefore, a learning curve was expected to appear in the modified SHAP results, when performing the test multiple times. For reliable and reproducible results, the learning curve should be flattened. For generating unbiased, reliable scores for the modified SHAP, a test planning was set up. The test planning is presented in Table IV. The initial planning consisted of four days of testing, with 24 test runs in total. When needed, extra test days could be added. Each day, both grippers were tested three times, in an alternating fashion. The gripper tested first was alternated as well each day, starting with the RPG. The alternating fashion was applied to eliminate the potential bias caused by changes in time, such as fatigue, boredom, or the changing level of skill. A 45 minute break was taken in between each test run, again to limit bias caused by fatigue and boredom. A full run of the modified SHAP took approximately 20 minutes, so a test day took approximately 6 hours. After the twelve tests for both grippers, the results were evaluated, to look at whether the LIFPP and W-LIF scores showed a flattened learning curve. This was the case, so no extra days of testing were needed. As final outcomes of the modified SHAP and SHAP, the mean of the results of the last three trials was taken.

TABLE IV: Planning for performing the modified SHAP, with a break of 45 minutes between each test

Day	Day 1						Day 2						Day 3						Day 4					
Test	1	2	3	4	5	6	1	2	3	4	5	6	1	2	3	4	5	6	1	2	3	4	5	6
RPG	•		•		•			•		•		•	•		•		•			•		•		•
4FH		•		•		•	•		•		•			•		•		•	•		•		•	

For each task of the modified SHAP and SHAP, the grippers started in fully open position. Before each task, the thumb of the 4FH was put in the desired mode. During the test runs, reasonably often an error was made in pressing the timer unit, due to which the correct task completion time was not recorded. In these cases, the task was redone, as well as in cases where other avoidable errors were made which heavily influenced the completion time.

Scoring of the EIT and AHAP both are not influenced by the level of skill. They are just based on the ability to perform certain tasks, disregarding time. Therefore, one run of the EIT and AHAP was regarded sufficient to generate reliable and unbiased scores.

Expectation

Before testing, it was expected that the 4FH would pass the EIT. Furthermore, the design of the 4FH was expected to allow for generating a significantly more robust grasp. This expectation can also be seen in the Harris profile, where the 4FH scores +2 and the RPG -2 for grasp stability. Consequently, it was expected that the 4FH would score significantly higher on the modified AHAP. For the modified and original SHAP it was expected that the scores would show learning curves, settling after a certain amount of trials. Considering the modified SHAP, a higher score was expected for the 4FH than for the RPG, but with less difference than for the AHAP. The SHAP namely mostly focuses on the speed of performing tasks and picking up certain shapes, of which most are not too complex. It was expected that the RPG could perform these simpler tasks as well without much problems.

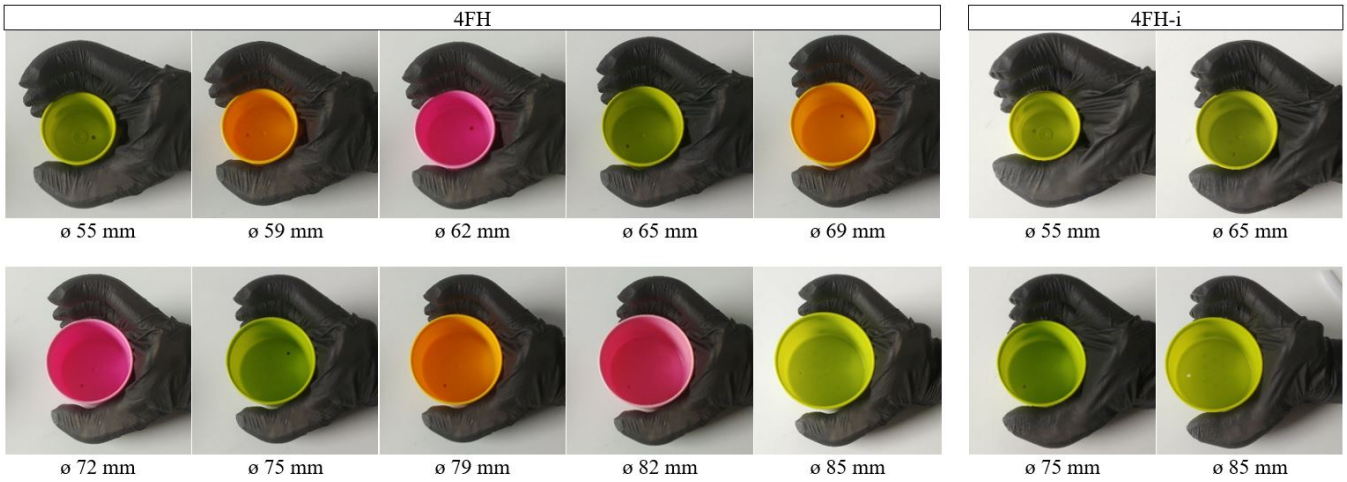

FIG. 22: Left: 4FH grasping cylindrical objects of various diameters. A gap can be seen between the distal phalanx and the larger objects. Right: Improved version of the 4FH, the 4FH-i, grasping the same range of cylindrical objects.

2.4. Potential improvement

The 4FH performed well during the testing procedure. Still, a design aspect was identified which could potentially be improved. It was identified that the fingers of the 4FH nicely form enclose around cylindrical objects with relatively small diameters. On the other hand, the shape conformity decreases for cylindrical objects with larger diameters. The difference is mainly visible when looking at the contact point(s) between the object and the thumb in the left side of Figure 22. For the smaller diameters, two contact points exist on the thumb, namely on the distal and proximal phalanx. For larger diameters, a gap exists between the thumb tip and the object. The larger the diameter gets, the larger the gap becomes. This means that on the thumb side, the larger cylindrical object is only supported by one contact point close to the palm of the hand. When approaching the problem in 2D, from the plane of the pictures, it can be seen that always at least two contact points exist on the index finger side of the gripper, namely on the finger tip and somewhere on the proximal phalanx. For form enclosing the object, at least three contact points are needed, such that the contact points cover more than half a circle. In other words, the minimal total angular distance between the contact points needs to be more than 180° for form enclosing. Evaluating the left side of Figure 22, it can be seen that for the largest presented items the contact points lay in one half of a the circle, so with a minimal angular distance of less than 180°. Therefore, form enclosing is not achieved for the largest cylindrical items. It could be argued that the object could be moved towards the thumb tip, such that two contact points are generated on the thumb. This would mean, however, that on the finger side the amount of contact points is reduced to one, viewing the 2D-scenario. Furthermore, the new set of three contact points would still not cover more than 180° for the largest item. Therefore, in both scenario's, the grasp stability for larger cylindrical objects is at risk.

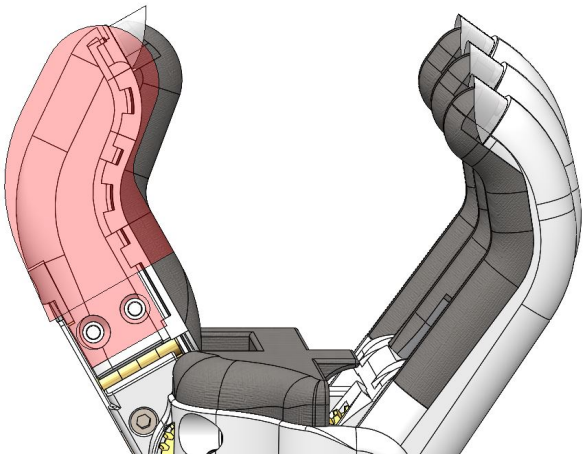

FIG. 23: Improved thumb design for the 4FH-i, compared to the shape of the original thumb of the 4FH (red)

The issue could be solved by modifying the ratio between the proximal and distal phalanx of the thumb, such that the gap between the thumb tip and the largest cylindrical objects is removed. This could mean, however, that a gap is introduced between the proximal pha-

FIG. 24: Final physical prototype of the 4FH-i, without glove

FIG. 25: Final physical prototype of the 4FH-i, with the glove fitted

lanx of the thumb and the smaller cylindrical objects. Further evaluation was needed to determine whether the modification could be an improvement. For this, the 2D-scenario of the gripper fingers in the plane of Figure 22 was considered. For smaller cylindrical objects, a gap between the proximal phalanx of the thumb and the object would still result in a form enclosed object, due to two or more contact points on the finger side and one on the thumb side, covering more than 180°. Therefore, the grasp stability for smaller cylindrical objects could be assumed to remain sufficient. Furthermore, in general, larger objects have a higher mass. Consequently, a higher level of grasp stability is desired for larger items than for smaller items. Following this reasoning, it was assumable that the gripper design would be improved by modifying the ratio between the proximal and distal phalanx of the thumb.

The improved thumb design in comparison to the original thumb design can be viewed in Figure 23. The shape of the original thumb is presented in red. The proximal phalanx was shortened by 6 mm. The distal phalanx was elongated such that the length of the thumb, between the tip and the axis of rotation at the base, was kept equal. From now on, the version of the 4FH with the improved thumb design is called the 4FH-improved (4FH-i). The right side of Figure 22 shows the 4FH-i grasping the same range of cylindrical objects, to allow for comparison.

The 4FH-i was assessed with the same assessments and in the same manner as described for the RPG and 4FH. Only the test planning differed. Furthermore, less test runs were needed for the 4FH-i. Experience in performing the tasks with the prosthesis simulator was already gained while assessing the RPG and 4FH. Therefore, the learning curve was flattened in less runs.

Expectation
The 4FH-i was expected to have improved grasp stability. Therefore, a higher score for the modified AHAP was expected, relative to the 4FH. For the modified SHAP, little or no significant improvement in score was expected, as this assessment does not directly assess grasp stability.

3. RESULTS

After building the 4FH and 4FH-i, they were subjected to the functional performance tests described in

Section 2.3.1. Also, general and mechanical properties were measured. Pictures of the final physical prototype of the 4FH-i can be found in Figure 24 and Figure 25. The 4FH looks the same, only with a small difference in the shape of the thumb.

3.1. General and mechanical properties

An overview of the specifications of the 4FH-i is presented in Table V. The specifications of the RPG are added as well, to allow for comparison. The specifications of the 4FH are almost identical those of the 4FH-i, so these values are not added to the table. The measured volume includes all components of the gripper. The volumes are presented for the grippers including and excluding the holders for the camera's. The mass is the mass of the complete gripper as how it would be used on the gripper. So the mass includes all components, and the mass of the 4FH-i also includes the glove. The maximum achievable pinch force was not measured, as this would damage the gripper. Instead, it was tested whether the gripper was able to achieve a pinch force higher than the required 30 N. The pinch force was measured using a hydraulic pinch force meter. The 4FH-i was able to pinch 35 N, without being damaged. The RPG damaged while trying to pinch 30 N. A teeth of the 3D-printed transmission broke off. The stroke width is the minimum distance measured between the the tips of the fingers. Please note that the gripper stroke of the 4FH-i can be slightly altered, by modifying the defined open position in the Arduino code. The mechanical maximum stroke width of the 4FH-i is 103 mm. The repeatability of opening and closing the gripper is defined as the distance the tip of the finger can be moved due to play in the system. The closing time is defined as the minimum time between fully open and fully closed position. Please note that this value can be slightly altered as well, by modifying the defined open position. A smaller stroke width results in a shorter closing time. The closing time presented in the table is related to the stroke width in the table.

3.2. Closed loop control

The closed loop control with the use of the force sensor, as described in Section 2.2, was tried out. First, the pinch force meter was positioned between the tips of the fingers, and the 4FH-i was closed. Then, the pinch force meter was positioned between the base of the fingers, and the gripper was closed again. The measured force applied on the pinch force meter was similar for both conditions.

TABLE V: General and mechanical specifications of the RPG and 4FH-i

	RPG	**4FH-i**
Volume closed	90x72x154 mm^3	105x115x194 mm^3
Volume open	165x72x152 mm^3	154x110x188 mm^3
Volume closed without holder	90x69x154 mm^3	95x90x194 mm^3
Volume open without holder	165x69x152 mm^3	154x90x188 mm^3
Mass	372 g	496 g
Pinch force	<30 N	>35 N
Stroke width	98 mm	92 mm
Repeatability	2 mm	3 mm
Closing time	0.7 s	0.69 s

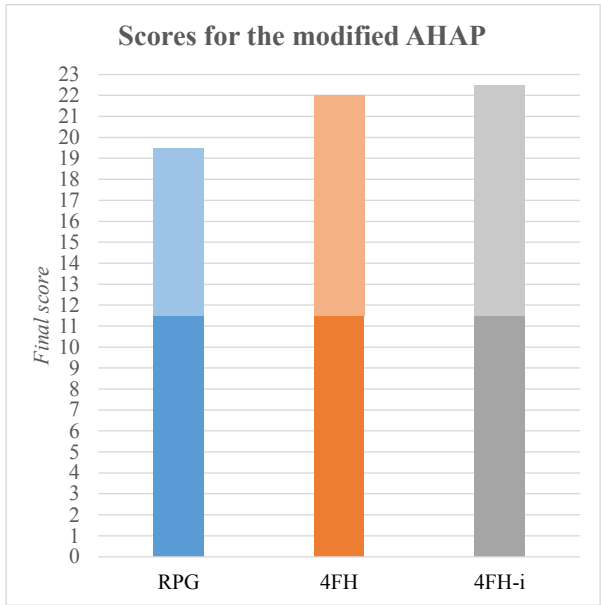

FIG. 26: Scores obtained for the modified AHAP by the three gripper designs. The lower halves of the bars represent the contribution to the scores for not dropping items. The upper halves represent the contribution for not showing relative motion.

3.3. Functional performance

EIT

The EIT was performed with the RPG, 4FH and 4FH-i, according to the description in Section 2.3.1. All grippers were able pick up each item from the list, both from ground level and from table height. Consequently, all grippers passed the EIT.

Modified AHAP

The three gripper designs were assessed using the modified AHAP as well. The test results are presented

in Figure 26. The maximum achievable score is 23 points, one point for each of the 23 items. None of the items were dropped during the test procedure, for any of the three grippers. This means that each each gripper scored 11.5 points for not dropping any items. These points are visualised in the bottom of the stacked bar plot in Figure 26. While assessing the RPG, relative motion between the object and gripper was seen for seven objects. For the 4FH, two objects showed relative movement, and for the 4FH-i one. Consequently, 8, 10.5 and 11 points were scored by the RPG, 4FH and 4FH-i respectively for the movement part. These scores are presented in the top of the bar plot in Figure 26. Only the skillet could not be rotated by any of the grippers without showing relative motion. Both the RPG and 4FH failed to prevent relative motion for the coffee can. The RPG additionally failed on this point for the skilled lid, plate, pitcher base, cracker box and power drill. An overview of the scores achieved for each item in tabular form can be found in Appendix K 1.

Modified SHAP

Outcomes of the modified SHAP consist of seven sub-scores, and one overall score. The sub-scores are named LIFPP, the overall score is named W-LIF. The LIFPP scores obtained by the RPG, 4FH and 4FH-i are presented in Figure 27a. The W-LIF scores for each gripper are presented in Figure 27b. Figure 27c and 27d show zoomed in versions of Figure 27a and 27b, to make differences between the scores and the uncertainties more visible. In Figure 27c and 27d, the significance of the results is presented as well. A result was regarded significant, when the p-value was smaller than 0.05. Insignificant p-values are written in orange. Appendix J shows how the uncertainties and statistical significance were determined. Regarding the W-LIF, the RPG scored 89.58 ± 0.25, the 4FH 92.33 ± 0.18 and the 4FH-i 92.47 ± 0.26. In Appendix K 2, the exact values of the overall score, sub-scores and scores for each individual task can be found. Also, graphs of the sub-scores and overall scores versus the test trial can be found.

SHAP

The SHAP was performed by the RPG and 4FH-i. As the SHAP is not a direct measure of the functional performance of the grippers, only the overall scores are presented here. The RPG achieved a W-LIF of 80.02 ± 0.20. The 4FH-i achieved a score of 85.34 ± 0.19. Diagrams showing all outcomes of the SHAP can be found in Appendix K 3. Additionally, tables with the exact outcomes can be found here.

4. DISCUSSION

4.1. Evaluation requirements

Below, an evaluation is presented whether each requirement was achieved. A tabular overview of which requirements were achieved is presented in Appendix L. The complete list of requirements set to the gripper is presented in Appendix B. The evaluation names the 4FH, but does also apply to the 4FH-i.

Overall requirements

The costs of the 4FH stayed well below budget. The total amount spend for the gripper was approximately €600, but the real cost of the gripper is much lower. For example, bolts and nuts were bought in bulk, while only few bolts and nuts are finally used in the gripper. Furthermore, the dimensions of the gripper are within the allowed ranges, although it can be noted that the total length of the gripper is close to the predefined maximum of 200 mm. The total mass of the 4FH is lower than the required maximum, but also here can be noted that the difference is very small.

Mechanical requirements

The 4FH was shown to be able to produce a pinch force higher than the 30 N required. The 4FH was also able to pick up items of 2 kg, tested with a grocery bag containing a weight of 2 kg. Due to the compliant material positioned at the hand-object contact points, objects will not damage easily. The contact area is spread out over at least 2 cm^2, assuming a pinch grip with 1 cm^2 per finger. The gripper stroke width between the tips of the fingers is 7 mm more than the required minimum. The requirement set to repeatability, however, was not achieved. A maximum of 1 mm was defined, but the tip op the fingers can be moved for approximately 3 mm, due to play. The play is mainly caused by space between the bearings and the driving shafts. Regarding robustness, the gripper was able to perform the complete testing procedure without breaking, as required. The time between fully open and fully closed position is 0.69 s, which is 0.08 s less than the required maximum.

Functional requirements

The 4FH was able to perform the complete EIT, and therefore it passed the test. For the modified SHAP, it was required that the 4FH would achieve a higher overall score than the RPG. The 4FH did indeed outperform the RPG, with a difference of approximately 3%. The 4FH also outperformed the RPG on the modified AHAP, as required, with a difference of 13%. The 4FH-i achieved a 15% higher score than the RPG.

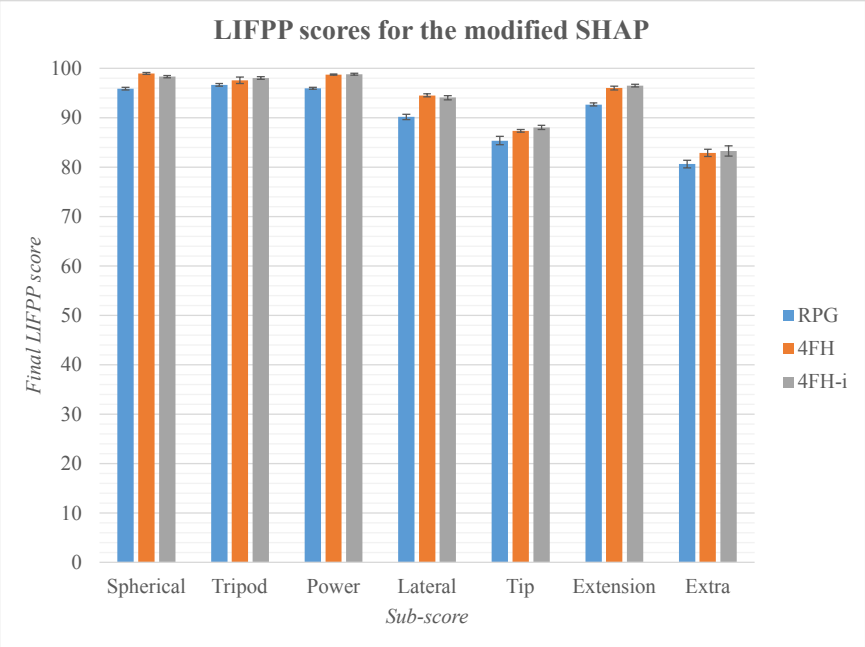

((a)) Sub-scores obtained for the modified SHAP

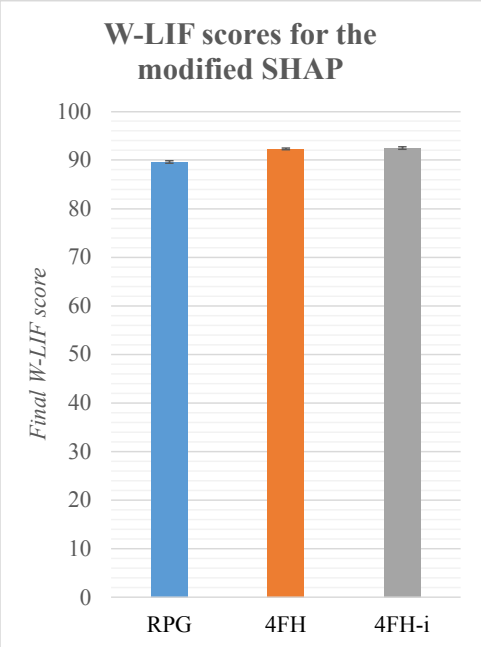

((b)) Overall scores obtained for the modified SHAP

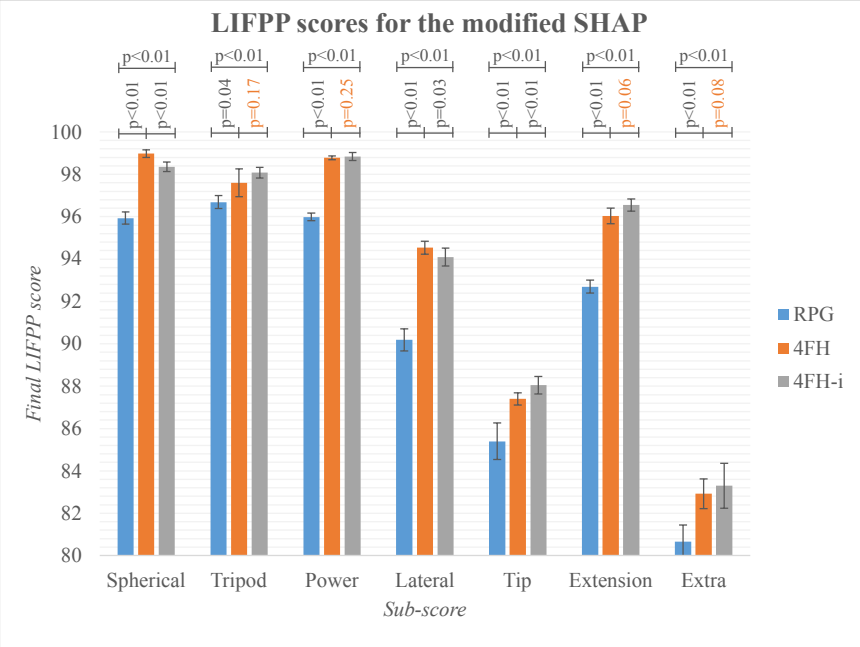

((c)) Zoomed in presentation of the sub-scores, including significance

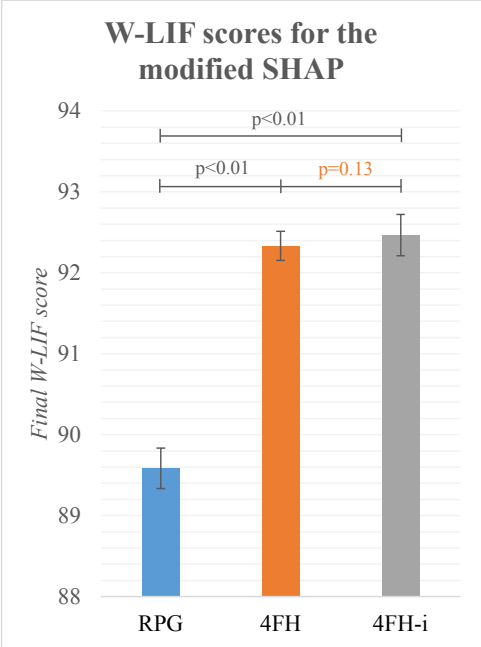

((d)) Zoomed in presentation of the overall scores, including significance

FIG. 27: Outcomes achieved by each of the grippers for the modified SHAP. The significance of the results is presented in Figure c and d. Insignificant relative results ($p>0.05$) are written in orange. The error bars show the standard deviation of the results.

Actuation and control requirements
The 4FH is powered with a power supply of 12 V, fulfilling the requirement. Simplicity of the control system was achieved using a servo as actuator, and limiting the amount of actuators and sensors to one. As required, a force sensor is integrated in the design, to allow for force feedback. Furthermore, the actuation mechanism did not overheat during the complete testing procedure.

Safety requirements
The outer surface of the 4FH was designed such that it does not have sharp points or edges. Furthermore, the nails on top of the fingers have low stiffness. Therefore, the risk of harming people is minimised. The wrist of the 4FH is specifically designed for high heat dissipation, making sure that the gripper does not reach temperatures which could harm people. During the complete testing procedure, the temperature of the gripper did not come close to the maximum allowed temperature.

Build up and casing requirements
The manufacturing of the 4FH was done in more than one week, as the design and 3D-printer settings needed several iterations. When the parts can be printed correctly at once, it is expected that the manufacturing time is shorter than a week, as required. Not much maintenance or replacement of parts was done. It is expected that each part can be replaced within one hour, when all needed parts are readily available. Only replacement of the palm of the gripper is expected to take longer. The palm, namely, is the basis of the gripper, to which almost all components are connected. Furthermore, all functional components are contained inside the gripper, and there are no exposed electrical wires. Only for testing the gripper with the prosthesis simulator, external electrical wires were needed. A holder for a camera is integrated in the design, of which the orientation can be adjusted, to allow for visual inspection during grasping tasks. The gripper is water resistant due to the disposable glove. Also, there is no possibility of dirt accumulation or corrosion, as required. For hygiene, the glove can be replaced after each use. In terms of looks, the 4FH resembles a human hand to a certain degree, but differences make sure that the gripper does not enter the uncanny valley. Therefore, it is expected that the gripper will not be frightening to clients.

Interfacing requirements
A bayonet-fitting is integrated in the gripper design, for mounting the gripper on the care-robot. The fitting is bolted to the rest of the gripper, to allow for simple interface change, as required.

To summarize, it can be concluded that only one of the 32 requirements was not achieved. The requirement that was not achieved, was the requirement for the repeatability of opening and closing the gripper.

4.2. Interpretation of results

Testing closed loop control
The outcome of testing the closed loop control was that the same force was applied on an object for pinching with the tip of the fingers and grasping between the base of the fingers. With the open loop control, without using the force sensor, a certain amount of torque would be applied on the driving shafts. When pinching with the tip of the fingers, the torque would have a much larger moment arm than for grasping with the base of the fingers. This would mean that a much lower force would be applied on the object for pinching, compared to gripping close to the palm. The fact that this was not the case for the closed loop control proves the concept of measuring grasp force and using this for controlling the gripper. It can be concluded that the design of the 4FH and 4FH-i allow for force feedback.

EIT
The outcome of the EIT is limited to pass or fail. The EIT was designed to create a baseline for a gripper in development, to check whether it has potential for application on the care-robot. When one of the objects could not be picked up, the gripper would fail the test. In this case, it should be concluded that the gripper design is not useful yet. Further iteration would be needed to improve the gripper. The RPG, 4FH and 4FH-i, however, each passed the EIT. From this can be concluded that each of the gripper designs at least show potential for application on the care-robot. Of course, for the RPG this was already established, as this gripper was the gripper previously used on the care-robot.

Modified AHAP
None of the 23 objects were dropped, but several objects showed relative movement with respect to the grippers. The objects that could not be stably held with the RPG were the skillet lid, plate, pitcher base, cracker box, coffee can, power drill and skillet. According to the AHAP protocol, the skillet lid and pitcher base are related to the hook grasp type, the plate and cracker box to the extension grip, the coffee can and power drill to the cylindrical grip, and the skillet to the diagonal volar grip. It can be

noted that for the hook grasp type, two of the two items could not be stably grasped. For the extension grip and cylindrical grip this is two out of three, and for the diagonal volar grip one out of three.

From this, several conclusions were drawn. The RPG is not suitable for stably grasping items with a handle, as it failed all items of the hook grasp. Furthermore, the RPG has difficulty to stably hold larger items with flat surfaces, being related to the extension grip. The chocolate box, however, could be stably held, and is also related to the extension grip. The chocolate box is the smallest and lightest object of the three. The reason this object did not show relative movement, is that the object could be grasped close to the centre of gravity, due to its smaller size. Therefore, the weight could only generate little torque. For the cylindrical objects, again the lightest and smallest of the three could be stably held, and the more heavy or larger ones not. From this can be concluded that the RPG cannot generate much torque between the fingers for cylindrical items as well, to cancel out torque generated by weight and distance to the centre of gravity. Regarding the diagonal volar grip, no direct conclusions could be drawn. Only one object could not be stably held, being the skillet. The skillet is a difficult item to stably hold. The skillet needs to be grasped at the handle, meaning that all weight is on one side of the gripper. This creates high amounts of torque while rotating the gripper, which should be counteracted by torques generated by the gripper. The RPG was not able to do so. The other two items related to the diagonal volar grip, however, did not impose any problems.

The two items showing relative movement with respect to the 4FH were the coffee can and the skillet. The coffee can is the cylindrical object with the largest diameter of the set. As described in Section 2.2.4, the 4FH has issues grasping cylindrical items with large diameters. For these items, a gap exists between the object and the thumb tip, due to which the object can not be form enclosed. This was the cause for the unstable grasp of the coffee can. As described above, stably holding the skillet is a difficult task. Therefore, it is not surprising or worrying that the 4FH is not able to stably hold this object.

For the 4FH-i, only the skillet showed relative movement. As described for the 4FH, this is not surprising or worrying. It can be noted that the 4FH-i is able to stably grasp the coffee can. Therefore, it can be concluded that the improvement of the thumb indeed improved the grasp stability of the gripper for larger cylindrical items. Furthermore, no other objects showed relative movement, so the improvement was not disadvantageous for stably grasping other types of objects.

Overall, it can be concluded that the 4FH and 4FH-i can generate significantly higher grasp stability than the RPG. This conclusion was also what was expected in the Harris Profile. The increase in grasp stability is thought to be mainly caused by the compliant material, finger shape and by having more than two fingers. Having three fingers on one side significantly increases the potential moment arm of the friction forces in the contact points. This is useful for generating counteracting torques against rotation of the grasped object. The compliant material increases shape conformity, due to which contact areas are spread out. This also increases potential moment arms to counteract rotation. Furthermore, the curved shape of the fingers of the 4FH and 4FH-i allow for form enclosing objects, improving grasp stability. The fingers of the RPG can only pinch, and do not provide the ability to form enclose.

Modified SHAP

The overall score and all sub-scores obtained with the RPG are lower than those obtained with the 4FH and 4FH-i, all with significant difference. The sub-score with clearly the largest significance in difference is the LIFPP for the power grip, with a z-score of 31.3 and 24.2 for the 4FH and 4FH-i respectively. The difference in outcome for the power grip is not surprising. In the Harris Profile, a score of +2 was assigned to the 4FH for power grasp patterns, while a score of -1 was assigned to the RPG. The LIFPP for the power grip is based on performance on five tasks. Three of the tasks showed little difference for the three grippers. The difference of the LIFPP is mainly caused by the task of using a door handle. The lower performance on this task by the RPG can be related to the low performance of the RPG on performing a hook grasp in the modified AHAP. The hook grasp is the common method to operate a door handle. The RPG is less suitable in performing the hook grasp than the 4FH and 4FH-i. The 4FH and 4FH-i, namely, have curved fingers ideal for performing the hook grip, while the RPG has straight finger tips. The difference in LIFPP for the power grip is also caused by a difference in performance of picking and placing a full jar. The difference can be explained as follows. The jar is of significant weight, as it is filled with water. Therefore, a stable grasp is needed to correctly perform the task. For the RPG, more care is needed for stably grasping objects than for the 4FH and 4FH-i, due to the lower grasp stability. The care needed increases the completion time.

Another LIFPP score showing a large significant difference between the RPG and the 4FH and 4FH-i is the LIFPP for the spherical grip. This LIFPP consists of three tasks. A clear difference can only be found in the completion time of one of the tasks, being carton pouring. The lower performance on this task by the RPG can be explained again by looking at results of the mod-

ified AHAP. It was concluded that the 4FH and 4FH-i are more suitable for stably grasping large items with flat surfaces, for which a human would apply an extension grip. A drink carton is such an item. Therefore, as for the filled jar, more care was needed to confirm stable grasping with the RPG, which costs time.

The three LIFPP scores with lowest significant difference were the scores related to the prehensile patterns tripod, tip and extension. These prehensile patterns are the precision grasp patterns. Less difference between the RPG and 4FH on these patterns was also expected. In the Harris Profile, namely, only one point difference was assigned between the performance on precision grasp patterns for the RPG and 4FH.

Very little differences were found between the scores of the 4FH and 4FH-i. The difference in W-LIF is insignificant, as is the case for four of the seven LIFPP. The difference in the LIFPP for the lateral grip also shows low significance, having a p-value of 0.03. The differences in the spherical and tip LIFPP are hard to explain. No significant differences would be expected, as the improvement is aimed only at increasing grasp stability for cylindrical items with larger diameters. In the modified SHAP, no such items are present. The difference in LIFPP for the tip might be explained by the fact that the gripper stroke is slightly reduced for the 4FH-i, as the thumb shape has changed. All objects related to the tip grip are thin, so in these tasks the gripper must be almost completely closed from open position. The slight reduction in stroke width results in a slight reduction of closing time, which could cause the slight decrease in completion times for the 4FH-i compared to the 4FH.

To summarise, the same conclusion can be drawn as for the modified AHAP. The increased grasp stability of the 4FH and 4FH-i relatively to the RPG can be concluded to cause the higher functional performance of the 4FH and 4FH-i. For the modified SHAP, no improved functional performance was found for the 4FH-i with respect to the 4FH.

SHAP

The original SHAP was not a direct measure of functional performance of grippers for care-robots. Therefore, for this study no conclusions can be drawn based on the scores obtained on this test. But in contrast to the other tests, the obtained scores can be compared to scores presented in literature, as the SHAP is a validated and well known test. Various papers present scores obtained with prostheses, using a prosthesis simulator. In 2016, Belter et al. assessed three body-powered prostheses using a prosthesis simulator [46]. The prostheses under test had 11, 1 and 2 DOFs. The overall scores achieved by the prostheses was 64.1, 64.8 and 65.0 respectively. In 2011, Kyberd presented SHAP outcomes for three single DOF myoelectric prostheses, tested using a prosthesis simulator [28]. The SHAP was performed with different control settings of the prostheses. In total, eight overall scores were obtained. The scores ranged between 81 and 94. In 2017, Kyberd assessed three myoelectric multi DOF and a myoelectric single DOF prosthesis with a prosthesis simulator [33]. The overall scores of the multi DOF prostheses were 83, 81 and 89. The single DOF prosthesis scored 94.

With an achieved SHAP score of 80 and 85 for the RPG and 4FH-i respectively, it can be concluded that both grippers have functional performance comparable to prostheses presented in literature. But note that it is hard to directly compare the outcomes. The control method of the grippers of this study differs from the control of the prostheses. In this study, the grippers were controlled by turning a button with the hand not under test. Some tasks, however, allow or require the use of an assisting hand. Therefore, for some tasks the hand not under test needed to switch between controlling the gripper and assisting in the task. This naturally costs time, which presumably has negatively influenced the results. On the other hand, controlling the gripper with a button is assumably easier than myoelectric or body-powered control. This potentially has influenced the results positively. Furthermore, it needs to be kept in mind that the alternative scoring method was used for generating the scores. Literature states that a three point difference with a standard deviation of three was found comparing both scoring methods.

Overall functional performance testing

When looking at all the results, one of the first things that can be noted is that only high scores were obtained. For the modified AHAP, the lowest score is 84.8% of the maximum obtainable score. In case of the modified SHAP, the lowest overall score is even 89.7% of the maximum. Before testing, a larger difference in scores was expected between the RPG and 4FH and 4FH-i. But when evaluating the results, it can be concluded that the RPG has high functional performance as well. Here can be noted that the RPG is already the result of six years of development, while the 4FH and 4FH-i are first prototypes. In the six years, various design iterations were made to improve the gripper. Amongst others, the actuator was improved, nails were added and friction pads were applied on the inside of the fingers. In 2016, the SHAP was performed by the company with an early version of the RPG without all the improvements. For this version, an overall SHAP score of 39 was achieved. When comparing this to the SHAP score achieved in the current study, it can be

concluded that the functional performance of the RPG has been improved significantly. Again, please note that the difference in control method and score computation could account for part of the difference in scores.

4.3. Strengths and limitations

A limitation of this study can be found in the set assessments. Validated methods were modified to fit the application of the gripper, as no relevant validated tests are presented in literature. This means that the reliability and validity of the modified SHAP and modified AHAP have not yet been verified. Another limitation is that the normative completion times for the added tasks of the SHAP can not be assumed free of bias. The normative completion times, namely, are generated by two subjects only. This study, however, mainly aims at evaluating relative scores, so the limitations in the assessments do not directly impose a problem to this study.

Strengths of this study can be found in the presentation of various design considerations to be made for a versatile robotic gripper for a care-robot. Many design choices, where applicable, are backed up by literature. Another strength is the newly developed set of assessments. The set is specifically aimed at measuring functional performance of versatile robotic grippers, in particular for care-robots. The set of assessments could fill the gap identified in literature, regarding functional assessments for versatile grippers.

4.4. Risk analysis

For safety, the gripper may not interfere with other devices, or be influenced by other devices. The Federal Communications Commission (FCC) has designed limits to protect against harmful interference between devices. The only electrical component in the gripper is the actuator. The actuator has been tested and found to comply with the norms set to such devices, according to part 15 of the FCC Rules [47].

The 4FH and 4FH-i have been designed such that they do not contain sharp points or edges, and do not reach harmful temperatures. Nevertheless, the possibility to accidentally harm clients is still existent. This could happen when the gripper accidentally bumps into a human, or makes an error and grasps a human. Both scenario's need to be avoided. When designing the control of the robot arm, attention must be directed to make sure that the robot will not touch people. A safety stop might be applied in case the robot arm is coming too close to a human. Ethically seen, a human should always be responsible for the actions of the robot.

4.5. Recommendations and future work

Considering the mechanical design of the gripper, several recommendations can be made. Evaluating the set of requirements indicated that one requirement was not achieved, namely the required repeatability due to play in the system. The play is mainly the result of play between the driving shafts and the bearings. Play in the transmission also adds to the issue. It is recommended to further look into the transmission and bearings to reduce play and achieve the requirement.

When industrialising the design, it is recommended to look at durability. The material or thickness of the nails might need to be reconsidered. The nails allow for high functional performance, but do not have high durability. During the complete test procedure, the nail of the thumb needed replacement twice, and the nail of the index finger thrice. The glove needed replacement twice during the complete test procedure. For disposable gloves, this durability could be considered high enough. Furthermore, considerable wear down occurs in the slots for the bi-stability of the thumb, due to movements of the pin. The slot did not need to be replaced during the test procedure, but wear down is visible. Therefore it is recommended to reconsider the manufacturing method and material for the slots. Durability would also be increased when threading would be applied directly in parts which are secured to driving shafts via set screws. In the current design, brass inserts in the 3D-printed material were used for the set screws. The inserts, however, can be pushed out of the material when considerable force is applied, for example due to considerable actuator force or weight of a grasped object. As a result of this, play is introduced between the driving shaft and the set screw, resulting in play of the fingers. Therefore, it is recommended to reconsider the material and manufacturing method of parts needing to be fastened to the driving shafts. The current material and manufacturing method, PLA and FFF, are not suitable for threading.

Application of a servo was mainly chosen for control simplicity. In later projects on this gripper, this requirement might be dropped, now the first prototype has been developed. In this case, a rotary electric motor could be chosen to replace the servo. Control design will become more complex, but there are also several advantages. Firstly, application of a rotary electric motor is likely to reduce weight and space. Furthermore, the motor can still be combined with worm gears, but with significantly lower gear ratio. An electric motor, namely,

generates a much higher angular velocity than a servo. Worm gears with significantly lower gear ratio have three advantages. The low gear ratio improves self-locking behaviour, and thus even less power is needed to maintain grip during a grasping cycle. Also, worm gears with low gear ratio have higher commercial availability and cost less. Lastly, the size of the worm gears can be reduced compared to the gears applied currently.

The 4FH and 4FH-i are only 6 mm shorter than the maximum as allowed in the requirements. Although the requirement has been achieved, a shorter gripper is assumably beneficial for the range of motion and for application in environments with little space. In the current design, approximately 30 mm of the 194 mm is needed for the interfacing with the robot, being the bayonet fitting. It is recommendable to look at possibilities to reduce the space needed for the interfacing. As discussed previously, application of an electric motor and worm gears with low ratio could result in a shorter gripper as well.

When using 3D-printing for a following version of the 4FH-i, the infill of the parts could be designed according to the force fields. This way, the weight of the gripper can be reduced while not compromising strength. Potential improvement due to a higher level of shape-adaptivity might be evaluated as well. To this end, a non-rigid or under-actuated thumb could be evaluated.

The assessment set designed in this study could be widely used as standard test method for grippers for care-robots, but only after future work. To this end, a study is required to validate and check reliability of the EIT, modified SHAP and modified AHAP. Also, reliable and non-biased normative completion times for the extra tasks of the modified SHAP need to be generated.

The gripper should be tested in an actual care environment in future studies. This way, the applicability for the care environment can be assessed, in terms of hygiene, safety and functionality. Also, acceptance of the gripper by the clients should be tested. This can be done by asking the the opinion of the clients on the gripper design.

Future work is also needed for designing the gripper control. This project should aim at creating a robust and easy to use control method, compatible with the robot. The control method should include controlling the force applied on objects, by integrating the force sensor. The use of a master gripper with haptic force-feedback is recommendable. Lowering torque for maintaining grasp after grasping should also be implemented, to lower power consumption and generated heat. During the control design, societal and ethical aspects must be kept in mind, to guarantee safe interaction with humans.

5. CONCLUSION

The goal of this study was to design, develop and assess a versatile gripper for a care-robot. The gripper designed in this study is the 4FH. An improved version was developed as well, called the 4FH-i. The 4FH and 4FH-i have four fingers, three on one side and a thumb on the opposite side. The fingers are rigid and can rotate only around the base of the finger. The thumb can also rotate sideways, such that the thumb tip can oppose the tip of the index or middle finger. This allows for two grasping modes, namely a pinch mode and a power grip mode. The middle finger is connected to its driving shaft with a spring. Consequently, the grippers have one actuated DOF and two non-actuated DOFs. The 4FH and 4FH-i are very similar, only the shape of the thumb is different.

The 4FH and 4FH-i were designed to fit the requirements for application in a care environment. Disposable gloves are fitted around the complete gripper. A used glove can be replaced for a clean glove to ensure hygiene. The grippers have no sharp points on the outer surfaces, do not reach unsafe temperatures and have no exposed electrical wires. Furthermore, the grippers have resemblances with a human hand, but stay far from the uncanny valley, so the aesthetics presumably do to not frighten the clients. In this study, however, the grippers have not been assessed in a care environment. Utility and suitability of the gripper in real world applications needs to be evaluated in future studies.

A set of assessments was drawn up for measuring the functional performance of a gripper for a care-robot, as was part of the goal. The set consists of the EIT, modified SHAP and modified AHAP. The EIT was designed in this study as a baseline test, to see whether the minimum required performance of a gripper for a care-robot could be achieved. The modified SHAP is a slight modification of the well-known SHAP. The modification was done in this study to make the SHAP representative for applications of a care-robot, instead of for a human. The AHAP, presented in 2019, was also slightly modified in this study, resulting in the modified AHAP. The modified AHAP is a measure of grasp stability. The modified AHAP does not measure the level of anthropomorphism, as is the case for the original AHAP.

As required, the 4FH and 4FH-i scored higher on functional performance than the gripper previously used on the robot, named the RPG. The 4FH and 4FH-i both passed the EIT. Regarding the modified SHAP, both grippers outperformed the RPG by approximately 3% on the overall score. The difference in score between the 4FH and 4FH-i was insignificant. The RPG was also outperformed on the modified AHAP. The 4FH scored 13% higher than the RPG, the 4FH-i 15%.

The higher scores on the set of assessments indicate higher functional performance of the 4FH and 4FH-i compared to the RPG. The set of assessments, namely, was designed as a direct measure of functional performance, representative for the application of the care-robot. An increase in grasp stability was assumably the main cause for the improved scores.

---

[1] Intermediair. Personeelstekorten in de zorg blijven oplopen. https://www.intermediair.nl/werk-en-carriere/beroepskeuze/personeelstekorten-in-de-zorg-blijven-oplopen\\-utrechtzorg?referrer=https\%3A\%2F\%2Fwww.google.com\%2F. Accessed: 13-7-2021.

[2] CBS. Arbeidsmarkt zorg en welzijn. https://www.cbs.nl/nl-nl/dossier/arbeidsmarkt-zorg-en-welzijn. Accessed: 13-7-2021.

[3] NOS. Ser slaat alarm: groot personeelstekort in de zorg dreigt. https://nos.nl/artikel/2337769-ser-slaat-alarm-groot-personeelstekort\\-in-de-zorg-dreigt. Accessed: 13-7-2021.

[4] EMTG. De oplossing voor het tekort aan zorgprofessionals (zorgpersoneel). https://www.skipr.nl/partnernieuws/de-oplossing-voor-het-tekort-aan-zorgprofession\\als-zorgpersoneel/. Accessed: 13-7-2021.

[5] P. Shubha and M. Meenakshi. Design and implementation of healthcare assistive robot. pages 61–65, 2019. cited By 2.

[6] PAL Robotics. Create your own tiago robot. https://pal-robotics.com/robots/tiago/#tiago-configurator. Accessed: 13-7-2021.

[7] A. Milojević, S. Linß, Z. Ćojbašić, and H. Handroos. A novel simple, adaptive, and versatile soft-robotic compliant two-finger gripper with an inherently gentle touch. *Journal of Mechanisms and Robotics*, 13(1), 2021. cited By 0.

[8] A. Mo, H. Fu, C. Luo, and W. Zhang. Concentric rotation pin array gripper for universal grasp. pages 112–117, 2019. cited By 1.

[9] Yang Liu and Hongnian Yu. A survey of underactuated mechanical systems. *Control Theory & Applications, IET*, 7:921–935, 05 2013.

[10] A.V. Sureshbabu, G. Metta, and A. Parmiggiani. A systematic approach to evaluating and benchmarking robotic hands-the ffp index. *Robotics*, 8(1), 2019. cited By 3.

[11] J.T. Belter and A.M. Dollar. Performance characteristics of anthropomorphic prosthetic hands. 2011. cited By 88.

[12] C.M. Light and P.H. Chappell. Development of a lightweight and adaptable multiple-axis hand prosthesis. *Medical Engineering and Physics*, 22(10):679–684, 2000. cited By 138.

[13] R. Vinet, Y. Lozac'h, N. Beaudry, and G. Drouin. Design methodology for a multifunctional hand prosthesis. *Journal of Rehabilitation Research and Development*, 32(4):316–324, 1995. cited By 59.

[14] A.D. Keller. *Studies to Determine the Functional Requirements for Hand and Arm Prosthesis*. Department of Engineering University of California, 1947.

[15] G. Smit, D.H. Plettenburg, and F.C.T. Van Der Helm. The lightweight delft cylinder hand: First multi-articulating hand that meets the basic user requirements. *IEEE Transactions on Neural Systems and Rehabilitation Engineering*, 23(3):431–440, 2015. cited By 25.

[16] E. Neha, M. Suhaib, and S. Mukherjee. Design issues in multi-finger robotic hands: An overview. *Lecture Notes in Mechanical Engineering*, pages 335–343, 2019. cited By 1.

[17] D. Che and W. Zhang. A dexterous and self-adaptive humanoid robot hand: Gcua hand. *International Journal of Humanoid Robotics*, 8(1):73–86, 2011. cited By 18.

[18] D.K. Kumar, B. Jelfs, X. Sui, and S.P. Arjunan. Prosthetic hand control: A multidisciplinary review to identify strengths, shortcomings, and the future. *Biomedical Signal Processing and Control*, 53, 2019. cited By 8.

[19] Industry association for standardizing information and communication systems. Safety of electronic equipment (ecma-287). *ECMA international*, ed. 2, 2002.

[20] P. Breedveld, J.L. Herder, and T. Tomiyama. Teaching creativity in mechanical design. In s.n., editor, *Diversity and Unity. Proceedings of IASDR2011*, pages 1–10. s.n., 2011. Diversity and Unity. Proceedings of IASDR2011, the 4th World Conference on Design Research ; Conference date: 31-10-2011 Through 04-11-2011.

[21] J.S. Cuellar, G. Smit, P. Breedveld, A.A. Zadpoor, and D. Plettenburg. Functional evaluation of a non-assembly 3d-printed hand prosthesis. *Proceedings of the Institution of Mechanical Engineers, Part H: Journal of Engineering in Medicine*, 233(11):1122–1131, 2019. cited By 3.

[22] Joseph T. Belter, Bo C. Reynolds, and A. Dollar. Grasp and force based taxonomy of split-hook prosthetic terminal devices. *2014 36th Annual International Conference of the IEEE Engineering in Medicine and Biology Society*, pages 6613–6618, 2014.

[23] Solomon's Metalen B.V. Silver steel data-sheet. https://salomons-metalen.nl/datasheets/SILVER_STEEL.pdf. Accessed: 19-3-2021.

[24] CV Protection. Materials of disposable gloves. https://cvprotection.com/materials-of-disposable-gloves-13/, 2014. Accessed: 26-3-2021.

[25] Immaculada Llop-Harillo, Antonio Pérez-González, Julia Starke, and Tamim Asfour. The anthropomorphic hand assessment protocol (ahap). *Robotics and Autonomous Systems*, 121:103259, 2019.

[26] R. Lewis, C. Menardi, A. Yoxall, and J. Langley. Finger friction: Grip and opening packaging. *Wear*,

263(7):1124–1132, 2007. 16th International Conference on Wear of Materials.

[27] P.J. Kyberd, A. Murgia, M. Gasson, T. Tjerks, C. Metcalf, P.H. Chappell, K. Warwick, S.E.M. Lawson, and T. Barnhill. Case studies to demonstrate the range of applications of the southampton hand assessment procedure. *British Journal of Occupational Therapy*, 72(5):212–218, 2009. cited By 58.

[28] P.J. Kyberd. The influence of control format and hand design in single axis myoelectric hands: Assessment of functionality of prosthetic hands using the southampton hand assessment procedure. *Prosthetics and Orthotics International*, 35(3):285–293, 2011. cited By 23.

[29] M. Saliba, A. Chetcuti, and M. Farrugia. Towards the rationalization of anthropomorphic robot hand design: Extracting knowledge from constrained human manual dexterity testing. *Int. J. Humanoid Robotics*, 10, 2013.

[30] S.R. Kashef, S. Amini, and A. Akbarzadeh. Robotic hand: A review on linkage-driven finger mechanisms of prosthetic hands and evaluation of the performance criteria. *Mechanism and Machine Theory*, 145, 2020. cited By 10.

[31] Philippe Gorce and Jean Guy Fontaine. Design methodology approach for flexible grippers. *Journal of Intelligent and Robotic Systems: Theory and Applications*, 15(3):307–328, 1996. cited By 19.

[32] N. Wang, K. Lao, and X. Zhang. Design of an anthropomorphic prosthetic hand with emg control. *Lecture Notes in Computer Science (including subseries Lecture Notes in Artificial Intelligence and Lecture Notes in Bioinformatics)*, 8917:300–308, 2014. cited By 0.

[33] P.J. Kyberd. Assessment of functionality of multifunction prosthetic hands. *Journal of Prosthetics and Orthotics*, 29(3):103–111, 2017. cited By 4.

[34] I. Llop-Harillo and A. Pérez-González. System for the experimental evaluation of anthropomorphic hands. application to a new 3d-printed prosthetic hand prototype. *International Biomechanics*, 4(2):50–59, 2017. cited By 7.

[35] Buryanov Alexander and Viktor Kotiuk. Proportions of hand segments. *International Journal of Morphology*, 28:755–758, 09 2010.

[36] J. Antonio Travieso-Rodriguez, Ramon Jerez-Mesa, Jordi Llumà, Oriol Traver-Ramos, Giovanni Gomez-Gras, and Joan Josep Roa Rovira. Mechanical properties of 3d-printing polylactic acid parts subjected to bending stress and fatigue testing. *Materials*, 12(23), 2019.

[37] I. Llop-Harillo, A. Pérez-González, and J. Andrés-Esperanza. Grasping ability and motion synergies in affordable tendon-driven prosthetic hands controlled by able-bodied subjects. *Frontiers in Neurorobotics*, 14, 2020. cited By 0.

[38] Interlink Electronics. FSR UX 400 Series. `https://www.interlinkelectronics.com/fsr-ux-400`. Accessed: 2021-06-02.

[39] I. Llop-Harillo, A. Pérez-González, and V. Gracia-Ibáñez. Anthropomorphism index of mobility for artificial hands. *Applied Bionics and Biomechanics*, 2019, 2019. cited By 1.

[40] C.M. Light, P.H. Chappell, and P.J. Kyberd. Establishing a standardized clinical assessment tool of pathologic and prosthetic hand function: Normative data, reliability, and validity. *Archives of Physical Medicine and Rehabilitation*, 83(6):776–783, 2002. cited By 198.

[41] J.G.M. Burgerhof, E. Vasluian, P.U. Dijkstra, R.M. Bongers, and C.K. van der Sluis. The southampton hand assessment procedure revisited: A transparent linear scoring system, applied to data of experienced prosthetic users. *Journal of Hand Therapy*, 30(1):49–57, 2017. cited By 5.

[42] M. Sinke. The delft pro simulator: An accessible and 3d-printable prosthesis simulator to simulate transradial limb absence. `http://resolver.tudelft.nl/uuid:cc7f1123-f246-40fd-b9aa-4c8be8fc8b29`, 2021.

[43] P.J. Kyberd. The influence of control format and hand design in single axis myoelectric hands: Assessment of functionality of prosthetic hands using the southampton hand assessment procedure. *Prosthetics and Orthotics International*, 35(3):285–293, 2011. cited By 24.

[44] P.J. Kyberd. Assessment of functionality of multifunction prosthetic hands. *Journal of Prosthetics and Orthotics*, 29(3):103–111, 2017. cited By 4.

[45] D. Latour and T. Passero. Assessment of functionality of multifunction prosthetic hands. *Journal of Prosthetics and Orthotics*, 31(3):165–166, 2019. cited By 0.

[46] J.T. Belter, M.T. Leddy, K.D. Gemmell, and A.M. Dollar. Comparative clinical evaluation of the yale multigrasp hand. volume 2016-July, pages 528–535, 2016. cited By 9.

[47] Robotis. Dynamixel xm430-w350 e-manual. `https://emanual.robotis.com/docs/en/dxl/x/xm430-w350/`. Accessed: 18-5-2021.

[48] H. van der Kooij, B. Koopman, and F.C.T. van der Helm. *Human Motion Control*. Delft University and Twente University, 2008.

[49] E.N. Marieb and K. Hoehn. *Human Anatomy and Physiology*. Pearson Education, San Fransisco, 8th edition, 2010.

[50] D.M. Ştefănescu and M.A. Anghel. Electrical methods for force measurement-a brief survey. *Measurement: Journal of the International Measurement Confederation*, 46(2):949–959, 2013. cited By 21.

[51] T. Nilsen, M. Hermann, C. Eriksen, H. Dagfinrud, P. Mowinckel, and I. Kjeken. Grip force and pinch grip in an adult population: Reference values and factors associated with grip force. *Scandinavian journal of occupational therapy*, 19:288–96, 02 2011.

[52] P.J. Kyberd, A. Clawson, and B. Jones. The use of underactuation in prosthetic grasping. *Mechanical Sciences*, 2(1):27–32, 2011. cited By 9.

[53] P. Breedveld. Lecture notes in bio-inspired design (me41095): Bioclamping – friction & biological grasping, October 2019.

[54] Framo Morat. Worm gear sets. `https://framo-morat.com/wp-content/uploads/Worm_gear_sets_en.pdf#23`. Accessed: 15-3-2021.

[55] A.F. Mills and C.F.M. Coimbra. *Basic Heat and Mass Transfer*. Temporal Publishing, 8 edition, 2015.

[56] Interlink Electronics. Fsr 408 data sheet. `https://cdn.sparkfun.com/datasheets/Sensors/Pressure/FSR408-Layout2.pdf`. Accessed: 15-7-2021.

[57] Berk Calli, Aaron Walsman, Arjun Singh, Siddhartha Srinivasa, Pieter Abbeel, and Aaron M. Dollar. Benchmarking in manipulation research: Using the yale-cmu-berkeley object and model set. *IEEE Robotics Automation Magazine*, 22(3):36–52, 2015.

Appendices

Appendix A:
Literature search for requirements

For setting up requirements for the Rose gripper, a small literature search was conducted. The literature search consisted of two parts. One part was done aiming at requirements set to upper limb prostheses, and the other part was done for finding requirements set to robotic grippers. Both searches were conducted by the author in January 2021, using the Scopus electronic database.

The search plan aimed at requirements for prostheses is presented in Table VI. Using this search plan, 126 papers were found by Scopus. Upon evaluation, a total of 19 papers contained useful information on the subject.

In order to find requirements set to robot grippers, the search plan shown in Table VII is used. As this initially resulted in many search results, the search was limited to the subject area Engineering. Finally, a total of 207 document results were presented by Scopus. Of the document results, 12 papers containing useful requirements were identified.

TABLE VI: Search plan used for finding requirements set to upper limb prostheses in literature

Concept 1: Requirements	**Concept 2: Prosthesis**
Requirement*	Upper-limb prosthe* Prosthe* hand

TABLE VII: Search plan used for finding requirements set to versatile robotic grippers in literature

Concept 1: Requirements	**Concept 2: Gripper**	**Concept 3: Design**
Requirement*	Robot* gripper Robot* hand Artificial hand	Design*

Appendix B: Requirements list

A list of requirements was drawn up to guide the design process of the gripper, shown in Table VIII.

TABLE VIII: Detailed list of all design requirements

Criteria	Description	Metric	Notes
R1	**Overall**		
R1.1	Cost of the gripper	Max: $8.000,-	*
R1.2	Volume of the gripper while closed	Max: 15x15x20 cm^3	**
R1.3	Mass of the gripper needs to be lower than current gripper	Max: 500 g	[11–13] **
R2	**Mechanical**		
R2.1	Grip and pinch force		
R2.1.1	Sufficient pinch force for enabling a broad range of activities	Min: 30 N	[14, 15] ***
R2.1.2	Able to pick up items with significant weight	Min: 2 kg	**
R2.1.3	The force at the contact points must be distributed over a sufficient area to avoid damaging objects	Min: 2 cm^2	*,**
R2.2	Gripper stroke width at the tip of the gripper	Min: 85 mm	**
R2.3	Repeatability of opening and closing the gripper	Max: 1 mm	*
R2.4	Sufficient robustness to complete the functional and mechanical testing procedure without being damaged	Pass/fail	
R2.5	Time between fully open and fully closed gripper position	Max: 0.7 s±10%	[11] *
R3	**Functional**		
R3.1	Able to pick up essential items, namely a pill box, credit card, keys, wallet, cloth, mug, plastic bottle, TV-remote and bowl from different heights: floor level and table height	Pass/fail	**
R3.2	Able to perform a self-modified version of the SHAP, specifically designed for applications of robot Rose, with an overall score higher than the RPG	Pass/fail	See Appendix I
R3.3	Able to perform a self-modified version of the AHAP, with an overall score higher than the RPG	Pass/fail	See Appendix I
R4	**Actuation and control**		
R4.1	Electrically powered, with a power supply of 12 V or 24 V	12 V or 24 V	****
R4.2	Simplicity of the control system	Pass/fail	
R4.3	Application of force sensor(s) to allow for force feedback	Pass/fail	Appendix D
R4.4	The actuation mechanism may not overheat	Max: 80° C	*****
R5	**Safety**		
R5.1	No sharp points or edges on the outer surface of the gripper	Pass/fail	
R5.2	Outer surface of the fingers and palm of the gripper may not exceed temperatures safe for continuously holding	Max: 43° C	Ref: ECMA
R5.3	Outer surface of the gripper, except the fingers and palm, may not exceed temperatures safe to touch for short periods (up to 10 s)	Max metallic: 55° C Max non-metallic: 65° C	Ref: ECMA
R6	**Build up and casing**		
R6.1	Short manufacturing time	Max: 1 w	
R6.2	Short time needed for maintenance and replacement of parts	Max: 1 h	
R6.3	Modular design		
R6.3.1	All functional components contained inside the gripper	Pass/fail	****
R6.3.2	No exposed electrical wires	Pass/fail	
R6.3.3	Integrate camera on the gripper for visual inspection	Pass/fail	*
R6.4	Function in wet and dirty conditions		
R6.4.1	Water resistant	Pass/fail	
R6.4.2	No possibility for dirt accumulation	Pass/fail	
R6.4.3	Corrosion resistant materials for outer surface of the gripper	Pass/fail	
R6.5	Allow for disinfection after each use	Pass/fail	
R6.6	Pleasant aesthetic, which will not frighten clients	Pass/fail	
R7	**Interfacing**		
R7.1	Bayonet-fitting for mounting the gripper on the robot arm	Pass/fail	****
R7.2	Bayonet-fitting bolted to the gripper, to allow for simple interface change for application on a different robot	Pass/fail	****

* Requirements by the company developing care-robot Rose

** Required to perform tasks and grasp objects, found relevant for robot Rose. Low weight is needed to have sufficient remaining payload of the robot arm for the tasks and objects

*** Highest pinch force named for tasks relevant to robot Rose, which is for lifting a book horizontally

**** Needed for compatibility with robot Rose

***** Specification of the specific actuator used in the gripper design

Appendix C:
Preceding literature study

Methods to assess and compare the functional performance of upper limb prostheses: A review

Fabian Matthias Verhage
TU Delft
(Dated: February 19, 2021)

Quantitative, reliable and validated assessments for measuring functional performance of upper limb prostheses are scarce, and no consensus exists in which assessment to use. Results of such tests are, however, essential for research and development of prostheses, to be able to make well-founded and objective conclusions regarding the prosthesis design. The goal of this study was to review existing tests to quantitatively assess and compare the functional performance of below elbow prostheses. A systematic search of the Scopus electronic database was conducted by the author. A total of 16 assessments were identified in literature. Only four of the identified assessments were concluded to be recommendable for functional performance testing in the prosthetic field, namely the Southampton Hand Assessment Procedure, the Anthropomorphic Hand Assessment Protocol, the Activities Measure for Upper Limb Amputees, and the Capacity Assessment of Prosthetic Performance for the Upper Limb. The first two named assessments are also suggested for application to robotic hands.

1. INTRODUCTION

For the research and development of upper limb prostheses, it is crucial to have reliable and valid quantified results of their performance. Only then, different designs can be objectively compared, benchmarking can be done, and well-founded conclusions can be drawn regarding design considerations and potential improvements [1, 2]. This is the basis for technological advancement. Not only for research and development, but also on the end of application, performance-based information regarding upper limb prostheses is essential [3]. Clinicians need reliable information to be able to objectively inform patients, and make evidence-based decisions on what prosthesis to prescribe [4].

There is, however, no consensus in what assessment to use for measuring performance of upper limb prostheses [3]. Numerous methods have been used, of which many are not validated for the field of prostheses, or mainly focus on the satisfaction of the user instead of performance of the prosthesis [5]. Many other assessments are very specific, only testing one area of performance, which makes it hard to draw conclusions about the performance of the complete prosthesis. Often, these specific tasks are used in combination with other tasks to cover the complete performance area, which results in long assessment sessions, a larger burden on the patient and less insightful results on overall performance [6–8]. Reliable assessment methods validated for testing and comparing different upper limb prosthesis designs for improving the performance of state of the art artificial hands are scarce [1]. The same problem is identified in the field of artificial hands applied to robotics [2]. No standard set of tests exists for holistic analysis and benchmarking of robotic hands [9].

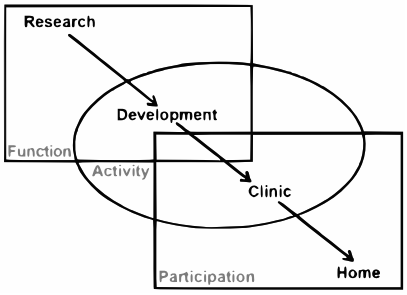

FIG. 1: International Classification of Functioning domains of prosthesis testing (grey) within the development cycle of prostheses (black) [8]

The goal of this study is to review existing methods for quantitative assessing and comparing of functional performance of below elbow prostheses. The methods do not necessarily need to be reliable or validated for the prosthetic field to be included in this review. The applicability of the identified methods to robotic hands will be discussed.

Three types of prosthetic assessments can be identified, based on the World Health Organization's International Classification of Functioning, Disability and Health (WHO-ICF) model, visualised in figure 1 [8]. This model was used by the Upper Limb Prosthetic Outcome Measures (ULPOM) group in 2009 to create a standard-

ised set of tests for assessing function for upper limb prostheses. The three types of assessments can be distinguished by the area in which they assess. The three area's are the function, activity and participation domain. The function domain involves the performance of the prosthesis, such as grasping and releasing. The activity domain is related to performing practical tasks based on Activities of Daily Living (ADLs). The participation domain consists of measuring the impact of the prosthesis in real-life situations, such as daily life at home, usually assessed using self-report.

As visualised in figure 1, each WHO-ICF domain covers two area's in the development cycle of prostheses. In this review, the focus is set on methods testing in the function and activity domain, as they are related to the research and development part of prostheses. The participation domain focuses mainly on the personal experiences and opinions of prosthetic users, and therefore does not provide useful insight and quantified results on prosthetic performance for research and development. Also assessments specifically designed for paediatric population are disregarded. These methods focus mainly on the performance of the children, which provides little usable information on the prosthetic performance itself.

Except for experimental testing methods, also various analytical methods are developed and used for assessing artificial hands [9–13]. For example, artificial hands can be assessed by computing their finger workspace and comparing this to the workspace of human fingers, or by simulated grasping with the prosthesis design in computer programs and evaluate contact properties. Such analytical approaches are, however, limited in providing reliable outcomes. Essential aspects for the performance of the artificial hand, such as friction and contact rigidity, are challenging to realistically integrate in an analytical model [1]. Therefore, in this study it is chosen to disregard analytical approaches.

Many assessments for measuring the mechanical performance of artificial hands are developed and applied as well [14–19]. Multiple mechanical properties of artificial hands, such as grip force and opening and closing speed, contribute to some extent to their functional performance. Numerical values for such properties, however, do not provide direct information on functionality. For example, slower artificial hands do not necessarily score lower on time-based functional tests [20]. Following this reasoning, it can be argued that experimental assessments of function provide more insight in functional performance than mechanical tests. Therefore, also mechanical assessment methods are not considered in this study.

In this study, the existing set of experimental quantitative assessments in the WHO-ICF function and activity domain for upper limb below elbow prostheses will be reviewed.

TABLE I: Search plan defined and applied for conducting the systematic literature search

Concept 1: Test	**Concept 2: Function**	**Concept 3: Prosthesis**	**Concept 4: Upper limb**
Test*	Function*	Prosthe*	Upper limb*
Benchmark*	Performance*	Artificial hand*	Hand
Assess*	Metric*		Hook*
	Grasp*		Upper extremit*
			Below elbow
			Gripper*

2. LITERATURE SEARCH METHOD

The review is based on a systematic search of the Scopus electronic database, conducted in November 2020 by the author. The defined goal for this study was divided in four concepts: "test", "function", "prosthesis" and "upper limb". These concepts, in combination with related terms to each concept, were used to create an initial search plan. A fifth concept, "review", was added to find relevant review papers for this study, in order to get a clear overview of the topic. Based on the review papers and inspection of the type of search results, the initial search plan was refined. The refined search plan is presented in table I.

In the search query, each row of the search plan is coupled using the OR operator, and each column is coupled using the AND operator. Upon inspection of the search results, it was noted that the term "hand" included irrelevant results, caused by papers containing "on the other hand" or "by hand". Therefore, these two terms are excluded from the search term "hand", using the AND NOT operator. A document search using the refined search plan presented over 2600 results. Based on evaluation of the results, the document search was limited to the three subject area's Engineering, Medicine and Health Professions, which resulted in approximately 2300 hits.

Like the initial search plan, the refined search plan was fitted with a fifth concept for finding review papers. The search resulted in five relevant review papers. After evaluating these, each seemingly relevant paper named in the references was noted.

A list of exclusion terms, for using with the AND NOT operator, was defined to refine the search results. Each exclusion term was carefully evaluated, by checking the relevancy of the papers that would be excluded by its use. If the term in question excluded papers on relevant subjects, or relevant papers noted from the review papers,

the exclusion term was disregarded. The final set of exclusion terms, including the topics they exclude from the results, is presented in table II. In the search query, the exclusion terms are combined with the OR operator.

The final version of the search query, including the refined search plan and exclusion terms, resulted in a set of 356 papers. Each of these results was individually checked for relevancy, based on the title and abstract. Finally, 53 papers from the list of search results were identified as potentially relevant for this study. An additional set of 10 relevant papers was found in the references of the relevant search results.

TABLE II: List of terms for excluding irrelevant papers, used with the AND NOT operator

Term	Excluded topics
Cod AND NOT Codevelop*	Encoding, decoding, auto-encoder (but not excluding papers using the term "codevelopment")
Recogni*	Recognising patterns and signals e.g. myoelectric signals
Algorithm*	Developing algorithms
Learn*	Deep learning, machine learning The effect of learning on using prostheses
Virtual reality	Using virtual reality for training or testing
Train*	Effect of training on using prostheses
Stroke Paralys* Spinal* Cerebral palsy	Pathologies not requiring prostheses, such as stroke, paralysis, spinal cord injury and cerebral palsy. Also excluding spinal cord signal modelling and detecting
Foot Ankle* Knee* Leg* Gait* Lower limb* Lower extrem*	Related to lower-limb prostheses, or about both upper- and lower-limb
Orthop*edic	Deformities of bones and muscles: orthopaedic and orthopedic
Stimul*	Electric stimulation or haptic feedback using tactile stimulation
Identific*	Identifying signals e.g. myoelectric signals or real time EMG
Survey* Questionnaire*	Assessment methods using self-report
Surgery*	The field of surgery
Satisfaction	Level of satisfaction of prosthetic users
Arthr	Disease or surgery of the joints, e.g. arthritis, arthrosis and osteoarthritis
Brace* Exo*skelet*	The field of supporting a limb, instead of using an artificial limb.
Child*	Prostheses, assessments and treatments focusing specifically on children
Vascul	The field related to blood vessels

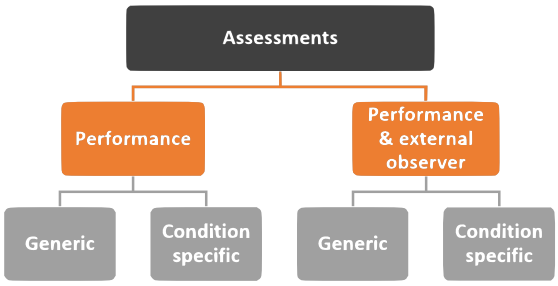

FIG. 2: Visualised structuring of the identified relevant assessments, using a tree structure

3. METHODS FOR TESTING THE FUNCTIONAL PERFORMANCE OF PROSTHESES

Various assessments, fitting the scope of this paper, were identified in literature. The assessments will be structured on basis of two characteristics: group focus and scoring.

The first characteristic concerns what group of subjects is targeted with the assessment. Three types of assessments can be distinguished: generic, population specific and patient specific [5]. The category of generic assessments involve tests which can be used not only in the prosthetic field, but also for human hands. Particularly in the early days of prosthesis testing, assessments developed for human hands were applied to prostheses. These tests also belong to the generic category. The category population specific assessments consists of the methods specifically developed for the prosthetic field. Patient specific assessments are methods which depend on the patient, so the exact assessment can be different for each individual patient. Such assessments are suitable for measuring individual progress of the patient in rehabilitation. The scope of this study involves objectively assessing and comparing functional performance of prostheses. Patient specific assessments are not useful for this goal, because scores of patient specific assessments can not be compared between patients as the exact assessment protocol varies. Therefore, the patient specific category is disregarded in this study.

The second characteristic, scoring, involves identifying what the score of the assessment is based on. The score can be based on the performance of the participant, evaluation of an external observer, self-report by the participant, or a combination of these [5]. Outcomes of self-reported assessments are generally considered more subjective than outcomes of the other two groups of assessments [21]. Generally, assessments in the performance domain of the WHO-ICF model are based on self-report.

No assessments focusing on the function and activity domain based on self-report have been found in literature. For these reasons, the self-report category will be disregarded. Furthermore, three assessments based on ratings of an external observer alone have been found in literature, namely the Assisting Hand Assessment (AHA), the University of New Brunswick (UNB) test and the Assessment of Capacity for Myoelectric Control (ACMC). These tests, however, do not fit the scope of this study, as the AHA and UNB test focus specifically on the paediatric population, and the ACMC is a patient specific measure. This means that no relevant assessments have been identified in the category external observer as well. Consequently, all assessments fitting the scope of this study can be structured in two categories: performance based methods on the one hand, and performance and external observer based methods on the other hand.

Structuring of the test methods is performed using a tree structure, visualised in figure 2. A total of 16 relevant assessments were found in literature, which are described in the following sections. None of the identified assessments fall under the second to left branch of the tree structure: performance based and condition specific methods.

3.1. Performance based

3.1.1. Generic

JTHF

The Jebson-Taylor Hand Function Test (JTHF) is aimed at measuring the functionality of a human hand using a set of seven tasks, representing ADLs [22]. The set consists of writing a simple sentence, page turning, eating using a teaspoon, stacking checkers, picking up small everyday items, such as paper clips, pennies and bottle caps, picking up a large lightweight object, represented by an empty can, and picking up a large heavy object, represented by a filled can of one pound.

The JTHF was standardized in 1969. In March 1986, the JTHF was chosen as the preferred measure for assessing hand dexterity by a panel of hand therapists. Therefore, it would be adopted as the classical hand function test [23].

The scoring system of the JTHF is completely time-based [5]. The time needed to perform each task is measured. A shorter time indicates better hand dexterity according to the JTHF. Each task may be completed in any amount of time.

Although originally developed and validated for assessing disability and rehabilitation progress related to the functionality of the hand, in 2009 the ULPOM group saw potential in using the JTHF also for assessing prostheses in the function domain [8]. However, validation for prosthetic users was still needed. Since then, the JTHF is used for testing the functionality of hand prostheses and for comparison of outcomes between several commonly used assessment methods and a new developed method. For example, this is the case for the development of CAPPFUL [3] and BAM-ULA [4].

FIG. 3: Test setup of the Nine Hole Peg Test [24]

Two modification are proposed for the JTHF by Resnik and Borgia (2012), as some tasks were assumed to be too hard for prosthetic users to complete, and the maximum duration of the test was too long for clinical use [5]. One change was to limit the allowed completion time of each task to 2 minutes, the other was to modify the scoring system. The modified scoring method is based on the amount of items completed per second, instead of the time to complete the full task. For example, the amount of words written in 2 minutes are counted, instead of measuring the time to write the 24-letter sentence. Testing reliability and validity showed, however, that this scoring method was not reliable for six of the seven tasks. No reasoning on the cause of this finding was presented. Only the page turning task showed reliability with the modified scoring method, but this task also showed a significant ceiling effect. Therefore, the modified scoring method is not recommended.

NHPT

The Nine-Hole Peg Test (NHPT) aims to assess manual dexterity, and more specifically finger dexterity [23, 24]. The test setup consists of a board with 9 holes positioned in a 3 by 3 array, and nine 32mm long pegs positioned in a concavity directly next to the holes, as shown in figure 3. The goal for the participant is to pick up all nine pegs from the concavity and place them into the nine holes. When all pegs are placed, the participant needs to remove the pegs from the holes and transfer them back to the concavity. Throughout the test procedure, the

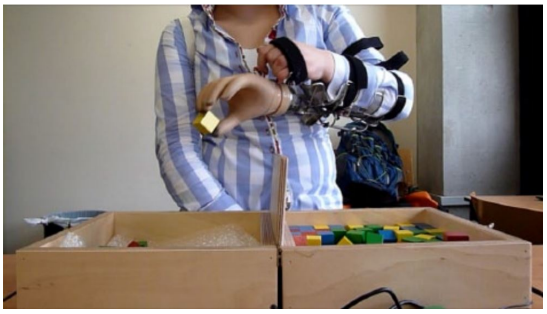

FIG. 4: Test setup of the Box and Blocks Test [24]

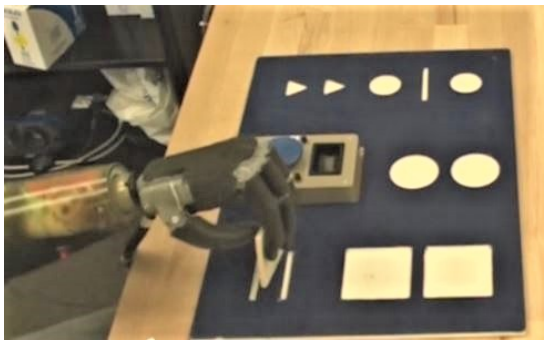

FIG. 5: The form board of the Southampton Hand Assessment Procedure, used for 12 abstract relocation tasks [28]

participant is free to choose in which order he fills and empties the holes, but the pegs must always be handled one by one.

The score of the test is equal to the amount of time needed per movement of the peg. If the test procedure was not completed in 90 seconds, the test is stopped. This means that the score is calculated by the completion time divided by the total of 18 movements, or by the 90 seconds divided by the amount of movements completed. Following from this method, a lower score is related to better performance.

Haverkate et al. (2014) used the NHPT for testing three different body-powered upper limb prostheses [24]. Testing yielded scores for the three prostheses with significant differences, showing that the NHPT is an useful assessment procedure for hand prostheses.

An advantage of the NHPT is the short duration of the test, which is 90 seconds or less. A disadvantage is that the test specifically aims at a part of the functionality of the hand, namely finger dexterity. This makes it difficult to draw conclusions about the functionality of the whole hand [23].

BBT

The original purpose of the Box and Blocks Test (BBT) was to assess gross dexterity of the hand for adults suffering from cerebral palsy [25]. But the test was used in a broader range of pathologies, and since 1985 normative data exists to which test results can be objectively compared [23].

The material needed for the test consists of 150 wooden cubes of 24mm and a box with an upright board in the middle, dividing the box in two. All blocks are positioned randomly in one side of the box, namely the side of the tested hand. A picture of the test setup is shown in figure 4. The goal for the participant is to transfer as many blocks as possible to the other side of the box in one minute, with as condition that the blocks are handled one by one [25].

The score of the test is equal to the amount of blocks successfully transferred from one side to the other [24]. Therefore, a higher score is related to better performance. In 2009, the ULPOM group selected the BBT as a testing method to consider for assessing upper limb prostheses in the function domain. For the BBT to be used eventually in prosthesis testing, a standard procedure still needed to be established for prosthetic users and reliability and validity needed to be retested for this standardization [8].

Various researchers have used the BBT since for assessing the functionality of below elbow prostheses [3, 24, 26, 27].

The BBT should be considered as a test for specific dexterity, like the NHPT, instead of a test for gross manual dexterity [23]. Compared to the NHPT, less fine motor skill, and thus less effort, is needed to perform the BBT [24].

SHAP

The Southampton Hand Assessment Procedure (SHAP) has been designed in 2002 to fill a gap in existing testing methods for measuring the functionality of the hand in patients with a pathology or prosthesis [29].

The gap was identified in 1999. As there was no consensus in how to measure functionality of natural and prosthetic hands, a new assessment was desired which should comply to 5 criteria. According to the criteria, the test must involve all prehensile patterns, should consist of reliable and valid sub-tests, should be scored objectively, should not be limited by current technology and should have a short duration and be low cost [23]. According to the developers, the SHAP complies to all criteria [29].

The SHAP consists of 26 tasks in total, 12 abstract tasks and 14 ADLs. The abstract tasks consists of transferring objects of six shapes, each executed in a light and heavy version, from one slot in the form board to the other. The form board can be seen in figure 5. Each

object shape is related to one of six prehensile patterns, namely the spherical, tripod, power, lateral, tip, and extension grip. The tasks based on ADLs consist of picking up coins, unbuttoning, cutting food, turning pages, opening a jar, pouring from a jug, pouring from a carton, pick up and place a heavy object, pick up and place a light object, lifting a tray, rotating a key, opening and closing a zipper, using a screwdriver and operating a door handle. The SHAP can be completed in 20 to 30 minutes [29].

Each task is timed by the participant himself, by pushing a button before and after the task. The scoring is completely based on the completion time. The SHAP presents a score for overall hand function (IOF), but also for the performance per grip type (IOFPP). The scores are normalized: a score of 100 indicates normal hand function. A lower score is related to lower functionality of the hand [29].

The SHAP was identified by the ULPOM group as a recommended assessment of prosthetic function, provided that the assessment would be validated for prosthetic use [8]. The same year, the developers of the SHAP published a paper which showed the wide range of capabilities of the SHAP [30]. Since then, the SHAP is a commonly used assessment to measure the functionality of upper limb prostheses [19, 20, 26–28, 31, 32].

The scoring method of SHAP is criticized, as the computation is not published [33]. Therefore, the equations can not be independently checked for errors, and the scores are more difficult to interpret for clinicians. Also the computation is non-linear and suspected to induce bias, as it is based on standard deviations of an earlier obtained set of results. Another disadvantage is that clinicians can not compute scores themselves and are forced to buy the expensive SHAP software license. For these reasons, alternative score computations are suggested by Burgerhof et al. (2017). With the new equations, the Linear Index of Function for the Prehensile Patterns (LIFPP) and its weighted version (W-LIF) are calculated, which replace the IOFPP and the IOF respectively. The modified indices have very high correlations with the original indices, although a difference of 3 points with a standard deviation of 3 is identified between the W-LIF and IOF score.

Various other generic assessments, originally aimed at human hand function, have been modified and applied to measure prosthetic hand function, without validating its use. For example, Agnew (1981) compared the functionality of a myo-electric and a split-hook prosthesis, using the Minnesota Rate of Manipulation Test (MRMT) and the Smith Test of Hand Function (STHF) [34].

The MRMT consists of 60 identical blocks and a form board with 4 rows and 15 columns. The complete test consists of five sub-tasks related to manipulating the blocks: placing in the slots, turning over, displacing, turning and placing with one hand and turning and placing with two hands [35]. Agnew modified the test, by using only 24 blocks and 6 columns of the form board, and limiting the test to only the sub-task placing [34]. The score obtained was equal to the completion time.

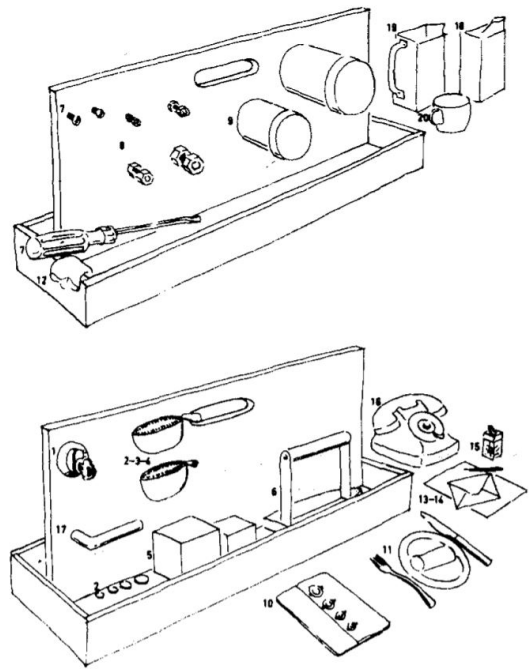

FIG. 6: Items for the Sollerman Hand Funtion Test, mounted in a box [37]

He also used a modified version of the STHF, which consists of three transferring tasks. The items to be picked and placed were nails, coins and three blocks of different sizes. The original STHF involved many more tasks, such as unbuttoning, loosening a belt and placing pegs in holes [36]. The scoring is based on the time needed to complete the tasks.

3.2. Performance and external observer based

3.2.1. Generic

SHFT

The Sollerman Hand Function Test (SHFT) was standardised in 1995, for evaluating the functionality of human hands [37]. The assessment consists of 20 ADLs, related to the seven most used grip types. The activities consist of using a key, picking and placing coins, using

a zipper, lifting wooden cubes and iron objects, using a screwdriver, picking up nuts, opening a jar, opening buttons, using a knife and fork, putting on stockings, writing, folding paper, using a paper-clip, lifting a telephone, turning a door-handle, and pouring water from a cup, jug and Pure-pak. For easy and quick application, all items required for the assessment are fitted in a box, visualised in figure 6. The maximum duration of the test is 20 minutes.

An external observer evaluates the performance on each task, and assigns a score ranging from 4 to 0 points. If the activity is successfully completed with the correct grip type and within 20 seconds, 4 points are awarded. In case the participant experiences difficulty while completing the task in 20 seconds, he earns 3 points. The same amount of points is assigned if 20 to 40 seconds are needed to complete the task, or when the used grip type is slightly different than prescribed. 2 points are given when the task completion takes 40 to 60 seconds, is completed with great difficulty or is performed with an incorrect grip type. If the task is only partially completed after 60 seconds, the participant scores 1 point. No points are earned if the participant can not perform the task at all. To obtain the overall score of the SHFT, the scores of the 20 tasks need to be added. The theoretical maximum score of 80 is related to the dominant hand function of a healthy person. Lower scores indicate worse functionality.

The SHFT has been named by the ULPOM group as a potentially useful assessment for prostheses in the function domain [8]. The test was, however, validated for assessing human hands, not for upper limb prostheses. Therefore, validation that the the assessment can reliably be applied in the prosthetic field as well was still needed [38]. Such validation work was not found in this literature study.

RCPRT

The Refined Clothespin Relocation Test (RCPRT) was presented in 2016 for measuring human and prosthetic hand function and compensatory movements [39]. The original version of the RCPRT, the Clothespin Relocation Test (CPRT), was based on the Rolyan Graded Pinch Exerciser, a training tool for upper limb rehabilitation.

The RCPRT is based on two tasks. Removing clothespins from a horizontal rod, and placing them on a vertical rod is the inside-out task of the assessment. The outside in task consists of placing back the clothespins on the horizontal rod. These tasks need to be performed with the hand under test. The test setup is shown in figure 7. The test is self-timed, by pressing a button before starting and after completing a task.

Compensatory movements are abnormal movements of limbs, caused by decreased achievable range of motion or strength. This decrease can be caused by impairment, amputation and sensation of pain. The use of compensatory movements can cause overuse injury, such as Repetitive Strain Injury (RSI). Identification of compensatory movements needs constrained movements to consider as normal.

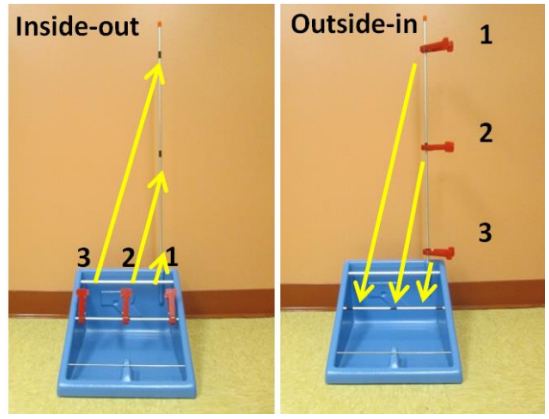

FIG. 7: Predefined order for performing the Refined Clothespin Relocation Test [39]

The major difference between the RCPRT and CPRT is that the RCPRT has a constrained assessment path as visualised in figure 7, to allow for evaluation of compensatory movement. The numbers in the figure represent the order of removing and placing the clothespins, the arrows represent the prescribed trajectories. Motion capture is used for tracking the participants movements. Participants are fitted with 26 reflective markers, which are tracked using 8 cameras.

A limitation of the RCPRT is that it can only be applied in clinics with access to the required motion capture technology. In 2019 the RCPRT was modified to ease clinical use [40]. The new version does not use motion capture, but applies a single video camera in the frontal plane instead. Only trunk lateral tilt and shoulder abduction are evaluated in the updated version. The remaining test protocol is identical to the original RCPRT.

An external observer scores the performance of the participant based on compensatory movements, using the recorded video. If excessive compensatory movement is used, the participant scores 1 point. In case the task is completed without any compensatory movements, 4 points are assigned. 2 or 3 points respectively are awarded if significant or little compensatory movements are present. This scoring system is applied to both tasks. For the inside-out task, the external observer evaluates trunk lateral tilt. For the outside-in task, the

score is based on shoulder abduction. The overall score can be calculated using the average completion time (t) of five trials and the average compensatory movement scores (S) of five trials. The equation for obtaining the score is shown below:

$$RCPRT - Score = \frac{S_{inside-out,avg} + S_{outside-in,avg}}{t_{inside-out,avg} + t_{outside-in,avg}}$$

The validity and reliability of the RCPRT for prosthetic function assessment is yet to be established by future study. The test is, however, used in 2019 for measuring prosthetic hand function [26]. In this study, significant correlation between RCPRT scores and SHAP and BBT scores was demonstrated.

ARAT

The Action Research Arm Test (ARAT) was aimed at assessing arm function after cortical damage, and in 2008 a standardized approach was presented which improved its reliability [41].

The ARAT uses 19 tasks related to the categories grasping, gripping, pinching and gross movements. The tasks related to the first category are grasping a ball, sharpening stone and blocks of various sizes. Tasks in the gripping category are pouring water, putting a washer over a bolt and displacing two tubes of different sizes. For the pinching category, six objects need to be pinched between thumb and one of the other fingers. Gross movement is evaluated using three activities, namely moving the hand to behind the head, above the head and to the mouth. All items required for performing the ARAT are fitted in a kit, which is shown in figure 8. The duration of the ARAT is approximately 5 to 15 minutes.

The 19 tasks are all scored from 0 to 3 by an external observer. Each task needs to be completed in 60 seconds. For movement equal to that of a healthy subject, 3 points are awarded. If the participant completes the task in more time than a healthy subject would need, 2 points are assigned. If the participant can only partially perform the task, or can not perform the task at all, the participant earns 1 or 0 points respectively. The overall score of the test can be obtained by adding the scores of each activity. Consequently, a maximum score of the 57 can be obtained. A lower score is related to a lower level of arm function.

Although the ARAT is originally developed for assessing human arm function, the test has been applied to assess prosthetic hand function as well [26]. The study showed significant correlation between ARAT scores and SHAP and BBT. No significant correlation was, however, found between ARAT scores and RCPRT. The study also showed floor effects, as completion times for the maximum score are rarely reached by prosthetic users. This could be due to the fact that the ARAT is originally not developed for prosthesis assessment.

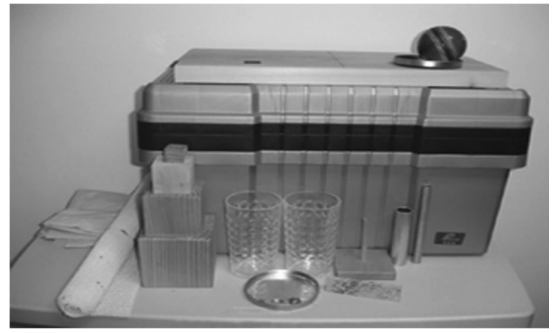

FIG. 8: Items of the kit used in the Action Research Arm Test [41]

3.2.2. Condition specific

KSCT

Kay (1970) developed a series of comparative tests for objectively testing the functionality of upper limb prostheses, using proposals given by Fishman (1970) [23]. This assessment will be referred to in this paper as Kay's Series of Comparative Tests (KSCT). The KSCT consists of three tasks, of which two abstract and one practical.

One of the abstract tasks is the form board test, which is developed to assess grasping functionality of prostheses. The subject is instructed to pick up various objects and place them in relevant slots in the form board. The set of objects cover various weights, sizes and rigidity. Scoring of the test is based on the completion time of each sub-task, as well as error count and a subjective evaluation of an external observer. The second abstract task is the pigeon-hole test. The test specifically aims at assessing grasping function at various heights. This is relevant as many body-powered prostheses are actuated by shoulder movement, which may influence the grasping ability in certain planes. The test involved moving various objects at mouth, chest, waist and knee height. The pigeon-hole test is scored the same way as the form board test, using completion time, amount of errors and subjective ratings. The practical task consists of 25 activities, which need to be performed with both hands.

Codd (1975) was not satisfied with the credibility of the KSCT and designed a modified version. No changes were made to the two abstract tasks, but different activities were picked for the practical task. In the modified version, also the use of correct grip types and the orientation of the prosthesis were identified to construct the

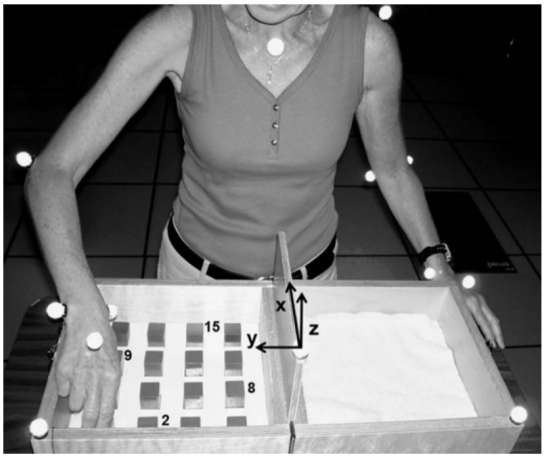

FIG. 9: Test setup for the Modified Box and Blocks Test, using motion capture [42]

subjective evaluation, with the aim to make scoring more consistent.

Critics argue that the reliability and validity of the KSCT is questionable, as the scoring is based on subjective ratings of external observers. In order to obtain more objective outcomes, the scoring system of the form board test has been modified by Edelstein and Berger (1993). The new version disregards the subjective evaluation, using only completion times and error counts for generating a score. The errors of the participant need to be identified and categorised by the external observer.

The modified form board test of Edelstein and Berger has been shown to have high reliability, arguably caused by minimising subjectivity in the scoring method.

MBBT

In order to assess not only quantitative performance but also quality of motion of prosthetic users, the Modified Box and Blocks Test (MBBT) is introduced in 2012 [43]. In contrast to the BBT, which falls under performance based tests in the tree structure of figure 2, the MBBT belongs in the category of performance and external observer based tests. The MBBT differs from the BBT on two points, whereas the rest of the test remains the same. Instead of 150 randomly positioned blocks, 16 blocks are positioned in an ordered fashion of 4 by 4 in one half of the box, as can be seen in figure 9. The participant is instructed to transfer the blocks to the other half in a specified order. Secondly, the MBBT uses motion capture to track the trajectories of the prosthesis and body parts. Because the task is cyclical, it is ideal for evaluating and comparing motions. The performance of the participant is judged by an external observer, based on kinematic trajectories and completion time. In terms of the WHO-ICF classification, the developers argue that the MBBT covers both the activity and function domain, as it is based on performance metrics and motion analysis [42].

Eight opto-electronic cameras are used to track the motions of reflective markers. The markers are positioned on nine anatomical locations. Furthermore a marker is placed on the divider and two markers are placed on the right and left sides of the box.

Resnik and Borgia (2012) have concluded that the MBBT is a valid assessment for upper limb prosthesis use, and have shown excellent reliability of the test [5].

Hebert et al. (2014) provided normative data for the MBBT, which allows clinicians to make well-founded evaluations [42]. The normative data consists of completion times, ranges of motion and maximum absolute velocities.

As motion capture requires a cyclic procedure, a limitation arises [42]. It is questionable whether a cyclic task with explicit defined execution such as the MBBT is representative of real-life tasks. The use of motion capture also limits the applicability of the MBBT to clinical centers having the required devices.

AM-ULA

The Activities Measure for Upper Limb Amputees (AM-ULA) is developed in 2013 as a performance based assessment for upper limb prostheses in the WHO-ICF activity domain [21]. A need for such an assessment was identified, as the ULPOM group found only one performance based measure of activity for adults. This measure was the Assessment of Capacity for Myo-electric Control (ACMC), which is patient specific and can only be used with users of myo-electric prostheses.

The AM-ULA consists of 18 ADLs. The activities were selected from the well-known Atkins ADLs checklist. Only activities from the checklist were chosen which were also used in the earlier developed and widely accepted UEFS from the OPUS assessment. The chosen tasks are: brush hair, put on and remove t-shirt, button a shirt, zip a jacket, put on socks, tie shoes, use a cup, use a fork and spoon, pour soda, write a word, use scissors, turn a door knob, use the phone, use a hammer, fold a towel and reach overhead. The duration of the complete test is 30 to 35 minutes [4].

An external observer evaluates the performance on each task on five elements, namely task completion, speed, movement quality, skillfulness of prosthetic use and independence [21]. For each element a score ranging from 0 to 4 is assigned. A higher score indicates a better performance. Only the lowest score of the 5 graded elements is assigned as the score of the task. Then the scores of the 18 tasks are averaged and multiplied by 10.

So, the maximum obtainable score is 40, where a lower score indicates a lower level of performance.

Upon evaluation, the AM-ULA has shown good reliability and validity. Although the AM-ULA is developed to be objective, it is argued that the score is based on the opinion of observers and thus that the test can be considered subjective [26]. It is also argued that multiple outcome scores for various domains of functioning would be preferable to the singular outcome score obtained with AM-ULA [3].

BAM-ULA

Five years after the AM-ULA was presented, a modified version named Brief Activity Measure for Upper Limb Amputees (BAM-ULA) was developed [4]. As the name suggest, this test was shorter in duration, but also easier to score than the AM-ULA.

The BAM-ULA uses 10 activities, which is 8 less than the AM-ULA. The activities involve tucking a shirt, lifting a heavy bag, opening a bottle, removing and replacing a wallet in a pocket, lifting a filled jug, pouring water from a jug, brushing hair, using a fork and turning a knob. The full test can be completed in 10 minutes.

Instead of judging performance in five categories, the observer evaluates only whether or not the activity is completed. A score of 1 or 0 is assigned respectively for a completed or non-completed activity. The overall score is calculated by the sum of the ten completion scores. Therefore, a higher score is related to better performance.

After evaluation, a ceiling effect is identified for the BAM-ULA scores. The suggestion is made that more difficult tasks should be included in the test [4].

SEEAPH

In 2017, the System for the Experimental Evaluation of Anthropomorphic Prosthetic Hands (SEEAPH) was presented for assessing prosthetic and robotic artificial hands [1]. The test consists of picking up 24 objects, selected from the Yale-CMU-Berkeley (YCB) Object and Model set. This set of objects is carefully composed for use in prosthetic and robot gripper design as well as for rehabilitation research, consisting of everyday items with different shapes, weight, sizes and rigidity [44].

The 24 items for SEEAPH are selected such that each of eight grip types are represented by three objects. The grip types are the pulp pinch, lateral pinch, diagonal volar grip, cylindrical grip, extension grip, tripod pinch, spherical grip and the hook. Examples of used objects for each grip type respectively are a marker, bowl, screwdriver, can, plate, golf ball, softball and skilled lid.

For performing the test, the participant is asked to grasp each object with the corresponding grip type, after the object was presented to him in the correct orientation for performing the prehensile pattern. Then, the participant should hold the object for three seconds. As an example, three items grasped with the correct grip type are shown in figure 10.

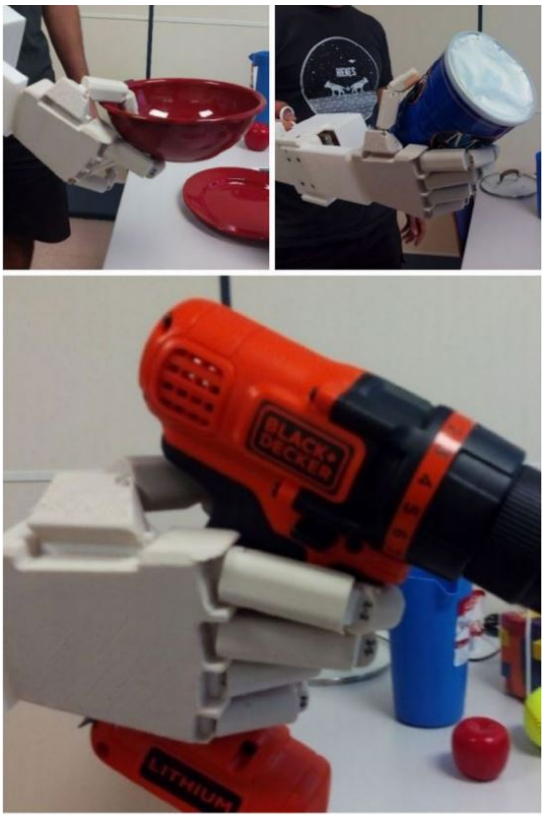

FIG. 10: Performing the System for the Experimental Evaluation of Anthropomorphic Prosthetic Hands on three example items using the correct grip type [1]

For each object, a score between 0 and 1 can be obtained. If the participant can hold the item for three seconds using the correct grip type, he scores 1 point. If the task can only successfully be completed on the second or third trial, a score of 0.6 or 0.4 respectively is assigned by the external observer. When the task is completed with a different grasping type, 0.2 points are given. The participant scores 0 points if he can not complete the task at all. Adding the scores of the three items in one category provides the score per grip type. The overall score is found by adding the scores of all items. A higher score suggests better performance [1].

The SEEAPH has not been statistically validated [2].

CAPPFUL

In 2018, the Capacity Assessment of Prosthetic Performance for the Upper Limb (CAPPFUL) was designed with the intention to fill a gap in the existing set of functional assessments by evaluating not only performance but also maladaptive compensatory movements [3]. The CAPPFUL was presented as a versatile measure of performance through broad and functional domain-specific testing.

The assessment consists of 11 ADLs, carefully chosen to assess the ability to perform multiple grip types in various planes and body positions. The activities are as follows: putting weights in a crate, carrying the crate, zipping up and down, picking up dice, tying shoelaces, lifting a plate, using a fork and knife, squeezing a bottle, turning a knob, placing coins in a slot and hanging a picture. During the tasks, five sub-functions are evaluated by an external observer, namely control skills, component utilization, maladaptive compensatory movement, adaptive compensatory movement and task completion. The duration of the complete CAPPFUL is 25 to 35 minutes.

The sub-functions adaptive compensatory movement and task completion are scored with 0 or 2 points. For task completion, a score of 2 is assigned if the task is completed within 90 seconds. Adaptive compensatory movement is judged by whether or not the prostheses required adjustment during the task, obtaining 2 or 0 points respectively. The remaining three sub-functions, control skills, component utilization, and maladaptive compensatory movement, are scored with 0, 1 or 2 points, where a higher score is related to better performance. For control skills, the amount of errors are counted in manipulating the object. The score of component utilization is based on the extent to which the participants use the prosthesis [45]. Maladaptive compensatory movement is scored by comparing the movements of the participant to 'normal' movements of non-amputees.

It is argued that the extent of maladaptive compensatory movement is hard to judge objectively. In order to improve the scoring of this sub-function, further research is done using motion capture to collect data on normative movements [45]. The research also provided normative completion times for each activity. The normative data provides the information clinicians need to make a more objective and consistent evaluation of the performance.

Sub-scores are obtained by summing up all 11 scores in a certain sub-function [3]. Higher scores are related to better performance for each sub-function except adaptive compensatory movement. The overall singular score of performance is calculated by adding all sub-scores except the sub-score for adaptive compensatory movement, minus 0.5 points for every adaptive compensatory movement.

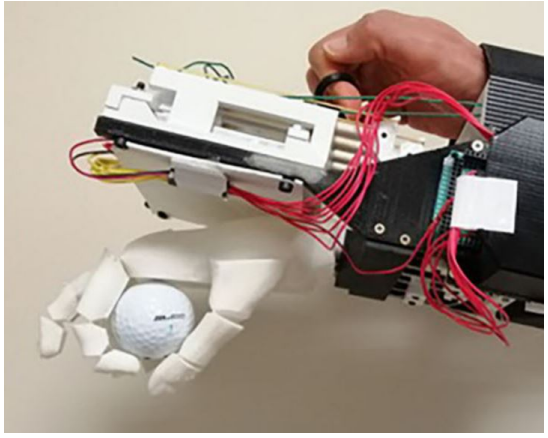

FIG. 11: An 180° rotated hand for performing one of the tasks of the Anthropomorphic Hand Assessment Procedure [46]

Excellent interrater reliability was shown for the CAPPFUL. The use of more standardized instructions was, however, suggested in order to obtain more similar movements between participants, which would improve the scoring of maladaptive compensatory movement [45].

AHAP

The Anthropomorphic Hand Assessment Protocol (AHAP) was presented in 2019 for measuring grasping performance under motion in anthropomorphic robotic and prosthetic hands [2]. The AHAP is based on the SEEAPH, and both are developed by the same researchers.

The AHAP uses an identical set of 24 objects for the test procedure, and adds two items. For assessing index pointing, pressing the button of a timer is added as task. A plate is used for assessing the platform prehensile pattern. Consequently, the ability to perform the eight most used human grip types and two non-grasping types can be measured using the AHAP. The assessment is not limited to assessing functionality, like the SHAP, but can also measure the human-like execution of grasping objects.

The first steps of the test protocol are identical to the procedure of the SEEAPH: an external observer hands the objects to the participant in the right orientation. The participant needs to grasp the objects with the correct grip type. But in comparison to the SEEAPH, where the participant only needs to hold the object for three seconds, the protocol of the AHAP is more elaborate. The participant is instructed to hold the object for three seconds, after which he needs to rotate the hand 180°

such that the palm is facing downwards. The rotated orientation can be seen in figure 11. After three seconds, the participant should rotate the hand back to the starting orientation. This sequence is repeated three times, while maintaining the correct grip type. Finally, the participant needs to hand the object back to the external observer. The protocol for using the timer consists of starting and stopping the timer three times, with intervals of three seconds. Rotating the hand is not used for assessing the platform prehensile pattern. The full assessment takes 80 to 100 minutes to complete.

The scoring system of the AHAP also differs from the SEEAPH. For each object, two scores are assigned by the external observer. One score is based on the ability to perform the correct grip types, the other on the performance under hand motion. Concerning the first, 1 point is assigned if the participant grasps the item with the correct grip type. If the object is grasped successfully, but with a different grip type than prescribed, 0.5 points are given. When the object can not be successfully grasped, no points are scored. For the second scoring category, the participant earns 1 point if no motion of the object with respect to the hand can be seen during rotation of the hand. In case of visible motion of the object, but without being dropped, 0.5 points are awarded. No points are earned if the object is dropped. The two non-grasping items are scored in a slightly different way.

The final scores of AHAP combine grasping performance and ability to hold the object under motion. They consist of an overall score, called the total Grasping Ability Score (GAS), and scores for each of the eight grip types, the partial GAS. The partial GAS can be calculated by summing the six scores obtained for the three objects per grip type. The total GAS can be obtained by summing all scores of all items. The scores can be normalized by dividing by the theoretical maximum amount of points. Consequently, a score of 100 indicates the level of hand function of a healthy human hand. A lower GAS indicates a lower level of performance.

In contrast to the SEEAPH, the AHAP has been statistically validated. The assessment has been applied to measure the functionality and human-like grasping ability of prosthetic hands [46].

4. DISCUSSION

This paper aimed to identify the set of existing assessments for experimentally testing the functional performance of upper limb prostheses. Assessments which were patient specific, analytical, for paediatric use, based on self-report, or fall in the participation domain of the WHO-ICF model were not considered. A total of 16 assessments fitting the criteria were found in literature.

The assessments were categorised on scoring system. The scoring can be based on performance, based on ratings of an external observer, or both. However, no relevant assessments were found in literature which fall in the external observer category, as paediatric and patient specific assessments did not fit the scope of this study. This raises the question whether this gap should be filled by developing new entirely external observer based assessments. Compared to results based on performance, the reliability and validity of results based on ratings of an external observer are questionable, and the results are regarded as less objective [23]. Therefore, assessments with results fully or partially based on performance can be regarded more useful for the research and development of prostheses. The conclusion can be drawn that there is no need for the development of new external observer based assessments.

A further subdivision of the assessments was made, based on the target group: generic or condition specific. When combining the the scoring and target group structuring, it was found that no performance based condition specific assessments were identified in literature. It could be argued, however, that some of the condition specific assessments based on performance and external observer are just based on performance. For instance, the score of the BAM-ULA is purely based on task completion. Therefore the role of the external observer is not significant. Also the SEEAPH and AHAP could be seen as assessments purely based on performance, although less clear than the BAM-ULA. The SEEAPH and AHAP are based on performing the right grip type and the AHAP also evaluates motion of the picked object relative to the hand, which makes the role of the external observer less insignificant than for the AM-ULA.

Of the 16 identified assessments, only few can be recommended for application to assess the functional performance of prostheses. First of all, some of the identified assessments are too specific, as they are based on only one task or grip type. Such methods individually can not provide a complete picture of overall functionality of the whole hand. To this end specific methods can be combined, but this will increase the burden on the participant and less insightful results will be obtained, compared to assessments aimed at the whole hand. Therefore, the specific tests, which are the NHPT, BBT, RCPRT and MBBT, are not recommended.

Concerning the remaining 12 assessments, many are never validated for the prosthetic field or have not shown sufficient reliability. The JTHF, MRMT, STHF, SHFT and ARAT were originally designed for human hands, and were never validated for the prosthetic field. The

modified version of the JTHF was not reliable for six of the seven tasks and showed floor and ceiling effects. The ARAT also showed floor effects. Although developed for prostheses, validation was not presented for the KSCT and SEEAPH. Statistical analysis of the BAM-ULA shows ceiling effects. The remaining 4 assessments however, the SHAP, AM-ULA, CAPPFUL and AHAP, have been statistically validated for application to upper limb prostheses, and have shown sufficient reliability. Therefore, these four methods are recommended for the prosthetic field. For the SHAP, the use of the alternative scoring system as suggested by Burgerhof et al. (2017) is recommended, to limit potential bias in the results, lower the cost, and make the scores easier to interpret.

It should be noted that with the use of the SHAP, CAPPFUL and AHAP, multiple outcome scores are obtained for various domains of functioning. This is useful for gaining insight in where the shortcomings of the prosthesis design lay, and in what areas improvement is desired. The AM-ULA provides only a singular outcome score. Therefore, the other three assessments may be preferred above the AM-ULA.

A further distinction needs to be made between anthropomorphic and non-anthropomorphic prostheses. Anthropomorphic hands can be scored on their ability to use the correct grip type, as they aim to resemble and imitate human hands. For other prosthesis designs, not resembling a human hand, assessments with scores based on grip type do not provide useful results. Of the four recommended methods, only the AHAP judges the performance based on applying the correct grip type. Therefore, for non-anthropomorphic prosthetic hands, only the SHAP, AM-ULA and CAPPFUL are recommended. For anthropomorphic prosthetic hands, all four tests are recommended.

As for upper limb prostheses, quantitative reliable and validated tests for assessing functional performance of robotic hands are scarce as well, and no standard protocol exists for benchmarking. Some of the recommended assessments for prosthetic hands could be applied to robotic hands as well, as prosthetic and robotic hands share many characteristics. For the evaluation of applicability of the assessments, an important note needs to be made. In the prosthetic field, scoring can be based on user related areas, such as compensatory movements and prosthesis utilization. For robotic hands, however, such areas are not useful for performance evaluation. Of the four recommended tests, the AM-ULA and CAPPFUL require the evaluation of such user related topics, while the SHAP and AHAP do not. Consequently, only the SHAP and AHAP are recommended for assessing robotic hands. Furthermore, the same distinction based on anthropomorphism needs to be made for the robotic field.

TABLE III: Recommended assessments for measuring functional performance of upper limb prostheses and robotic hands

	Prosthetic	**Robotic**
Anthropomorphic	SHAP AM-ULA CAPPFUL AHAP	SHAP AHAP
Non-Anthropomorphic	SHAP AM-ULA CAPPFUL	SHAP

Both the SHAP and AHAP can be applied to anthropomorphic robotic hands, but only the SHAP can be applied to non-anthropomorphic robotic hands.

An overview of the recommended test methods for each named type of artificial hand under test is presented in table III.

Although the SHAP test is significantly more commonly used than the AHAP in the prosthetic field, it has not yet been used in and validated for the robotics field in literature. The AHAP is, however, already partly designed and validated for robotic hands. Therefore, future research is suggested for statistical validation of applying the SHAP to robotic hands.

5. CONCLUSION

This review identifies existing experimental tests aimed at measuring functional performance of upper limb prostheses. A total of 16 assessments fitting the criteria of this study have been found in literature. Their scoring is either based on performance of the participant, or on the performance of the participant combined with ratings from an external observer. Part of the identified set of tests are generic in nature, as they are developed for assessing human hands as well, or even originally designed specifically for human hands. The remaining part of the tests are condition specific in nature, developed specifically for the prosthetic field.

Majority of the 16 identified assessments have not been validated for the prosthetic field or sufficient reliability has not been established. Results of several tests show floor or ceiling effects. Other methods are too specific for providing complete insight in the functionality of the whole prosthesis. Consequently, only four of the identified assessments can currently be recommended for application in the prosthetic field, namely the SHAP, AM-ULA, CAPPFUL and AHAP. If in future research more of the 16 assessments will be validated and are shown to have good reliability, more assessments can be rec-

ommended. This does not apply for the NHPT, BBT, RCPT and MBBT, which were found to be too specific. For the SHAP, the alternative scoring computations as suggested by Burgerhof et al. (2017) are recommended. Of the four tests, the AM-ULA may be the least preferred, as it provides a singular outcome score whereas the other three assessments establish multiple outcome scores for different areas of performance. If the prosthesis under test is non-anthropomorphic, only the SHAP, AM-ULA and CAPPFUL are recommended.

For measuring functional performance of anthropomorphic robotic hands, the SHAP and AHAP can be applied. For non-anthropomorphic robotic hands, only the SHAP is suggested. Statistical validation for applying the SHAP in the robotics field is recommended.

[1] I. Llop-Harillo and A. Pérez-González. System for the experimental evaluation of anthropomorphic hands. application to a new 3d-printed prosthetic hand prototype. *International Biomechanics*, 4(2):50–59, 2017. cited By 7.

[2] I. Llop-Harillo, A. Pérez-González, and V. Gracia-Ibáñez. Anthropomorphism index of mobility for artificial hands. *Applied Bionics and Biomechanics*, 2019, 2019. cited By 1.

[3] N.T. Kearns, J.K. Peterson, L. Smurr Walters, W.T. Jackson, J.M. Miguelez, and T. Ryan. Development and psychometric validation of capacity assessment of prosthetic performance for the upper limb (cappful). *Archives of Physical Medicine and Rehabilitation*, 99(9):1789–1797, 2018. cited By 3.

[4] L. Resnik, M. Borgia, and F. Acluche. Brief activity performance measure for upper limb amputees: Bamula. *Prosthetics and Orthotics International*, 42(1):75–83, 2018. cited By 4.

[5] L. Resnik and M. Borgia. Reliability and validity of outcome measures for upper limb amputation. *Journal of Prosthetics and Orthotics*, 24(4):192–201, 2012. cited By 25.

[6] V. Wright. Prosthetic outcome measures for use with upper limb amputees: A systematic review of the peer-reviewed literature, 1970 to 2009. *Journal of Prosthetics and Orthotics*, 21(SUPPL. 9):P3–P63, 2009. cited By 59.

[7] H.Y.N. Lindner, B.S. Nätterlund, and L.M.N. Hermansson. Upper limb prosthetic outcome measures: Review and content comparison based on international classification of functioning, disability and health. *Prosthetics and Orthotics International*, 34(2):109–128, 2010. cited By 60.

[8] W. Hill, P. Kyberd, L. Norling Hermansson, S. Hubbard, Ø. Stavdahl, and S. Swanson. Upper limb prosthetic outcome measures (ulpom): A working group and their findings. *Journal of Prosthetics and Orthotics*, 21(SUPPL. 9):P69–P82, 2009. cited By 50.

[9] A.V. Sureshbabu, G. Metta, and A. Parmiggiani. A systematic approach to evaluating and benchmarking robotic hands-the ffp index. *Robotics*, 8(1), 2019. cited By 3.

[10] M.V. Liarokapis, P.K. Artemiadis, and K.J. Kyriakopoulos. Quantifying anthropomorphism of robot hands. pages 2041–2046, 2013. cited By 30.

[11] T. Feix, J. Romero, C.H. Ek, H.-B. Schmiedmayer, and D. Kragic. A metric for comparing the anthropomorphic motion capability of artificial hands. *IEEE Transactions on Robotics*, 29(1):82–93, 2013. cited By 46.

[12] F.J. Andrés, A. Pérez-González, C. Rubert, J. Fuentes, and B. Sospedra. Comparison of grasping performance of tendon and linkage transmission systems in an electric-powered low-cost hand prosthesis. *Journal of Mechanisms and Robotics*, 11(1), 2019. cited By 3.

[13] I. Llop-Harillo, A. Pérez-González, and V. Gracia-Ibáñez. Anthropomorphism index of mobility for artificial hands. *Applied Bionics and Biomechanics*, 2019, 2019. cited By 1.

[14] A. Chan, E. Kwok, and P. Bhuanantanondh. Performance assessment of upper limb myoelectric prostheses using a programmable assessment platform. *Journal of Medical and Biological Engineering*, 32(4):259–264, 2012. cited By 3.

[15] G. Smit, D.H. Plettenburg, and F.C.T. van der Helm. Design and evaluation of two different finger concepts for body-powered prosthetic hand. *Journal of Rehabilitation Research and Development*, 50(9):1253–1266, 2013. cited By 3.

[16] R. Mio, M. Sánchez, and Q. Valverde. Mechanical testing methods for body-powered upper-limb prostheses: A review. pages 170–176, 2018. cited By 2.

[17] R. Mio, M. Sanchez, Q. Valverde, J. Lara, and F. Rumiche. Mechanical testing methods for body-powered upper-limb prostheses: A case study. *Advances in Science, Technology and Engineering Systems*, 4(5):61–68, 2019. cited By 0.

[18] F. Negrello, M. Garabini, G. Grioli, N. Tsagarakis, A. Bicchi, and M.G. Catalano. Benchmarking resilience of artificial hands. volume 2019-May, pages 8374–8380, 2019. cited By 3.

[19] J.S. Cuellar, G. Smit, P. Breedveld, A.A. Zadpoor, and D. Plettenburg. Functional evaluation of a non-assembly 3d-printed hand prosthesis. *Proceedings of the Institution of Mechanical Engineers, Part H: Journal of Engineering in Medicine*, 233(11):1122–1131, 2019. cited By 3.

[20] P.J. Kyberd. The influence of control format and hand design in single axis myoelectric hands: Assessment of functionality of prosthetic hands using the southampton hand assessment procedure. *Prosthetics and Orthotics International*, 35(3):285–293, 2011. cited By 23.

[21] L. Resnik, L. Adams, M. Borgia, J. Delikat, R. Disla, C. Ebner, and L.S. Walters. Development and evaluation of the activities measure for upper limb amputees. *Archives of Physical Medicine and Rehabilitation*, 94(3):488–494.e4, 2013. cited By 48.

[22] B. Rider and C. Linden. Comparison of standardized and non-standardized administration of the jebsen hand function test. *Journal of Hand Therapy*, 1(3):121–123, 1988. cited By 21.

[23] C.M. Light, P.H. Chappell, P.J. Kyberd, and B.S. Ellis. A critical review of functionality assessment in natural and prosthetic hands. *British Journal of Occupational Therapy*, 62(1):7–11, 1999. cited By 18.

[24] L. Haverkate, G. Smit, and D.H. Plettenburg. Assessment of body-powered upper limb prostheses by able-bodied subjects, using the box and blocks test and the nine-hole peg test. *Prosthetics and Orthotics International*, 40(1):109–116, 2016. cited By 17.

[25] M.A. Saliba, A. Chetcuti, and M.J. Farrugia. Towards the rationalization of anthropomorphic robot hand de-

sign: Extracting knowledge from constrained human manual dexterity testing. *International Journal of Humanoid Robotics*, 10(2), 2013. cited By 8.

[26] S. Salminger, I. Vujaklija, A. Sturma, T. Hasenoehrl, A.D. Roche, J.A. Mayer, L.A. Hruby, and O.C. Aszmann. Functional outcome scores with standard myoelectric prostheses in below-elbow amputees. *American Journal of Physical Medicine and Rehabilitation*, 98(2):125–129, 2019. cited By 1.

[27] J.T. Belter, M.T. Leddy, K.D. Gemmell, and A.M. Dollar. Comparative clinical evaluation of the yale multigrasp hand. volume 2016-July, pages 528–535, 2016. cited By 7.

[28] S.A. Dalley, D.A. Bennett, and M. Goldfarb. Functional assessment of a multigrasp myoelectric prosthesis: An amputee case study. pages 2640–2644, 2013. cited By 3.

[29] C.M. Light, P.H. Chappell, and P.J. Kyberd. Establishing a standardized clinical assessment tool of pathologic and prosthetic hand function: Normative data, reliability, and validity. *Archives of Physical Medicine and Rehabilitation*, 83(6):776–783, 2002. cited By 198.

[30] P.J. Kyberd, A. Murgia, M. Gasson, T. Tjerks, C. Metcalf, P.H. Chappell, K. Warwick, S.E.M. Lawson, and T. Barnhill. Case studies to demonstrate the range of applications of the southampton hand assessment procedure. *British Journal of Occupational Therapy*, 72(5):212–218, 2009. cited By 58.

[31] P.J. Kyberd. Assessment of functionality of multifunction prosthetic hands. *Journal of Prosthetics and Orthotics*, 29(3):103–111, 2017. cited By 4.

[32] S.A. Dalley, D.A. Bennett, and M. Goldfarb. Preliminary functional assessment of a multigrasp myoelectric prosthesis. pages 4172–4175, 2012. cited By 19.

[33] J.G.M. Burgerhof, E. Vasluian, P.U. Dijkstra, R.M. Bongers, and C.K. van der Sluis. The southampton hand assessment procedure revisited: A transparent linear scoring system, applied to data of experienced prosthetic users. *Journal of Hand Therapy*, 30(1):49–57, 2017. cited By 5.

[34] P.J. Agnew. Functional effectiveness of a myo-electric prosthesis compared with a functional split-hook prosthesis: A single subject experiment. *Prosthetics and Orthotics International*, 5(2):92–96, 1981. cited By 26.

[35] D.S. Gloss and M.G. Wardle. Use of the minnesota rate of manipulation test for disability evaluation. *Perceptual and motor skills*, 55(2):527–532, 1982. cited By 18.

[36] H.B. Smith. Smith hand function evaluation. *American Journal of Occupational Therapy*, 27(5):244–251, 1973. cited By 59.

[37] C. Sollerman and A. Ejeskär. Sollerman hand function test: A standardised method and its use in tetraplegic patients. *Scandinavian Journal of Plastic and Reconstructive Surgery and Hand Surgery*, 29(2):167–176, 1995. cited By 264.

[38] L.A. Miller and S. Swanson. Summary and recommendations of the academy's state of the science conference on upper limb prosthetic outcome measures. *Journal of Prosthetics and Orthotics*, 21(SUPPL. 9):P83–P89, 2009. cited By 33.

[39] A. Hussaini and P. Kyberd. Refined clothespin relocation test and assessment of motion. *Prosthetics and Orthotics International*, 41(3):294–302, 2017. cited By 13.

[40] A. Hussaini, W. Hill, and P. Kyberd. Clinical evaluation of the refined clothespin relocation test: A pilot study. *Prosthetics and Orthotics International*, 43(5):485–491, 2019. cited By 1.

[41] N. Yozbatiran, L. Der-Yeghiaian, and S.C. Cramer. A standardized approach to performing the action research arm test. *Neurorehabilitation and Neural Repair*, 22(1):78–90, 2008. cited By 286.

[42] J.S. Hebert, J. Lewicke, T.R. Williams, and A.H. Vette. Normative data for modified box and blocks test measuring upper-limb function via motion capture. *Journal of Rehabilitation Research and Development*, 51(6):919–931, 2014. cited By 22.

[43] J.S. Hebert and J. Lewicke. Case report of modified box and blocks test with motion capture to measure prosthetic function. *Journal of Rehabilitation Research and Development*, 49(8):1163–1174, 2012. cited By 38.

[44] Berk Calli, Aaron Walsman, Arjun Singh, Siddhartha Srinivasa, Pieter Abbeel, and Aaron M. Dollar. Benchmarking in manipulation research: Using the yale-cmu-berkeley object and model set. *IEEE Robotics & Automation Magazine*, 22(3):36–52, Sep 2015.

[45] A. Boyle, B. Prejean, L. Ruhde, K. Pool, C. Bollinger, J. Miguelez, D. Conyers, T. Ryan, and K.L. Kontson. Capacity assessment of prosthetic performance for the upper limb (cappful): Characterization of normative kinematics and performance. *PM and R*, 12(9):870–881, 2020. cited By 0.

[46] I. Llop-Harillo, A. Pérez-González, and J. Andrés-Esperanza. Grasping ability and motion synergies in affordable tendon-driven prosthetic hands controlled by able-bodied subjects. *Frontiers in Neurorobotics*, 14, 2020. cited By 0.

Appendix D:
Gripper sensorization

The human hand is considered the most versatile gripper found in nature. The human hand can perform numerous tasks, pick up items of a large range of size, shape, weight and rigidity, and can even perform in hand manipulation. Also, the hand can detect many external stimuli.

As this study was focused on designing a versatile gripper, the human hand can be seen as an ultimate example of a gripper for inspiration. Therefore, the human hand was taken as basis for evaluating which sensors could be useful in the robotic gripper.

Sensations of the human hand are of two natures; exteroreceptors and propriocepsis. Exteroreceptors are the sensors in the human skin, and the sensations are therefore based on touch. In the skin, various receptors are located, which are the endings of nerves [48]. In Figure 28, various receptors in the human finger are visualised. Three types of receptors exist: mechanoreceptors, thermo-receptors and nociceptors. Together, these receptors can sense touch, dynamic pressure, static pressure, vibration, skin stretch, temperature and pain. With these sensations, humans can also detect force, slip, texture and geometrical information such as contact area and geometrical shape of the contact [49]. The other type of sensation, propriocepsis, is based on kinematics. Proprioception of the hand consists of four sensations. Joint receptors, located in joint's capsule, can sense whether a joint is close to its extreme angle. The amount of force applied by a muscle is sensed by Golgi tendon organs, located in the tendons. Muscle spindles, positioned around muscle fibers, detect both length and contractile velocity of a muscle.

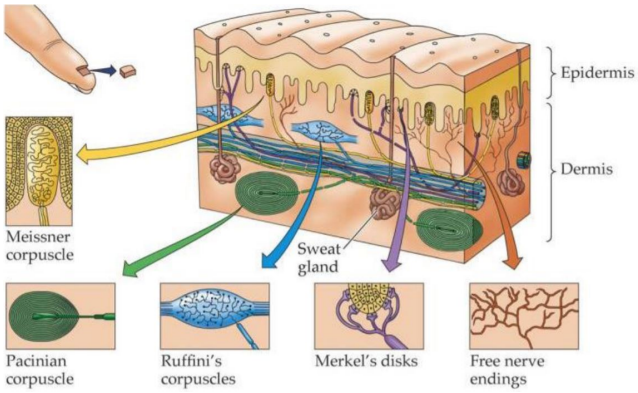

FIG. 28: Skin sensation is based on receptors in the skin of the hand [49]

TABLE IX: Overview of human hand sensorization. Based on potential usefulness and commercial availability, the last column presents whether a category of sensorization should be considered for the robotic gripper design.

Exteroreceptors	**Usefulness for gripper**	**Commercial Availability**	**Conclusion**
Pressure/force	✓	Good	✓
Simple geometry	∼	Good	∼
Contact	∼	Good	∼
Vibration	×	Good	×
Slip	✓	Scarce	×
Texture	×	N.A.	×
Temperature	×	Good	×
Pain	×	N.A.	×
Propriocepsis			
Extreme angles	∼	Good	∼
Actuator force	✓	Good	✓
Actuator orientation	✓	Good	✓
Actuator velocity	✓	Good	✓

For robotic grippers, muscle force can be translated into actuator force, muscle length into orientation or position of the actuator, and muscle contractile velocity into actuator velocity.

Each sensation was critically evaluated on potential for the robotic gripper design. The potential was based on two criteria, namely on how useful the sensation is for the robotic gripper, and on the commercial availability of such type of sensor. Table IX shows an overview of the evaluation. The second column shows how useful a sensation could be for the robotic gripper. A ✓indicates that a sensation was found potentially useful, ∼ indicates doubtfully useful and × indicates not useful. The third column presents the commercial availability, and implicitly affordability, of the sensor category. The last column presents whether the sensation should be considered for the robotic gripper design. Here a ✓indicates that a category of sensorsization should be considered for the gripper design, ∼ indicate less relevant considerations and × indicates that it should not be considered. The conclusion shown in the last column was based on the two columns on the left. The worst score of the two columns was taken for the conclusion column.

Some notes need to be made regarding the commercial availability presented in Table IX. It is shown that most types of sensors can easily be bought commercially. For slip sensors, this is different. Slip sensation is a technology which is currently in the research phase. Various research papers dig in to this topic. However, slip sensors are only scarcely available on the market, and are

high-priced. Second, commercial availability of texture and pain sensors are presented as non applicable. This is because sensors specifically for these sensations do not exist. Third, for propriocepsis each sensation is marked with good commercial availability. This is because actuator force, (extreme) orientation and velocity can all be detected by the actuator itself, if the correct actuator is applied.

In the evaluation, it has been concluded that only force measurement need to be considered for the robotic gripper design. Propriocepsis sensations could be useful as well, but no extra sensors need to be applied if the correct actuator is used in the design. Sensors for simple geometric shape and contact were concluded to have some useful potential for a robotic gripper, but not enough to balance the extra complexity of the system when such sensors are applied.

Consideration force sensor

By the use of force measurement, objects can be picked up more carefully as compared to without force feedback, as the applied force on the object is known. This way, force can be systematically increased, based on force feedback, to a certain value which is still safe to apply to a specific object without causing damage. It needs to be noted that most household objects do not damage easily, so force measurement is of less importance in this area. Various kinds of groceries can, however, be damaged or deformed easily, e.g. fruits and vegetables, bread, various products in thin carton packaging, chips, et cetera. Therefore, implementation of force sensors could be beneficial for the functional performance of the gripper design.

Various types of force sensors exist. For application on robot Rose, the force sensor must be electrical. Ştefănescu and Anghel (2013) presented a survey on 12 types of electrical force transducers, namely resistive, inductive, capacitive, piezoelectric, electromagnetic, electrodynamic, magnetoelastic, galvanomagnetic, vibrating wires, microresonators, acoustic and gyroscopic [50].

The applicability of each method for the robotic gripper was evaluated using two criteria. As first criteria, the range of force that can be sensed needs to cover the order of magnitude of 1 N to 0.5 kN. This was partially based on human grip and pinch force. For males, average grip force is 0.4±0.1 kN, and average pinch force is 0.08±0.02 kN. For females, average grip force is 0.2±0.06 kN, and pinch force 0.04±0.01 kN [51]. Note that the grip and pinch force vary over age and hand side. Forces much smaller than 1 N were deemed irrelevant for gripping performance.

Ştefănescu and Anghel have presented a graphical representation of the range of each type of electrical force

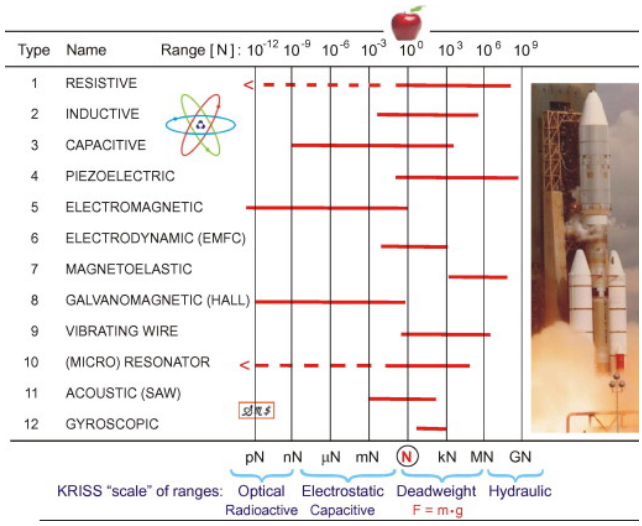

FIG. 29: Graphical representation of force ranges of various classical electrical measurement methods [50]

transducer, see Figure 29. Using the data of their study, it can be concluded that electromagnetic, magnetoelastic, galvanomagnetic, acoustic and gyroscopic force transducers are not applicable based on their ranges.

The second criteria involved that the type of force transducer needed to have good affordability and availability on the commercial market, in order to be implemented in the gripper design. Ştefănescu and Anghel described in their paper that vibrating wire force transducers are complex and expensive mechanical devices. Furthermore, they argued that microresonator force transducers are even more complex. Therefore, these two types were disregarded as well for this study.

From the two criteria was concluded that five types of force transducers were potentially applicable: resistive, inductive, capacitive, piezoelectric and electrodynamic force transducers.

Upon research of the five types of force transducers, various commercially available force transducers were found with potential for application on the gripper. Potential was evaluated on the base of size, force range and price. The found force transducers could be categorised in four categories: strain gauge, button, pad and force & position. Of each category, a short description will be given, complemented with advantages and disadvantages related to the gripper design.

Strain gauge: Strain gauges measure strain in material, which can be used to calculate stresses in the material using Hooke's law. The stresses can then be used to determine the force applied on the material. The stresses at the strain gauge are, however, not only dependent on the magnitude of the force, but also on the orientation and position of the applied force, as this in-

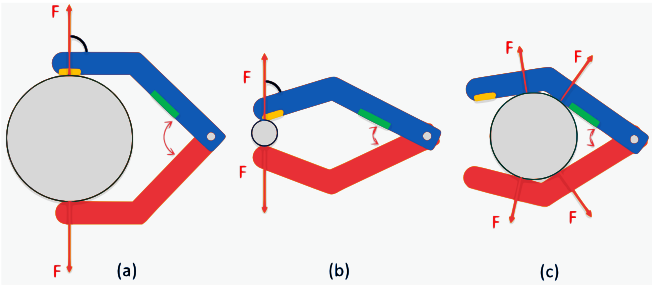

FIG. 30: Visualisation of a strain gauge (green) and button (yellow) force transducer applied on a simplistic exemplary gripper design grasping various sized objects

fluences the moment arm. To visualise the problem, Figure 30 presents an exemplary simplistic gripper design, which grasps items of various sizes. A strain gauge is positioned on the blue finger of the exemplary gripper design, and is visualised in green. As can be seen when comparing Figure 30a, b, and c, the orientation of forces and the moment arm relative to the strain gauge depend respectively on the size of the grasped object and the position of contact on the finger. Apart from the size of the object, the orientation of the fingers can also be used to determine the angle of the force relative to the strain gauge. The orientation of the fingers could be measured by the use of a rotary potentiometer, or, if applicable, by the position feedback of the actuator. For measuring the position of contact, another sensor would be needed. A flexible linear potentiometer could be applied to this end. It needs to be noted, however, that a linear potentiometer can only sense the closest contact point. This is a disadvantage, because multiple contact positions can occur, as visualised in Figure 30c, or large contact area's can occur in case of flexible materials. Therefore, grasping cases exist in which position measurement would be inaccuarate, resulting in inaccurate force determination. The multiple sensors needed for strain gauge force measurement also make physical implementation and control implementation more complex. Integrating data from multiple sensors will decrease the precision of the measurement as well, compared to the precision of the strain gauge only.

Another note that needs to be made about strain gauges, is that it is inconvenient to place them on 3D-printed material. 3D-printed material is an-isotropic and does not have a smooth surface area, which are both disadvantageous for strain gauge implementation. Therefore, if the gripper is produced using 3D-printing, it is advised to place a metal part in the finger for strain measurement, or to make use of an off-the-shelf load cell. Load cells with the force range defined earlier are, however, of significant size, which makes it hard to implement in a gripper finger. For placing a metal part in the finger, effort should be made to not lower the robustness of the finger, especially at the interfaces between the metal and 3D-printed parts.

Button: Button type force transducers measure force based on displacement of a button-like structure on top of the sensor. For evaluating applicability of button force transducers, Figure 30 is used again. In this figure, the button force transducer is positioned in the blue finger, and visualised in yellow. As can be seen, in Figure 30a the force can be measured as desired: the force is applied on the force transducer. In Figure 30b and c, however, two cases are presented in which the button force transducer will not measure the correct force. The error is the result of varying contact positions, while the button force transducer can only measure force at one specific position. To solve this issue, multiple button force transducers could be applied, although this increases the complexity of physical implementation significantly.

Pad: Force transducers are also available in the form of a pad. Capacitive pad force transducers and Force Sensing Resistors (FSRs) exist. Pad force transducers measure force applied anywhere on the pad, irrespective the position on the pad. FSR force transducers in particular exist in many shapes, including circular, square, rectangular and oblong. For implementation on the gripper, a pad should be applied with a shape matching the finger shape. In this case, any force applied on the finger can be measured directly, irrespective of the contact position and finger orientation. Also the total amount of force can be directly measured in case of a large contact area, or in case of multiple contact positions. This eliminates the need for extra sensors, which is advantageous as argued in the paragraph discussing strain gauges. Another advantage of FSRs is that they are flexible, resulting in simple physical integration.

Pad force transducers have disadvantages as well. Force measurements of pads have lower precision than strain gauges. Also, effort needs to be made to guide all forces through the sensor pad. Otherwise, forces can go through the surrounding rigid, non-sensing parts of the pads, resulting in inaccurate force measurements.

Force & position: Some force transducers can simultaneously measure the position of the applied force. Examples of such transducers are FSR matrices and Force Sensing Linear Potentiometers (FSLPs). FSR matrices consist, as the name implies, of multiple FSRs positioned in an array. FSLPs can be described as a combination of an oblong FSR and a flexible linear potentiometer. Although position measurement was needed for strain gauges, it does not provide essential feedback for the force measurement with a FSR. Therefore, force & position sensors can be regarded as unnecessarily complex, causing unnecessary cost.

Actuator: Finally, in case of using an actuator which provides torque feedback, force applied to the object can also be determined based on actuator torque. The main advantage of this solution is its simplicity, as no force transducers need to be implemented in the design. However, as for strain gauges, for accurate determination of the force, contact position and orientation of the finger are needed. As for the case of strain gauges, orientation of the fingers can be based on actuator position feedback, and contact position can be measured using a linear potentiometer. So, for accurate force measuring, implementation of a sensor is still needed, eliminating the main advantage of using actuator force feedback. In addition, a main disadvantage of measuring force at actuator level can be identified. Forces determined using actuator force feedback include transmission losses and accelerations of moving parts, meaning that the determined forces have low accuracy.

When an actuator with torque feedback is applied in a design using a force transducer, the torque feedback can be used as a supplement for extra data. The extra data will not be essential, but additional evaluations can be made possible, such as determining transmission losses and forces due to accelerations. Also, the torque feedback can function as some sort of back-up or second opinion, when the force transducer does not work or gives unsound values.

Please note that Figure 30 only presents a single exemplary gripper design. Many other designs are possible. For each design, categories of force transducers can be more or less applicable. The description above tries to provide general aspects of the types of force transducers. In the design phase, however, the applicability of each type of force transducer must be evaluated for the specific gripper design.

Appendix E:
Morphological overview and ACRREx method

The ACCREx method, designed by Breedveld, Herder and Tomiyama (2011), was used in combination with a morphological overview for the systematic and structural design of the gripper [20]. In Figure 3, the application of the ACCREx method is shown for two sub-functions, but the method has been applied to more of the sub-functions present in the morphological chart. Initially, the morphological chart was generated based on knowledge, brainstorming and literature. The ACCREx method was used to elaborate and fill gaps in the morphological chart, for both sub-functions and design solutions.

In Figure 4, the morphological chart can be seen. The chart consists of 12 sub-functions and 67 design solutions. Below, a more detailed description is given for each sub-function, and notes are made on several design solutions.

1 - Amount of fingers: The amount of fingers of a gripper can theoretically vary between zero and infinite. Zero, two, three and five fingers are most commonly applied to grippers. Examples of zero finger grippers are magnetic or suction based grippers. Five fingered grippers are most commonly applied in prostheses and humanoid robots. Research has concluded that three fingers are needed to grasp any 2-D object [30]. To grasp any 3-D item, a minimum of four fingers are needed. Other research concluded that the human hand without a functioning little finger achieved practically the same score on several functional tests as a fully functioning human hand, indicating that a fifth gripper finger is no necessity [29]. Another reasoning of why more than two fingers are beneficial can be found in grasp stability. In previous gripper design projects for robot Rose, developing two-fingered grippers, the issue was named that objects rotated while being lifted. This phenomenon occurs, as two opposing fingers provide very little moment arm to generate torque to prevent rotation. The points of contact are in the same line, and therefore torque around that line can only be generated by the of-center contact area of the finger. A solution could be to make the contact area of significant size, although this would result in a bulky gripper. Another solution is to apply three or more fingers, which can span a plane of contact points. Distance between fingers create moment arms for generating torque to prevent rotation and to provide a more stable grasp.

2 - Finger relative orientation: When the fingers do not make contact with other fingers during the closing cycle of the gripper, the finger orientation is classified as "No finger interference". In other words, the fingers are out of phase. Fingers directly opposing each other, are classified as "Face to face". In this case, the fingers are in phase. Fingers of a gripper can be out of plane with the other fingers, in which case the gripper falls under the "Angled" category. The gripper of this study is required to perform a pinch grip, see Appendix B. Therefore, the gripper design can not consist solely of fingers that do not interfere.

3 - Finger movement: According to Gorce and Fontaine (1996), four types of finger movement can be distinguished. They also give an overview of advantages and disadvantages of the four categories. Angular and prismatic joint parallel movements are seen as simple mechanisms, while quasi-parallel and rotoid joint parallel movements are seen as more complex [31]. Quasi-parallel and parallel movements are identified to have a good force transmission, while for angular movement this depends on the orientation. Furthermore, they state that angular movement is mainly suitable for grasping of cylindrical parts, quasi-parallel for cylindrical and prismatic parts, and parallel movement for cylindrical, prismatic and thin parts. Last, for prismatic joints the drawback is named that they are prone to wear and are not suitable in dirty environments.

4 - Finger DOFs: Theoretically, each finger can have zero up to infinite DOFs. It is however argued that the least amount of DOF should be used with which the gripper can fit its purposes [32]. Increasing the amount of DOF namely increases the complexity, weight and volume, and reduces robustness of the gripper. For executing precision grasp patterns, single DOF fingers are preferred above fingers with multiple DOFs [30]. For power grasp patterns, multiple DOFs are, however, preferred to enable shape adaptivity. It needs to be noted that more DOFs in the gripper do not necessarily result in higher functional performance. A good example of this can be found in the work of Kyberd (2017), in which he assesses the functional performance of four hand prostheses: a single DOF prosthesis and three multiple DOF prostheses [33]. The functional performance is assessed using the SHAP. The single DOF prosthesis outperforms the multiple DOF prostheses on every part of the SHAP.

5 - Actuation: As the robot is electrically powered, the gripper must be electrically powered as well. Four types of electrical actuators are distinguished, namely a rotary electric motor, servo motor, stepper motor and linear electric motor. Of the four types, servo and stepper motors are the easiest to control.

6 - Shape adaptivity: It is preferable to have gripper fingers which adapt to the shape of the item to grasp.

This way, less force needs to be applied for a stable grip. Shape adaptivity can be established by means of under-actuation or compliance. Various different under-actuation types can be distinguished [9]. There are linkage, compliant and tendon based under-actuated mechanisms. When contact forces in linkages are negative, as a result of specific orientations, grasps of linkage based under-actuated mechanisms are unstable [30]. In this case, the ejection phenomenon occurs, which is complex to prevent in under-actuated mechanisms. Tendon based mechanisms also include pulley systems. For tendon based under-actuation mechanisms is argued that they are generally less robust and need more maintenance [52]. Soft robotics are known for being compliant and their characteristic of shaping around objects. Furthermore, shape adaptivity can be obtained by applying material at contact points with high compliance, or by applying springs. The principle of differential gears can be applied as well, as they allow for different output movements for a certain input movement, by balancing the torque generated at both sides. The whippletree mechanism is a system which balances multiple output forces for a given input force, which can therefore also be used to obtain shape-adaptivity. The under-actuation mechanism of a whippletree mechanism is built up out of multiple seesaw mechanisms, which is why this principle can also be referred to by the seesaw mechanism [9]. For this mechanism needs to be noted that springs are needed to guide the backwards movement, such that all fingers can be extended together [52]. The whippletree mechanism has for example been applied in a non-assembly 3D-printed hand prosthesis [21]. Finally, also active shape adaptivity can be achieved by the application of multiple actuators, sensors and a feedback system. The complexity needed for such a system makes the gripper less reliable and more expensive, compared to passive shape adaptivity [17]. Active shape adaptivity provides, however, increased stability and dexterity of grasping.

7 - Hygiene: The robot is being developed to operate in a care environment. Therefore, the requirement is imposed that the gripper must be cleanable, water resistant and has no possibility for dirt accumulation. To solve this issue, gloves can be applied. Off-the-shelf disposable or cleanable gloves could be used, or self-produced gloves. The self-produced glove in the picture in the morphological chart is produced in a previous gripper design project for robot Rose. Self-produced gloves have the advantage of freedom of shape of the gripper. In the previous project it was found, however, that self-producing a glove is time-consuming and complex to get the correct compliance at the joints. In general, disposable gloves have lower stiffness than cleanable or self-produced gloves. Other solutions for hygiene involve having rigid cleanable surface materials with flexible surface materials at the joints, or using flexible surface material for the whole gripper, as can be seen in soft robotics.

8 - Enhancing grip: In order to decrease required grip or pinch force for grasping an item, it is desired to enhance friction grip. The importance of friction for functional performance is highlighted in literature [21]. Enhancing friction grip can be done in various ways [53]. As friction force depends on normal force and friction coefficient, friction force can be enhanced by influencing these factors. A high friction coefficient can be achieved by using a material with this characteristic for the contact areas. Many off-the-shelf gloves consist of material with a reasonably high friction coefficient, including latex rubber and nitrile rubber [26]. Therefore, various gloves can also be viable solutions for achieving a high friction coefficient. An increased normal force, without applying a higher pinching or gripping force, can be achieved by suction. This is, however, limited to items with smooth contact areas. The direction of normal force can also be adapted to get a higher resulting grip force. Teeth or shape adaptivity can be used to this end. Note that the needed friction force is not required in this case to generate grip force. Further, note that teeth can only be applied in case of grasping objects with deformable contact surfaces. Last, adhesion can be used as well to enhance grip, by enlarging the contact area. As the gripper of this study is required to grasp a large variety of objects with different contact surfaces, it can be concluded that teeth and suction are not viable options.

9 - Actuator heat dissipation: During gripper usage, the actuation of the gripper will generate heat. This heat needs to be dissipated to prevent overheating. The actuator can be directly cooled by means of natural convection or forced convection. This solution implies the need for air flow along the actuation system. The gripper, however, must be water and dirt resistant, making free air flow impossible. Other options are to indirectly cool the actuation system, by first conducting the heat through the enclosing outer surface of the gripper, after which convection can cool the outer surface. To enhance cooling, the outer surface must have a high conductivity and a large area in contact with the environment air.

10 - Transmission: Between the actuator and fingers, one or multiple types of transmissions need to be used. There are many different transmission methods. For cables, it is argued that robust transmission is still difficult to obtain, and require frequent maintenance [52]. Furthermore, all transmission mechanisms in the morphological chart but two work equally well for forward and backward transmission directions. Worm gears and spindles in contrary have a most efficient direction of transmission. Depending on the lead angle, the transmission can

even be self-locking in backwards direction. Advantage of less backdrivable or self-locking transmission mechanisms is that unwanted opening of the fingers is limited, without need for active actuation. Disadvantage of self-locking gears is that they are in general less efficient than fully backdrivable gears.

11 - Production: Production of non-off-the-shelf parts for the gripper can be done in various ways. However, it should be kept in mind that fast manufacturing is required. To this end, additive manufacturing is most suitable. Another advantage of additive manufacturing is the ability to produce parts with higher shape complexity. Disadvantages of additive manufacturing are lower accuracy, poorer surface finish, lower strength and anisotropic parts. In specific cases, anisotropy can, however, be seen as an advantage.

12 - Force measuring: For measuring the force applied by the gripper, actuator feedback or force transducers can be used. Three types of force transducers can be distinguished, namely button-like sensors, sensing pads and strain gauges. For more detailed descriptions and considerations, see Appendix D.

Appendix F:
Concept selection: Harris Profile

For selecting the most promising gripper design concept, in a well-grounded and systematic manner, a Harris Profile was used. The final Harris Profile, including scoring, is presented in Table II. The criteria, presented in the left column, are subdivided regarding the related category of requirements. The design concepts and the previous gripper design, named in the Harris Profile, are presented in Table I and visualised in Figure 5.

For clarification, the criterion 'orientation independence' aims at the ability of the design concept to grasp objects in various relative orientations of the gripper. Furthermore, it needs to be noted that the criterion 'production simplicity' includes glove production and sensor integration as well, when applicable. 'Ease of disinfection' also includes changing of disposable gloves, when applicable.

Scores presented in the Harris Profile were determined with the notes presented in Appendix E in mind. To create more reliable outcomes, the author determined scores for all criteria and designs twice, with a day in between and without reviewing the previous determined scores, resulting in two reasonably independent evaluations. Afterwards, scores of both evaluations were compared. In case the same score had been assigned twice, the score was taken as final score. When the scores differed, the scores were critically evaluated again. Comparing the two Harris Profiles, most scores corresponded, and non-corresponding scores never differed more than one point.

Looking at the final Harris Profile, it was concluded that the UALG and the RPG score lowest overall. Although having good functional properties, the UALG is of significant design complexity relative to the other concepts, which could be appointed as the main reason for a low overall score. For the RPG, it is the other way around. The design is simple, relative to the other concepts. However, this design does not provide high functional properties for versatile tasks. Another major drawback is that the RPG can not be disinfected.

Based on the Harris Profile, the remaining concepts could be ranked as follows, from best to worst: 4FH, SHG, WTH. The SHG scored well mainly due to its simplicity, but functional properties for versatile tasks are lower, similar but to less extend than was found for the RPG. Looking at the final Harris Profile, the 4FH was concluded to provide the best balance between all criteria. Although it does not often score the highest amount of points (+2), it scores positively on almost all of the criteria, and never scores the lowest amount of points (-2). This can not be said for any of the other designs. It was concluded that the 4FH fits all aspects of the design problem sufficiently, and does not require significant concessions. Therefore, the 4FH was chosen as the design to continue with.

Appendix G:
Design calculations and evaluations

1. Actuation

A minimum pinch force of 30 N was required. An actuator with sufficient torque was to be chosen to enable a pinch force of 30 N. However, the achievable pinch force with a given actuator torque is dependent on the gear ratio, which also relates to the closing time of the gripper. A duration of closing the gripper of less than 0.7 s was required. The required angular velocity of the fingers to achieve the required closing time is dependent on the minimum gripper stroke, which was 85 mm, and the finger length. The relation is shown in Equation G1.

$$\begin{aligned} \omega_f &= \frac{\theta}{t} \\ \theta &= sin^{-1}(\frac{s}{2L}) \end{aligned} \tag{G1}$$

Where ω_f is the angular velocity of the fingers, t is the required closing time, s is the required stroke width, L is the finger length and θ is the angular distance the fingers must open to obtain the required stroke width.

The gear ratio, angular velocity and torque are related as shown in Equation G2.

$$i = \frac{\omega_a}{\omega_f} = \frac{T_f}{T_a} \tag{G2}$$

Where i is the gear ratio between the fingers and actuator respectively, ω_a is the angular velocity of the actuator, T_f is the torque of the fingers and T_a is the torque of the actuator.

The transmission of the gripper, however, consists of two worm gears positioned on opposite sides of the worm. Therefore, the torque transferred from the worm to each worm gear is halved, as presented in Equation G3.

$$i = \frac{\omega_a}{\omega_f} = 2\frac{T_f}{T_a} \tag{G3}$$

As actuator, the Dynamixel XM430-W350-R servo was chosen, which has 4.1 Nm stall torque and an angular velocity of 46 rpm without load. However, efficiency is lower than 1, as there is friction in the transmission and bearings, and worm gears are known to have a relatively low efficiency compared to most transmission systems. An efficiency, η of 0.8 has been assumed, based on a datasheet on worm gear sets by Framo Morat, manufacturer of the used gear set [54].

Equation G3 can be rewritten as follows, to obtain the achievable pinch force, F.

$$\begin{aligned} T_f &= \frac{T_a\ \omega_a}{2\ \omega_f} \\ T_a &= \eta\ T_{stall} \\ F &= \frac{T_f}{L} \\ F &= \frac{T_a\ \eta\ \omega_a}{2\ L\ \omega_f} \end{aligned} \tag{G4}$$

Now the equations can be filled in with the given values, the no load angular velocity for ω_a and a finger length L of 0.09 m. The finger length was chosen to fit the gloves and is discussed in Section 2.2. The outcome of the achievable pinch force, resulting from the equations, is 1.25E2 N, which is more than sufficient compared to the required 30 N. It was concluded that the servo does not need to be used at full capacity.

2. Transmission

For the transmission, it was important to chose the right gear ratio i. The required gear ratio could be determined by combining Equation G1-G4 and filling in the given values. Resulting from these equations, the required gear ratio was found to be 6.86:1. The worm gear set was allowed to have a lower gear ratio, but not higher. A lower gear ratio than required would result in a small decrease in achievable pinch force, and a small decrease in closing time. The decrease in pinch force was expected not to form a problem, as the achievable pinch force was shown to be much larger than required. A decrease in closing time is actually beneficial, as this would result in a faster gripper, or an increased gripper stroke for the same closing time. Worm gears with such low ratio's are scarce. A worm gear set, approaching the required gear ratio, was chosen, which has a gear ratio of 4.5:1.

To check the consequences of using a gear ration of 4.5:1, the pinch force and closing time were recalculated. Recalculating the achievable pinch force was done by rewriting G4, where the angular velocity ratio could be replaced by the gear ratio, as seen in Equation G3. Equation G5 shows the calculation for the achievable pinch force with the used gear ratio.

$$F = \frac{T_a\ \eta}{2\ L} i \tag{G5}$$

Filling in the given values in Equation G5 resulted in an achievable pinch force of 82 N. This pinch force is still an order of 3 times higher than required, so the decrease in gear ratio did not impose a problem for the pinch force.

For the effect of the gear ratio on the closing time, Equation G1 and G4 could be combined into Equation G6.

$$\begin{aligned} t &= \frac{\theta}{\omega_f} \\ \theta &= sin^{-1}(\frac{s}{2L}) \\ \omega_f &= \frac{\omega_a}{i} \end{aligned} \tag{G6}$$

When recalculating the closing time with Equation G6, a value of 0.46 s was obtained. As expected, the closing time with the lower gear ratio is lower than the required closing time of 0.7 s. This means that either a faster gripping cycle could be fulfilled, or the gripper stroke could be increased. Using Equation G7, the maximum stroke width can be determined for which the closing time is equal to the required maximum time. Equation G7 is obtained by rewriting Equation G1 and G4.

$$\begin{aligned} s_{max} &= 2\ L\ sin(\theta) \\ \theta &= \omega_f\ t_{req} \\ \omega_f &= \frac{\omega_a}{i} \end{aligned} \tag{G7}$$

Here, t_{req} is the maximum closing time as set by the requirements. Filling in the equation, a maximum stroke width was obtained of 123 mm. It has to be noted that this maximum stroke width is purely based on the maximum closing time. The actual maximum stroke width of the gripper is also dependent on the physical design.

The specific worm gear set was also chosen for its small axis to axis centre distance and relatively low lead angle. Worm gear sets with comparable gear ratio's mostly have a larger centre distance and lead angle. A larger centre distance results in an increase in gripper size, and an increase in distance between the rotation points of opposing fingers. Keeping the distance between opposing fingers to a minimum has the advantage that the movement of the fingertips towards the palm is kept to a minimum. In other words, the fingertips rotate less inwards towards the palm just before contact between two opposing fingertips. This way, the extreme reach of the finger tips farthest away from the palm approximates the reach when fully closed. The relatively low lead angle, given the gear ratio, results in a less backdrivable mechanism, meaning that a torque in the fingers will not as easily rotate the servo as the other way around. This has the advantage that an object can be held after gripping, without actively providing the full force in the fingers with the servo. The lead angle of the worm gear set is 21°50. It needs to be noted that for worm gear sets in general, this lead angle is still relatively large. In general, the maximum lead angle for static self-locking in worm gears is 5° [54].

3. Driving shafts

The stresses developed in the driving shafts by the actuator torque should not plastically deform the driving shafts. The maximum shear stress in a circular shaft for a given torque is given by Equation G8

$$\begin{aligned} \tau_{max} &= \frac{T\ c_{max}}{J_c} \\ J_c &= \frac{\pi d^4}{32} \\ c_{max} &= \frac{d}{2} \end{aligned} \tag{G8}$$

Where T is the torque in the driving shaft, J_c is the polar moment of inertia of a circular shaft, and d is the diameter of the driving shaft.

A scenario is assumed, where no loads are present except for the load applied on the shaft by the torque of the actuator. Applying the circle of Morh, the principle stresses σ could be found. The principle stresses are related to the maximum shear stress as presented in Equation G9. The maximum stress in the driving shaft is equal to σ_1.

$$\begin{aligned} \sigma_1 &= \tau_{max} \\ \sigma_2 &= 0 \\ \sigma_3 &= -\tau_{max} \end{aligned} \tag{G9}$$

There are three driving shafts in the gripper. One is directly connected to the actuator and drives the worm. The other two are connected to the fingers, one for the thumb and one for the index, middle and ring finger, and are driven by the worm gear. The maximum torque in the driving shaft connected to the actuator is equal to the stall torque of the actuator, namely 4.1 Nm. The torque in the driving shaft on the other side of the transmission, connected to the fingers, could be calculated using the gear ratio i, actuator torque T_a and the gear efficiency f, as presented in Equation G10.

$$T_f = f\ i\ T_a \tag{G10}$$

Combining and rewriting equations G8 to G10, expressions could be found for the minimum diameter of the finger driving shafts, $d_{f,min}$, and of the actuator driving shaft, $d_{a,min}$. As the shafts may not plastically deform,

the maximum stress is equal to the yield point of the material, σ_y. The rewritten equations are presented in Equation G11.

$$d_{f,min} = \sqrt[3]{\frac{16T_f}{\pi\sigma_y}}$$
$$d_{a,min} = \sqrt[3]{\frac{16T_a}{\pi\sigma_y}} \tag{G11}$$

For the shafts, the material silver steel was chosen. The yield point of silver steel lays between 480 MPa and 690 MPa [23]. For safety, the lowest yield point was assumed, namely 48 MPa.

Filling in Equation G11, $d_{f,min}$ and $d_{a,min}$ could be obtained. For $d_{f,min}$ a value was obtained of 5.4 mm, and for $d_{a,min}$ a value of 3.5 mm. Based on these calculations, 6 mm diameter shafts were chosen for all three driving shafts. It needs to be kept in mind that the maximum torque will very rarely occur, as the maximum torque was shown to generate a force much higher than required.

The angle of twist of the driving shafts under the maximum torque loads is of interest as well, as it is not desired that the fingers rotate for large angles due to the load. The angle of twist was calculated with Equation G12.

$$\phi = \frac{TL}{GJ_c} \tag{G12}$$

Here L is the length of the shaft between the torque load T and where it is clamped. G is the modulus of rigidity. J_c is the polar moment of inertia of a circular shaft, as presented in Equation G8. For silver steel, the modulus of rigidity is 83 GPa [23]. The free length L is different for the three shafts. In the gripper design, the free length of the actuator shaft, L_a, is equal to 9 mm. The free length of the thumb shaft, L_t, is 12.5 mm. The maximum free length of the finger shaft, L_f, is 36 mm.

Filling in the values, and keeping in mind that torque T_a is applied on the actuator shaft and T_f on the thumb shaft and finger shaft, the angle of twist could be determined. This way, it can be shown that the angle of twist for the actuator shaft is equal to 0.2°, for the thumb shaft 1.0° and for the fingers 2.9° under maximum torque. The fingers are 90 mm in length, so the 2.9° angular twist of the finger shaft could be translated to a displacement of the fingertips of 4.5 mm. With the determined small angular twists and displacements, no problems for the performance of the gripper were foreseen.

4. Heat dissipation

In stall, which is the case during grasping, the electrical power consumed by the actuator is converted to heat. When heat is not dissipated enough, there is risk of actuator overheating or unsafe surface temperatures of the gripper. The amount of heat to be dissipated, as well as an evaluation of the heat dissipation capacity of the gripper design, is described in this section.

Maintaining grasp

After grasping an object with a certain actuator force, the actuator torque can be lowered while maintaining the grip force applied on the object. This is caused by the the low backdrivability properties of the worm gears. Lowering the actuator torque during grasping cycles decreases the required electrical power and thus the heat needing to be dissipated. To evaluate to what fraction of the initial actuator torque the torque can be lowered, without lowering the grip force, following equations were be used.

Equation G13 presents the pinch force resulting from an actuator force. In this case, the torque is transmitted from the worm on the actuator side to the worm gears on the side of the fingers. This direction will be called the forward direction. Equation G13 is taken from Equation G5.

$$F = \frac{T_a\ \eta}{2\ L} i \tag{G13}$$

After applying the force on the object, it is desired to maintain the force while lowering the actuator torque. In this scenario, the torque on the worm gear side, as a result of the force on the fingers, is transmitted to the worm side. This direction of torque transmitting through the transmission will be referred to as the backwards direction. In the equations, the backwards direction will be indicated with an apostrophe. For the backwards direction, the torque generated by the pinch force is $T_{f'}$. The torque at the actuator side, as a result of the torque at the finger side, is $T_{a'}$. Equation G14 shows the relations for the torques.

$$T_{a'} = \frac{T_{f'}\ \eta'}{i}$$
$$T_{f'} = 2\ F\ L \tag{G14}$$

Here, η' is the efficiency of the backwards direction. Combining, rewriting and simplifying Equation G13 and G14 results in Equation G15.

$$\frac{T_{a'}}{T_a} = \eta\ \eta' \tag{G15}$$

According to the manufacturer of the gear set, the backwards efficiency can be calculated with Equation G16 [54]. This equation includes that the starting efficiency, when the gears are not running, is approximately 30% lower than the running efficiency.

$$\eta' = 0.7\ (2 - \frac{1}{\eta}) \tag{G16}$$

Combining Equation G15 and G16, a relationship could be determined between the initial actuator torque for gripping and the minimum lowered actuator torque during gripping. The relationship is only dependant on the forward efficiency, as can be seen in Equation G17.

$$\frac{T_{a'}}{T_a} = 1.4\eta - 0.7 \tag{G17}$$

As described in Section G 1, the forward efficiency η is approximately 0.81 [54]. Therefore, the ratio between the actuator torque needed to maintain the grip force, and the initial actuator torque for gripping, is 0.42. In other words, theoretically the actuator torque can be lowered to 42% of the original actuator torque, without lowering the grip force applied on the object.

Generated heat

An evaluation is made regarding the total amount of heat to be dissipated. During grasping and maintaining grasp, the actuator is in stall, so all electrical power is converted to heat. The needed electrical power, however, is highly dependent on the task. For the worst case scenario, a task was evaluated in which the gripper grasps for 25% of the time, and maintains the grip force for 75% of the time. The pinch force evaluated for the worst case scenario was 30 N, which is sufficient to allow for a broad range of activities [14]. The required actuator torque to grasp an object can be calculated with Equation G18, which is a rearranged version of Equation G13.

$$T_a = \frac{2\ F\ L}{\eta\ i} \tag{G18}$$

The required actuator torque to maintain grip can be calculated using Equation G17. Doing the calculations, it was obtained that 1.5 Nm is needed to initiate a pinch force of 30N, and 0.63 Nm to maintain the force. Using the performance graph of the actuator in the gripper, the required current for the torques were determined [47]. For 1.5 Nm and 0.63 Nm, A current is needed of 0.95 A and 0.44 A respectively. The average required electrical power, and thus generated heat, for the worst case scenario can be calculated with Equation G19.

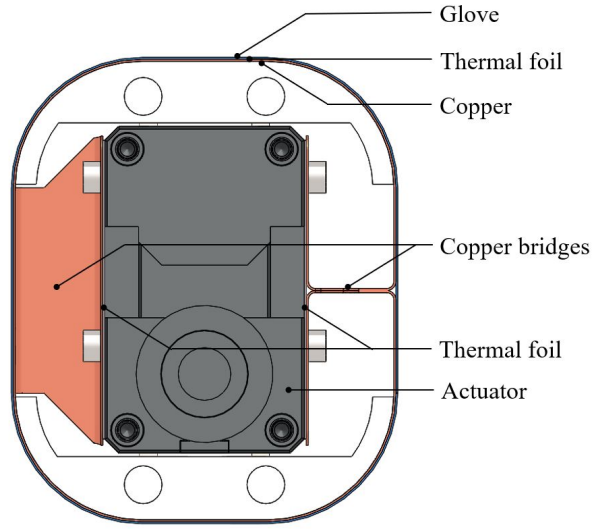

FIG. 31: Cross-section of the wrist design of the gripper.

$$P_{elec} = \dot{Q} = 0.25\ V\ I_{grasp} + 0.75\ V\ I_{maintain} \tag{G19}$$

In this equation, $\dot{Q}$ is the generated heat to be dissipated, V is the potential difference and I is the current for grasping and maintaining grasp. The potential difference of the actuator is 12 V. By filling in the equation, the generated heat in the worst case scenario can be determined, namely 6.8 W.

Heat dissipation gripper

The actuator is positioned in the wrist of the gripper, so the wrist design must allow for high heat dissipation. For the design, the requirement was kept in mind that the gripper must be water resistant and disinfectable, and could therefore not make use of airflow through the wrist.

The wrist design of the gripper is presented in Figure 31. The heat flows from the actuator to the outside air, via thermal foil, copper bridges, copper sheet, thermal foil and the glove respectively. The thermal foil on top of the actuator needs to ensure high thermal conductivity between the actuator and copper bridges, by eliminating air gaps. The copper bridges are folded pars of the copper sheet surrounding the wrist, and are needed to conduct the heat from the actuator to the outside of the wrist. The material copper was chosen, as it has the highest thermal conductivity of all affordable and feasibly manufacturable materials. The copper sheet surrounding the wrist is needed to ensure approximately equal temperature distribution at the surface of the wrist, instead of having peaks in

temperature where the copper bridges are positioned. The glove around the wrist is needed for disinfectability of the gripper. The thermal foil between the glove and the copper sheet is filler material, but with a specific reason. As described in the requirements, the wrist must be safe to touch for a contact period up to 10 s. According to the ECMA Standard for safety of electronic equipment, the surface temperature may be 10° C higher for non-metallic materials than for metallic materials considering safety [19]. If the metallic material, however, is covered with a non-metallic material of at least 0.3mm, the surface material can be considered non-metallic. As the surface of the wrist must be cooled with natural convection and radiation, both strongly correlated with the temperature difference, a higher surface temperature is highly beneficial for the heat flow. Therefore, the thermal foil in combination with the glove was used to create a non-metallic cover of more than 0.3mm, allowing for a safe high temperature surface. The thermal foil is connected to the copper and copper bridges using thermal glue, having high thermal conductivity.

Figure 32 shows a simplified representation of the realistic wrist design in Figure 31. Under the simplified representation, an indicative graph is shown, visualising the heat transfer through each layer of the wrist. It can be seen that the shape of the wrist has been simplified to a circular shape, instead of the rounded rectangular shape. This simplification was done in order to make heat transfer analysis less complex. A circular shape could be considered a good approximation of the actual rectangular shape, as the rectangular shape has highly rounded edges. In the equations, the diameter of the circular wrist was taken such that its circumference equals that of the actual wrist design. Figure 32 was taken as basis for the equations below.

Heat flow through each layer of the wrist is in series. Therefore, the total amount of heat flow through each layer must be equal, and is also equal to the total amount of heat dissipated. Equation G20 shows this in formula form.

$$\dot{Q} = \dot{Q}_1 = \dot{Q}_2 = Q_3 = \dot{Q}_4 = Q_5 = \dot{Q}_6 \tag{G20}$$

Heat flows $\dot{Q}_1$ up to $\dot{Q}_5$ are in the form of conductive heat transfer, as they pass through solid materials. Heat flow to the environment, $\dot{Q}_6$, consists of radiative and convective heat transfer.

The copper sheet, thermal foil and glove surrounding the wrist have negligible thickness compared to the radius of the wrist. Therefore, the conductive heat transfer were approximated as heat transfer through flat sheets,

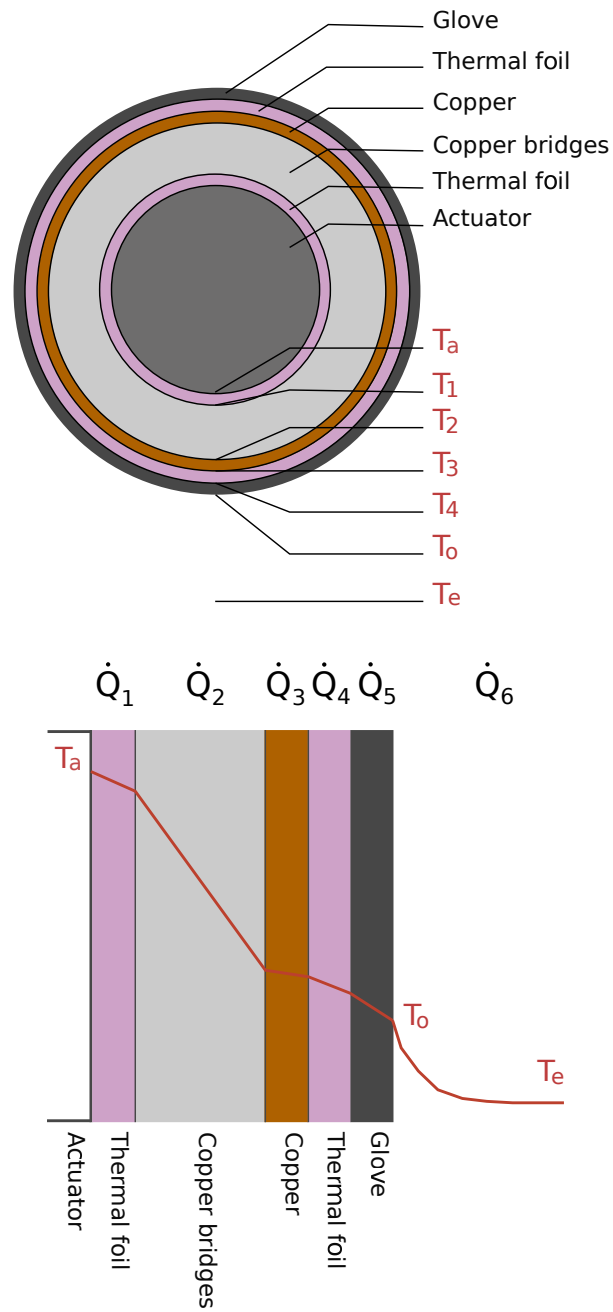

FIG. 32: Simplified representation of the wrist cross-section and graph of the heat transfer through each layer.

instead of cylindrical shells. Furthermore, the assumption was made that each layer wall is isothermal. This assumption will be checked for validity later in this section. Thermal glue and potential films of air between layers have been neglected. Also, no heat transfer is assumed through the flat ends of the cylinder. 3D printed material, namely, encloses the wrist design in both axial directions. The 3D-printed material, PLA, and the enclosed pockets of air in the parts, result in high isolating

properties compared to radial direction. Following these assumptions, the conductive heat transfer through each layer could be described with Fourier's law, as presented in equationG21.

$$\begin{aligned}\dot{Q}_1 &= \frac{k_{f1}A_{f1}}{L_{f1}}(T_a - T_1)\\ \dot{Q}_2 &= \frac{k_b A_b}{L_b}(T_1 - T_2)\\ \dot{Q}_3 &= \frac{k_c A_c}{L_c}(T_2 - T_3)\\ \dot{Q}_4 &= \frac{k_{f2}A_{f2}}{L_{f2}}(T_3 - T_4)\\ \dot{Q}_5 &= \frac{k_g A_g}{L_g}(T_4 - T_o)\end{aligned} \tag{G21}$$

Here, the subscript $f1$ is used for the thermal foil on the actuator, b for the copper bridge, c for the copper sheet, $f2$ for the thermal foil surrounding the wrist and g for the glove. Furthermore, k is the thermal conductivity, A the cross-sectional area, L the thickness of the material, and T is the temperature. The temperatures T are defined in Figure 32. T_a indicates the temperature of the actuator, T_o is the temperature of the outer surface and T_e is the environment temperature.

The heat transfer between the outer surface of the wrist and the environment, Q_6, consists of radiative and convective heat transfer, as presented in Equation G22.

$$\dot{Q}_6 = \dot{Q}_{rad} + \dot{Q}_{conv} \tag{G22}$$

The radiative heat transfer between the outer surface of the wrist and the environment can be calculated using Equation G23.

$$\dot{Q}_{rad} = \frac{\sigma(T_e^4 - T_o^4)}{\frac{1-\epsilon_o}{A_o\epsilon_o} + \frac{1}{A_o F_{o\to e}} + \frac{1-\epsilon_e}{A_e\epsilon_e}} \tag{G23}$$

In this equation, σ is the Stefan–Boltzmann constant, ϵ is the emissivity of the surface, and $F_{g\to e}$ is the view factor. The subscript o indicates the outer surface of the wrist, which is the same as the outer surface of the glove. The subscript e is used for the environment.

For the radiation, the assumption is made that the gripper is in a empty room with uniform temperature and uniform emissivity. Following this assumption, the view factor $F_{g\to e}$ is equal to one. The total surface of the room has insignificant influence on the radiative heat transfer, but for the sake of quantitative calculations a room has been assumed of 100 m^2.

At the outer surface of the glove, heat transfer is also caused due to natural flow of the environment air across the wrist. This convective heat transfer can be calculated with Equation G24.

$$\dot{Q}_{conv} = h_c A_g (T_o - T_e) \tag{G24}$$

In the equation, h_c is the convective heat transfer coefficient. The equation for the convective heat transfer coefficient can is presented in Equation G25.

$$h_c = \frac{k_e}{D_o}\overline{Nu}_D \tag{G25}$$

Here, k_e is the thermal conductivity of the environment air, evaluated at mean film temperature. D_o is the outer diameter of the wrist, and is therefore equal to the outer diameter of the glove. The Nusselt number is denoted as Nu_D. As presented in Figure 32, the shape of the wrist is simplified to a cylinder. The assumption was made that the wrist of the gripper is horizontal for most tasks. Therefore, the Nusselt number for natural flow on a horizontal cylinder was used to approximate the natural convection on the wrist. The equation for the Nusselt number on a horizontal cylinder is given by Equation G26 [55].

$$\begin{aligned}\overline{Nu}_D =& 0.36 + \frac{0.518 Ra_D^{1/4}}{[1 + (0.559/Pr)^{9/16}]^{4/9}},\\ &\text{if } 10^{-4} < Ra_D \simeq 10^9\end{aligned} \tag{G26}$$

In this formula, Pr is the Prandtl number and Ra_D is the Rayleigh number, both evaluated at mean film temperature. The Rayleigh number can be determined using Equation G27.

$$Ra_D = \frac{\beta \Delta T g D_o^3}{\nu^2} Pr \tag{G27}$$

Here, β is the thermal expansion coefficient, ΔT is the temperature difference between the outer surface of the wrist and the environment air, g is the gravitational acceleration, D_o is the outer diameter of the wrist, ν is the kinematic viscosity, and Pr the Prandtl number.

Equation G28 describes the mean film temperature T_{mf}, at which the preceding properties of the air must be evaluated.

$$T_{mf} = \frac{\Delta T}{2} = \frac{T_o - T_e}{2} \tag{G28}$$

Quantitative evaluation and results

The situation considered for the heat dissipation is the worst case scenario load cycle, as described before. Under these conditions, the maximum heat dissipation will

be evaluated. The maximum heat dissipation will occur when the outer surface of the wrist has reached the maximum temperature allowed for safety, or at the maximum operating temperature of the actuator, whichever is reached first.

The quantitative values used for calculating the heat transfer are given in Table X. Using Matlab, the presented set of equations is solved to determine the heat transfer capacity and temperatures of each layer surface. The results can be viewed in Table XI.

As presented in the table, the heat dissipation capacity of the gripper wrist is 7.72 W. The generated heat in the worst case scenario is 6.8 W, as calculated earlier. Therefore, it could be concluded that the wrist has the capacity to dissipate the heat generated by the actuator in any scenario.

Evaluating the table, it can also be seen that with the maximum allowed surface temperature of the wrist, the motor does not reach the overheating temperature of 80° C.

Assumption validation

As described, for the preceding heat transfer calculation it was assumed that each layer has an isothermal surface area. For most layers this approximation is intuitive, as the preceding layer has approximately the same surface area. For the copper sheet however, the heat flows from the bridges to the copper sheet, so from a relatively small cross-sectional area to a large one. In this case, heat must not only flow in radial direction, but also in tangential direction to flow through the copper sheet.

Determining the exact tangential heat flow, to check whether the isothermal assumption is valid, is very complex. Many aspects of heat transfer interact. For example, when heat flows through the copper sheet in tangential direction, the average temperature of the copper sheet will increase. This will increase the convection and radiation on the outer surface of the wrist, as these are both strongly related to the temperature difference with the environment. Therefore, the heat flow to the environment will increase, which results in a decreased relative heat flow in tangential direction, increasing again the temperature difference in the copper sheet.

To validate the isothermal assumption, the complex problem has been simplified. Validation of the isothermal assumption was based on thermal resistance. It is known that heat follows the road of least resistance. If the tangential thermal resistance in the outside of the wrist would be lower than the radial thermal resistance, an isothermal copper sheet could be seen as an acceptable estimation of the real world.

The heat flow in tangential direction can flow through the copper sheet, thermal foil and the glove. Heat flow in the three layers is in parallel. The thermal resistance of the wrist in tangential could therefore be determined using Equation G29.

TABLE X: Values for physical quantities used in the heat transfer equations

	Value	**Unit**	**Notes**
T_o	338	K	Max. allowed
T_e	293	K	Assumed room temperature
T_{mf}	315.5	K	
k_e	0.0278	W/mK	At mean film temperature
β	2.5e-03		For ideal gas
ν	1.699e-05	m^2/s	At mean film temperature
Pr	0.69		At mean film temperature
g	9.81	m/s^2	
k_{f1}	6.5	W/mK	Value given by manufacturer
k_b	401	W/mK	Value given by manufacturer
k_c	401	W/mK	Value given by manufacturer
k_{f2}	6.5	W/mK	Value given by manufacturer
k_g	0.24	W/mK	Value for nitril
L_{f1}	0.25	mm	
L_b	11.5	mm	
L_c	0.3	mm	
L_{f2}	0.25	mm	
L_g	0.085	mm	
σ	5.670e-08	$Wm^{-2}K^{-4}$	
$F_{o\rightarrow e}$	1		
ϵ_o	0.97		Value taken for black rubber
ϵ_e	0.93		Value taken for brick
D_o	67.4	mm	Based on circumference real wrist
A_{f1}	2,647	mm^2	Measured in CAD model
A_b	29.18	mm^2	Measured in CAD model
A_c	13,817	mm^2	Measured in CAD model
A_{f2}	14,353	mm^2	Measured in CAD model
A_g	14,389	mm^2	Measured in CAD model
A_e	100	m^2	Assumption

TABLE XI: Results regarding heat transfer through the wrist, following the equations and values presented.

	Value	**Unit**	**Description**
$\dot{Q}_{rad}$	4.50	W	Radiative heat transfer
$\dot{Q}_{conv}$	3.22	W	Convective heat transfer
$\dot{Q}$	7.72	W	Maximum heat dissipation
T_a	72.90	$°C$	Temperature outside actuator
T_1	72.79	$°C$	Temperature outside foil 1
T_2	65.21	$°C$	Temperature outside copper bridge
T_3	65.21	$°C$	Temperature outside copper
T_4	65.19	$°C$	Temperature outside foil 2
T_o	65.0	$°C$	Temperature outside glove
T_e	20.0	$°C$	Temperature environment air

$$
\begin{aligned}
R_{tan,c} &= \frac{L_{tan}}{A_{tan,c}\ k_c} \\
R_{tan,f2} &= \frac{L_{tan}}{A_{tan,f2}\ k_f 2} \\
R_{tan,g} &= \frac{L_{tan}}{A_{tan,g}\ k_g} \\
R_{tan} &= (\frac{1}{R_{tan,c}} + \frac{1}{R_{tan,f2}} + \frac{1}{R_{tan,g}})^{-1}
\end{aligned}
\tag{G29}
$$

In these equations, the subscript c is used for the copper sheet, $f2$ for the thermal foil and g for the glove. Furthermore, L_{tan} is the furthest point in tangential direction from one of the copper bridges, so the maximum distance the heat needs to travel through the layers. For the wrist design A_{tan} is the cross-sectional area of the layer in tangential direction. For the wrist design, L_{tan} is 45 mm, $A_{tan,c}$ is 20.4 mm^2, $A_{tan,f2}$ is 17 mm^2 and $A_{tan,g}$ is 5.78 mm^2.

The thermal resistance in radial direction, starting from the copper sheet, consists of the thermal resistance of conductance through the thermal foil, conductance through the glove and convection and radiation to the environment. Resistance due to convection and radiation are in parallel, and these two are in series with the convection resistances. Therefore, the thermal resistance in radial direction can be determined using Equation G30

$$
\begin{aligned}
R_{radial,f2} &= \frac{L_{f2}}{A_{f2}\ k_f 2} \\
R_{radial,g} &= \frac{L_g}{A_g\ k_g} \\
R_{conv} &= \frac{1}{h_c\ A_g} \\
R_{rad} &= \frac{1}{\epsilon_o\ \sigma\ A_g\ (T_o^2 + T_e^2) * (T_o + T_e)} \\
R_{radial} &= R_{radial,f2} + R_{radial,g} + (\frac{1}{R_{conv}} + \frac{1}{R_{rad}})^{-1}
\end{aligned}
\tag{G30}
$$

Doing the calculations with the presented values, it was obtained that R_{tan} and R_{radial} are 5.4 K/W and 5.9 K/W respectively. The thermal resistance in tangential direction was therefore shown to be lower than the thermal resistance in radial direction. This means that heat will flow relatively easily through the whole circumference of the wrist, making the isothermal assumption of each layer reasonable. It has to be noted, however, that in reality the layers can not be completely isothermal, resulting in surface areas with lower temperatures. The small differences in temperature result in a minor decrease in heat dissipation. Furthermore, no air gaps have been assumed in between layers. In reality, some air will be trapped, resulting in higher thermal resistance and thus a somewhat lower heat dissipation. Also, on a warm day the environment air will be higher than 20° C, which also lowers the heat dissipation. On the other hand, no heat transfer trough the flat ends of the cylindrical wrist has been assumed. In reality, some heat will flow through these ends, increasing heat dissipation. Also, no air flow across the wrist was assumed, but in reality the gripper will often move through the environment. Due to the movements, air flow across the wrist is generated, which means that the convective heat transfer and thus the heat dissipation is increased. Taking each notion into account, the approximation of the heat dissipation is assumabbly reasonable.

Appendix H:
Gripper control

For testing the RPG, 4FH and 4FH-i, an open loop control scheme was designed. The electrical circuit of the open loop control consists of a potentiometer, servo, Arduino, Arduino shield and a 12 V power supply. How the components are connected in the electrical circuit is shown in Figure 34. In the setup used for testing, the potentiometer was pinned on a breadboard. This was done to make operating the potentiometer easier. For simplicity of the visualisation of the electrical circuit, the breadboard was disregarded.

For proving the potential usefulness of the force sensor in the 4Fh and 4FH-i, a closed loop control scheme was designed. The electrical circuit of the closed loop control consists of the same items as the open loop control, in combination with a FSR sensor for force sensing. The electrical circuit for the closed loop control is presented in Figure 35. A resistor is needed for the connection of the FSR. A resistor with resistance in the range of 3k - 100k needs to be used. The resistance influences the sensitiveness of the FSR. See Figure 33 for an indication of how the FSR output is influenced by the choice of resistor. Please note that the diagram is for the same type of FSR, but with a different sensing range. The sensing range of the FSR in the diagram is 0.2 N to 20 N. The sensing range of the FSR used in the 4FH and 4FH-i has a sensing range from 0.5 N to 150 N. Therefore, Figure 33 should be used as an indication of relative behaviour only.

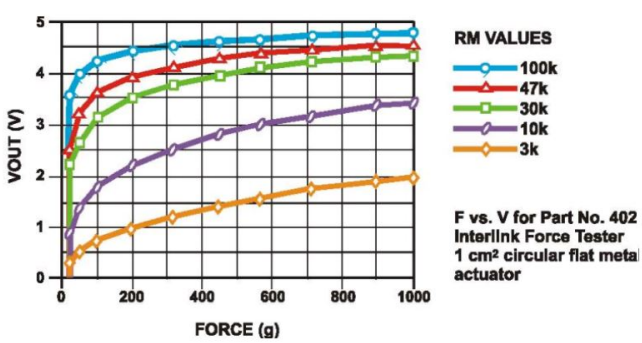

FIG. 33: Indication of the influence of the resistance on the sensitiveness of the FSR [56]. Note that the scheme is for the same type of FSR, but with a different sensing range.

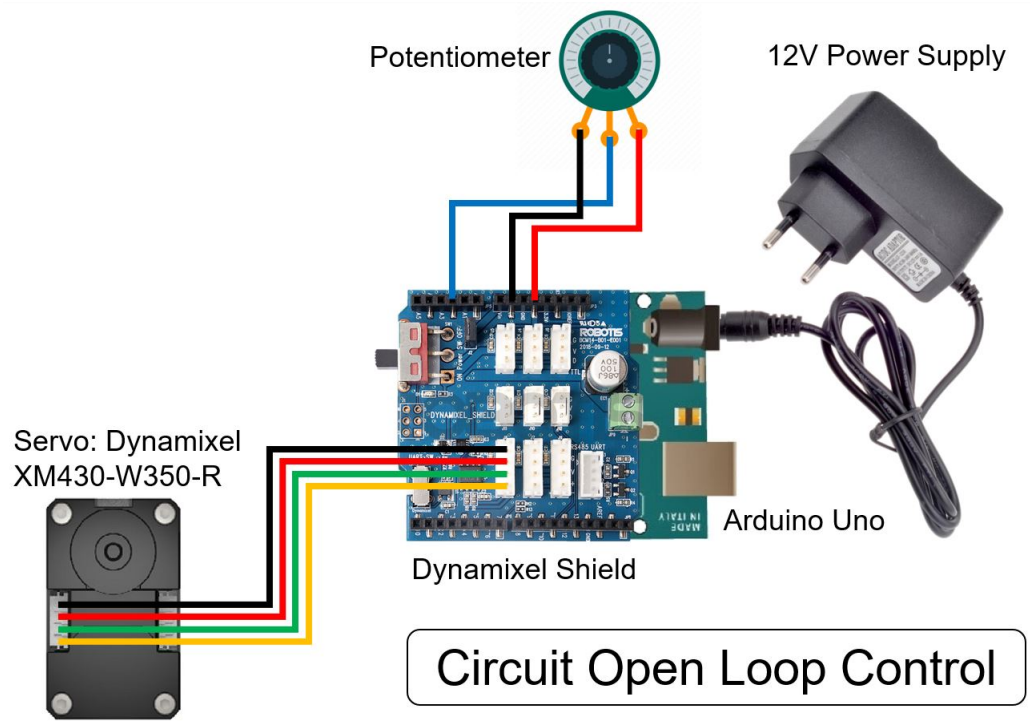

FIG. 34: Electrical circuit of the open loop control used for testing the RPG, 4FH and 4FH-i

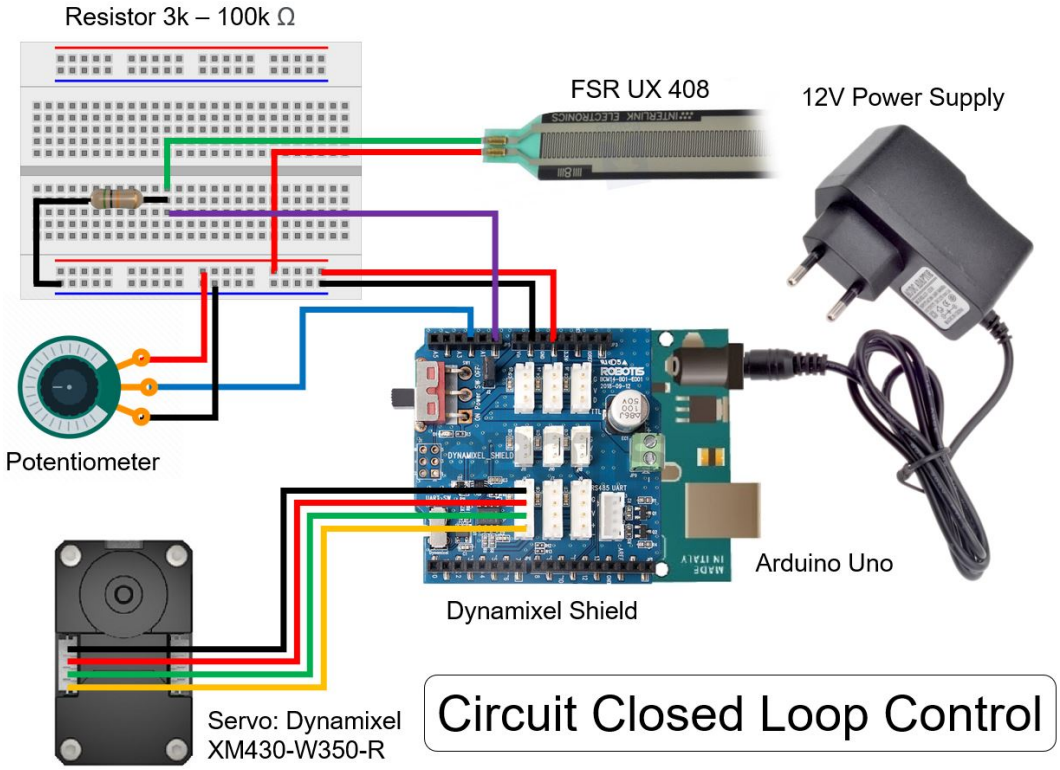

FIG. 35: Electrical circuit of the closed loop control used for proof of concept of the FSR in the 4FH and 4FH-i

Appendix I:
Functional performance testing

1. EIT

For the Essential Items Test (EIT), nine objects need to be used. The objects are presented in Table XII, including their weights and sizes. A picture of the set of objects can be found in Figure 36.

Each object must be positioned in the conventional non-supported orientation of the object. For clarification, the conventional non-supported orientation of each object will be described. The pill box should lay flat, so with the largest side parallel to the surface of the table or ground. The credit card should be laid flat as well. The keys can just be laid on the table or ground without concern about the orientation. The wallet and cloth should be laid flat as well, with the largest side parallel to the supporting surface. The mug should be positioned as normal, so with the open side on top. The same is true for the plastic bottle and bowl. It is advisable, however, to close the bottle with a bottle cap to avoid spillage. The tv-remote should be positioned such that the buttons are facing up.

The cloth should be folded through the middle three times before performing the test. The 0.5L plastic bottle should be filled with water. The mug, however, should be empty. For the keys item, a key chain with 5 keys was used. More or less keys may be used as well, provided that it remains a key chain and not one single key.

The prescribed height of the table to perform the EIT on is 75 to 80 cm. This height was chosen, because this is the most occurring table height, and thus a good representation of a real environment.

TABLE XII: Detailed list of specifications for items used for the Essential Items Test

Essential item	Mass [g]	Size [mm]	Notes
Pill box	18	120x50x18	
Credit card	3	86x54x0.7	
Keys	54	80x60x20	5 keys
Wallet	120	105x80x20	
Cloth	76	600x480x1	Folded trice
Mug	331	85x97	Empty
Plastic bottle	521	60x225	0.5L, filled
TV-remote	176	235x50x35	
Bowl	105	130x70	

FIG. 36: Set of nine objects used for the Essential Items Test (EIT)

2. Modified AHAP

The modified AHAP has been conducted for assessing grasp stability of the 4FH compared to the RPG. The original AHAP consists of 24 objects, and 26 tasks. The developers have selected the list of objects from the Yale-CMU-Berkeley (YCB) Object and Model set. This set of objects is carefully composed for use in prosthetic and robot gripper design as well as for rehabilitation research, consisting of everyday items with different shapes, weight, sizes and rigidity [57]. Therefore, each object of the AHAP can be found in the YCB Object and Model set, including the prescribed weights and sizes. One object of the AHAP, however, is not named in the YCB Object and model set, being task T_{19}, "Wood blocks with rope". T_{19} refers to the original numbering of each task, presented by the developers of the AHAP [25]. Due to the absence of this item in the YCB Object and Model set, no prescribed weights and sizes could be found for task T_{19}. Therefore it has been chosen to disregards this task. Furthermore, the two non-grasping tasks of the AHAP, T_{09} and T_{18} for index pressing a timer and holding a plate with platform grip respectively, were disregarded as well in this study. Both tasks originally are scored on performing the correct grip type only. As described in Section 2.3.1, however, this type of scoring was not found relevant for the gripper of this study.

TABLE XIII: Detailed list of specifications for object of the AHAP, as used in this study and as described in literature [25, 57]

Task		Object	Mass [g]	Size [mm]
T_{01}	Used	Skillet lid	512	250x40
	Prescribed	Skillet lid	652	270x10x22
T_{02}	Used	Apple	139	70
	Prescribed	Plastic apple	68	75
T_{03}	Used	Large marker	14	16x138
	Prescribed	Large marker	15.8	18x121
T_{04}	Used	Plate	255	200x18
	Prescribed	Plate	279	258x24
T_{05}	Used	Empty bottle	122	70x230
	Prescribed	Chips can	205	75x250
T_{06}	Used	Screwdriver	55	30x180
	Prescribed	Philips screwdriver	97	31x215
T_{07}	Used	Bowl	116	135x70
	Prescribed	Bowl	147	159x53
T_{08}	Used	Small marker	6	10x130
	Prescribed	Small marker	8.2	8x135
T_{09}	Used	N.A.	-	-
	Prescribed	Timer	N.A.	N.A.
T_{10}	Used	Pitcher base	275	220x110x250
	Prescribed	Pitcher base	178	108x235
T_{11}	Used	Play ball	183	90
	Prescribed	Softball	191	96
T_{12}	Used	Tuna can	107	70x35
	Prescribed	Tuna can	171	85x33
T_{13}	Used	Cracker box	144	70x125x140
	Prescribed	Cracker box	411	60x158x210
T_{14}	Used	Glass jar	412	100x124
	Prescribed	Coffee can	414	102x139
T_{15}	Used	Spatula	26	30x80x330
	Prescribed	Spatula	51.5	35x83x350
T_{16}	Used	XS clamp	17	90x70x12
	Prescribed	XS clamp	19.2	85x65x10
T_{17}	Used	Pear	213	63
	Prescribed	Plastic pear	33	59
T_{18}	Used	N.A.	-	-
	Prescribed	Plate	279	258x24
T_{19}	Used	N.A.	-	-
	Prescribed	Wood blocks on rope	-	-
T_{20}	Used	Kids soccer ball	65	110
	Prescribed	Mini soccer ball	123	140
T_{21}	Used	Ping-pong ball	1	40
	Prescribed	Golf ball	46	42.7
T_{22}	Used	Gravy mix box	125	35x125x85
	Prescribed	Chocolate pudding box	187	35x110x89
T_{23}	Used	Power drill	923	45x180x200
	Prescribed	Power drill	895	35x46x184
T_{24}	Used	Skillet	809	250x25x50
	Prescribed	Skillet	950	270x25x30
T_{25}	Used	Key	3	20x54x4
	Prescribed	Key	10.1	23x43x2.2
T_{26}	Used	Washer 10mm	1	10
	Prescribed	Washer 10mm	0.7	10

In Table XIII, the prescribed objects for the AHAP are presented, including sizes and weights, as described in the YCB Object and Model set. Some of the objects were not available in this study, in which case an object was chosen closely resembling the prescribed object. The objects actually used for the modified AHAP of this study, including sizes and weights, are presented in Table XIII as well, to allow for comparison.

Figure 37 presents pictures of testing both grippers. Here, the used objects for the test can be seen, as well as the used orientation of the object and gripper for each task.

3. Modified SHAP

a. *Scoring*

Scores for the conducted SHAP were generated using the alternative scoring method presented by Burgerhof et al. in 2017 [41]. The alternative method computes a score for overall functional performance, named the W-LIF. Also, separate sub-scores for six prehensile patterns can be generated, named the LIFPP. Following the alternative method as presented in literature, the scores could be obtained as follows.

For each task, normative completion times, n, are presented by the developers of SHAP, based on completion times for healthy human hands. The time limit, m, for completing each task is eight times the normative completion time. The time in which a task is completed during the assessment is to be transformed to a value between 0 and 100. Here, 0 indicates a completion time equal to or higher than the maximum, and 100 indicates a completion time equal to or lower than the norm. The transformed time score, T_s, is calculated as presented in Equation I1.

$$\begin{aligned} T_s &= 100\frac{8n-t}{8n-n} \\ &= 100\frac{8n-t}{7n} \end{aligned} \tag{I1}$$

The LIFPP score is the mean of all transformed time scores, related to the prehensile pattern in question. Consequently, the LIFPP scores can be obtained using Equation I2.

$$LIFPP = \frac{1}{k}\sum_{j=1}^{k} T_{s_j} \tag{I2}$$

Here, k represents the amount of tasks related to the specific prehensile pattern.

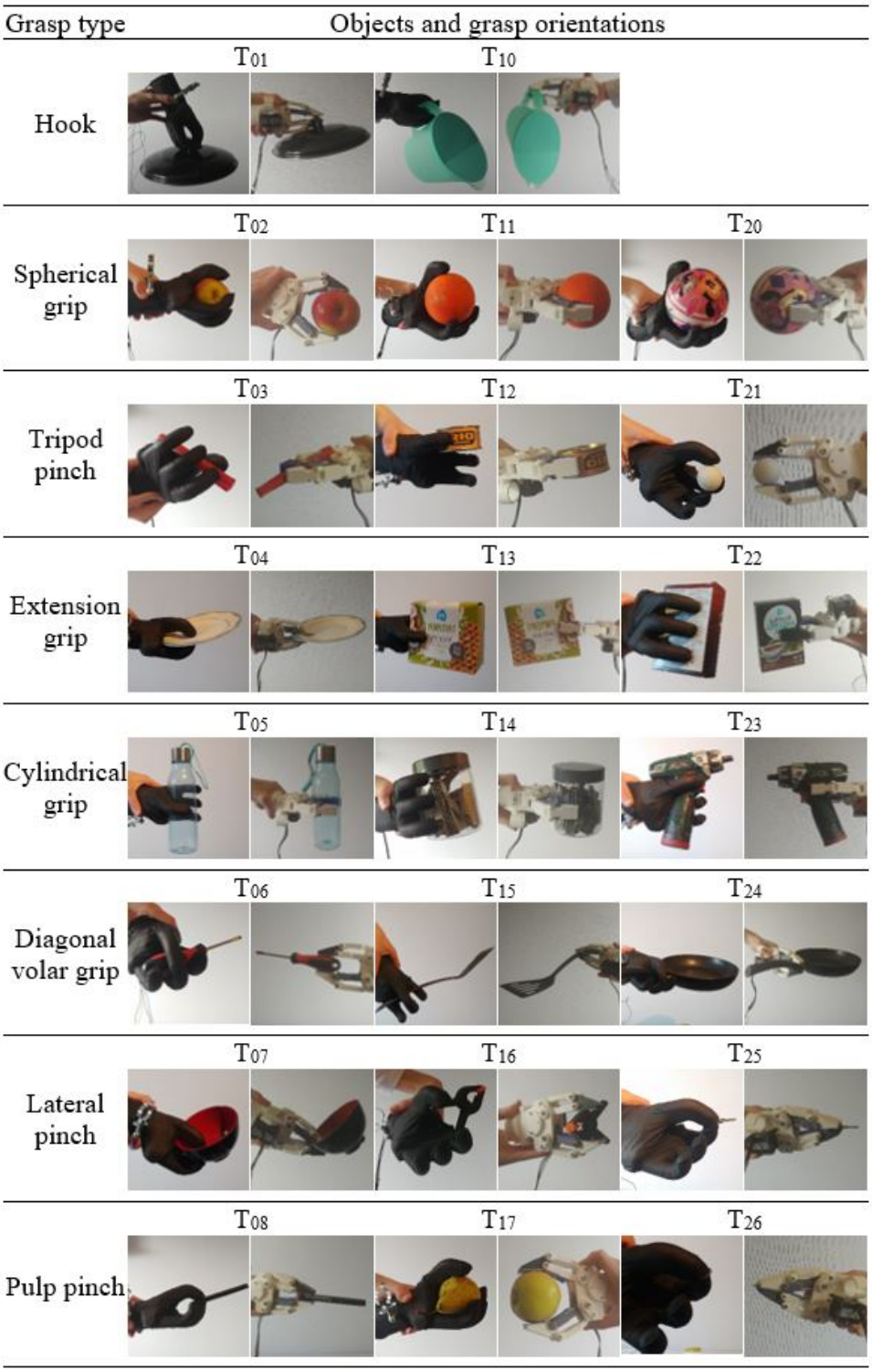

FIG. 37: Presentation of how the AHAP was conducted for both grippers, showing the object orientations and grasps used for each item.

Some of the tasks of the SHAP are each related to two prehensile patterns. These tasks are said to reflect important aspects of functional performance, and should therefore weigh more for the overall score. Therefore, the overall score of the SHAP, the W-LIF, is not simply equal to the mean of all transformed time scores. The W-LIF is a weighted mean of all LIFPP scores. Equation I3 shows how to compute the W-LIF, as presented in literature.

$$
\begin{aligned}
W-LIF =& \frac{1}{a}\ (k_{spherical}LIF_{spherical} + k_{tripod}LIF_{tripod} + \\
& k_{power}LIF_{power} + k_{lateral}LIF_{lateral} + \\
& k_{tip}LIF_{tip} + k_{extension}LIF_{extension}) \\
a =& k_{spherical} + k_{tripod} + k_{power} + k_{lateral} + \\
& k_{tip} + k_{extension}
\end{aligned} \tag{I3}
$$

As before, k indicates the amount of tasks, related to the prehensile pattern of the annotation. It can be noted that with this computation, tasks related to two prehensile patterns have a higher impact as other tasks.

In this study, a modified version of the SHAP has been used, in which some tasks were disregarded and some were added. It has been chosen to generate a separate LIFPP sub-score for the added tasks, hereafter named LIF_{extra}. The extra tasks could also be subdivided over the sub-scores for the prehensile patters, but this has not been done for multiple reasons. The extra tasks would need to be evaluated on which prehensile pattern(s) it relates to. If an incorrect prehensile pattern is chosen, the scores become less reliable. Also, by keeping the set of tasks related to a certain prehensile pattern the same, the scores present validated test results for the prehensile patterns, not spoiled by extra non-validated tasks. Furthermore, a separate sub-score for the extra tasks allows for easy evaluation of the performance on the extra tasks. Therefore, all added tasks were grouped to form an extra sub-score, the LIF_{extra}. The W-LIF computation for the modified SHAP therefore becomes as presented in Equation I4

$$
\begin{aligned}
W-LIF =& \frac{1}{a}\ (k_{spherical}LIF_{spherical} + k_{tripod}LIF_{tripod} + \\
& k_{power}LIF_{power} + k_{lateral}LIF_{lateral} + \\
& k_{tip}LIF_{tip} + k_{extension}LIF_{extension}) + \\
& k_{extra}LIF_{extra} \\
a =& k_{spherical} + k_{tripod} + k_{power} + k_{lateral} + \\
& k_{tip} + k_{extension} + k_{extra}
\end{aligned} \tag{I4}
$$

In Table XIV is presented which tasks are related to which prehensile patters, and thus to which sub-scores. The normative completion times, presented in literature, can be found in this table as well [41]. The tasks in the table in grey are the tasks disregarded for the modified SHAP. From this table, the k values for Equation I2 to I4 can be determined. For the modified SHAP, the k values are 3, 2, 5, 5, 5, 2 and 6 respectively for the prehensile patterns spherical, tripod, power, lateral, tip and extension, and the extra tasks.

TABLE XIV: Presentation of which tasks are related to which sub-scores of the modified SHAP. Also, normative completion times are presented. The tasks in grey are the SHAP tasks disregarded for the modified SHAP

Task	**Prehensile pattern and sub-score**	**Norm time**
Abstract objects - Lightweight		
Spherical	Spherical	1.63
Tripod	Tripod	1.66
Power	Power	1.77
Lateral	Lateral	1.77
Tip	Tip	1.59
Extension	Extension	1.78
Abstract objects - Heavyweight		
Spherical	Spherical	1.84
Tripod	Tripod	1.58
Power	Power	1.76
Lateral	Lateral	1.84
Tip	Tip	1.61
Extension	Extension	1.71
Activities of Daily Living		
Coins	Tip	4.41
Button board	Tripod and tip	6.77
Cutting	Tripod and power	3.12
Page turning	Extension	1.8
Jar lid	Spherical	2.26
Jug pouring	Lateral	4.66
Carton Pouring	Spherical	5.79
Full Jar	Power	2.1
Empty tin	Power	1.77
Tray lift	Lateral and extension	3.02
Key	Lateral and tip	1.78
Zip	Lateral and tip	2.43
Screwdriver	Power	3.9
Door handle	Power	1.49
Extra tasks		
Credit card	Extra	*1.32
Plate	Extra	*1.42
Cloth	Extra	*1.36
Mug	Extra	*1.26
Grocery bag	Extra	*2.67
Drawer	Extra	*2.18

* Self-determined normative completion time, see Table XV

For the extra tasks of the modified SHAP, naturally no normative completion times can be found in literature. Therefore, normative completion times were generated in this study. The norm times were determined by repetitively executing the extra tasks with a healthy dominant hand. Two subjects executed each task 20 times. The mean of all obtained completion times was taken as the normative completion time for the scoring of the modified SHAP. Completion times for the normative time genera-

TABLE XV: Generation of normative completion times for scoring the extra tasks of the modified SHAP

Subject 1 Age: 21 Gender: Female Dominant hand: Right

Task	**Time [sec]**																						
Trial	**1**	**2**	**3**	**4**	**5**	**6**	**7**	**8**	**9**	**10**	**11**	**12**	**13**	**14**	**15**	**16**	**17**	**18**	**19**	**20**	**Mean**	**Deviation**	**Mean both**
Credit card	1.56	1.25	1.35	1.66	1.32	1.31	1.35	1.41	1.50	1.50	1.37	1.31	1.34	1.32	1.37	1.38	1.41	1.31	1.38	1.34	1.39	0.10	1.32
Plate	1.53	1.35	1.47	1.53	1.35	1.53	1.37	1.44	1.47	1.50	1.53	1.44	1.50	1.63	1.57	1.47	1.47	1.53	1.44	1.44	1.48	0.07	1.42
Cloth	1.44	1.66	1.56	1.56	1.53	1.38	1.47	1.53	1.47	1.59	1.53	1.44	1.37	1.50	1.56	1.46	1.43	1.41	1.40	1.50	1.49	0.08	1.36
Mug	1.31	1.41	1.37	1.32	1.28	1.25	1.28	1.29	1.29	1.25	1.25	1.22	1.25	1.37	1.25	1.19	1.13	1.18	1.31	1.35	1.28	0.07	1.26
Grocery bag	2.78	2.81	2.66	2.78	2.72	2.71	2.88	2.81	2.62	2.78	2.72	2.75	2.97	2.84	2.72	2.59	2.78	2.59	2.84	2.50	2.74	0.11	2.67
Drawer	2.37	2.25	2.31	2.25	2.22	2.19	2.38	2.16	2.25	2.22	2.25	2.28	2.31	2.22	2.47	2.32	2.38	2.44	2.34	2.19	2.29	0.09	2.18

Subject 2 Age: 23 Gender: Male Dominant hand: Right

Trial	**1**	**2**	**3**	**4**	**5**	**6**	**7**	**8**	**9**	**10**	**11**	**12**	**13**	**14**	**15**	**16**	**17**	**18**	**19**	**20**	**Mean**	**Deviation**	**Mean both**
Credit card	1.40	1.41	1.25	1.15	1.25	1.25	1.15	1.31	1.31	1.22	1.19	1.16	1.16	1.22	1.22	1.28	1.37	1.28	1.28	1.21	1.25	0.08	1.32
Plate	1.41	1.43	1.37	1.37	1.38	1.38	1.37	1.34	1.28	1.41	1.31	1.31	1.35	1.35	1.44	1.28	1.35	1.25	1.40	1.31	1.35	0.05	1.42
Cloth	1.19	1.15	1.31	1.19	1.19	1.31	1.22	1.15	1.13	1.22	1.31	1.22	1.28	1.31	1.25	1.29	1.22	1.15	1.22	1.22	1.23	0.06	1.36
Mug	1.31	1.31	1.28	1.31	1.28	1.19	1.15	1.31	1.25	1.13	1.22	1.22	1.25	1.16	1.25	1.22	1.25	1.22	1.19	1.28	1.24	0.06	1.26
Grocery bag	2.81	2.56	2.78	2.91	2.62	2.66	2.54	2.62	2.56	2.66	2.50	2.53	2.56	2.37	2.40	2.78	2.56	2.56	2.44	2.62	2.60	0.14	2.67
Drawer	2.00	2.07	2.06	2.25	2.00	2.06	2.10	1.97	2.28	1.97	2.03	2.03	1.94	2.06	2.15	2.28	2.06	1.91	2.06	2.16	2.07	0.11	2.18

Comparison with normative completion times presented in literature

Trial	**1**	**2**	**3**	**4**	**5**	**6**	**7**	**8**	**9**	**10**	**11**	**12**	**13**	**14**	**15**	**16**	**17**	**18**	**19**	**20**	**Mean**	**Deviation**	**Norm literature**
Light sphere	1.13	0.91	0.97	1.06	1.13	1.00	0.97	1.16	0.97	1.07	0.97	0.94	0.97	0.94	0.97	1.10	1.12	0.91	1.00	0.97	1.01	0.08	1.63

tion can be found in Table XV. This table also presents information about the two subjects.

In order to be able to compare the newly determined norm times for the extra tasks to norm completion times in literature, one subject also performed the lightweight sphere task 20 times with his dominant healthy hand. It was found that a significantly lower norm time was obtained in this study for the lightweight sphere as the norm time presented in literature. Therefore, it can be assumed that the norm times determined for the extra tasks are on the low side, and thus result in lower functional performance scores. For generating completely unbiased norm times, many more subjects would be needed. For the testing and scoring of this study, however, the potential bias in the norm times did not impose problems. The scoring and evaluation in this study, namely, was aimed at comparing functional performance between grippers of this study, each tested exactly identically. This way, mainly the relative scoring is of importance, not the absolute scoring.

FIG. 38: Set of objects used for the six added tasks of the modified SHAP

b. *Protocols extra tasks*

As presented before, the extra tasks of the modified SHAP consist of picking and placing a credit card, plate, cloth, mug and grocery bag, and opening and closing a drawer. A picture of the set of objects used can be found in Figure 38. Weights and dimensions of each object can be found in Table XVI. For the task of the grocery bag, a 1 kg weight is added to the bag.

Setting up

As for the original SHAP, the participant should be seated at a table. The table should be at elbow height. The SHAP form-board should be positioned on the table directly in front of the participant, with approximatley 8 cm space between the board and the table edge. For the extra tasks, the board should be with the white side facing up, being the side for the activities of daily living.

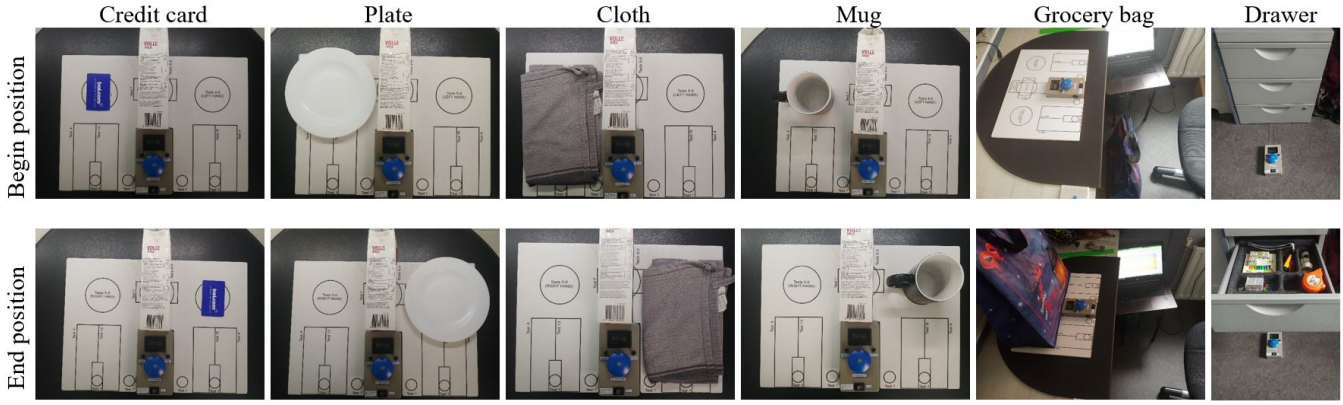

FIG. 39: Visualisation of the protocols for the added tasks of the modified SHAP

TABLE XVI: Detailed list of specifications for extra objects used for the added tasks of the SHAP

Extra task	Mass [g]	Size [mm]	
Credit card	3		86x54x0.7
Drawer	-	Handle size:	150x17
		Height from floor:	143
		Draw-out distance:	460
Plate	255		200x18
Grocery bag	112	.	403x218x443
	Added: 1101	Handle size:	140 x120
Cloth	76		600x480x1
Mug	331		85x97

Then perform each extra task according to the protocols below, in the presented order. The prescribed begin and end position of each item is also visualised in Figure 39.

Credit card

Place the credit card in the circle of the form board designated for test 5 to 9, on the left side for assessing (a gripper or prosthesis attached to the) right hand, and on the right side for the left hand. Use the empty carton to create a barrier, by placing it lengthwise along the middle of the form board, as done in ADL task 8 and 9 of the original SHAP. Start the timer with the hand or gripper under test. Lift the credit card over the carton, and place the credit card in the related circle on the other side of the board. Then, stop the timer with the hand or gripper under test.

Optional: If the credit card can not be picked up directly, it may be picked up using any method, as long only the hand or gripper under test is used. For example, the credit card may be slid to the edge of the board first. This option is also presented in the original SHAP for the task of picking up coins.

Plate

Center the plate on the same circle as used for the credit card. Leave the carton in the designated area in the middle of the board, to form a barrier. Start the timer with the hand or gripper under test. Lift the plate over the carton, and place the plate on the related circle on the other side of the board. Then, stop the timer with the hand or gripper under test.

Optional: As for the credit card task, it is allowed to pick up the plate using any method, when directly picking it up from its place is not possible. The plate may be slid to the edge of the board first.

Cloth

Fold the cloth through the middle thrice . Place the cloth on the left side of the board when assessing the right hand, and on the right side when assessing the left hand. The cloth should be laid flat, positioned in the middle between the top and bottom of the board, and touching the timer unit. Leave the carton in the designated area in the middle of the board. Start the timer with the hand or gripper under test. Lift the cloth over the carton, and place the cloth on the other half of the board. The cloth must remain folded and may not be crumpled after the pick and place task. Then, stop the timer with the hand or gripper under test.

Mug

Place the mug on the same circle as used for the credit card. Leave the carton in the designated area in the middle of the board. Start the timer with the hand or gripper under test. Lift the mug over the carton, and place the mug on the related circle on the other side of the board. Then, stop the timer with the hand or gripper under test.

Grocery bag

Move back the chair in which the participant is seated.

The distance between the chair and the edge of the table should be more than sufficient to place the grocery bag in between. Put the 1 kg weight in the middle of the grocery bag. Place the grocery bag on the ground, directly in front of the participant, between his or her feet and not under the table. The carton must be removed from the board. Start the timer with the hand or gripper under test. Pick up the grocery bag, and place it on the board behind the timer unit. Then, stop the timer with the hand or gripper under test.

Drawer

Let the participant sit directly in font of a drawer, with the handle of the drawer at elbow height. Position the timer unit 15 cm in front of the drawer. Start the timer with the hand or gripper under test. Open the drawer, until the drawer is fully opened. Then, close the drawer by completely guiding it, not by giving the drawer a push. When the drawer is fully closed, stop the timer with the hand or gripper under test.

Appendix J:
Statistical analysis

1. Uncertainty analysis

The EIT and modified AHAP were tests not based on skill. Both the assessments are based on true/false (sub)-scores. Therefore, no different outcome can be expected when the assessment is done multiple times. Therefore, these tests were only conducted once. Statistical analysis is not applicable to these scores.

The modified SHAP, however, is based on skill. The score is completely based on task completion time. Therefore, a different outcomes were expected for different runs. This was also the case. The obtained scores per run showed a learning curve. To create reliable scores, the test was repeated until the learning curve had flattened, meaning that at least three trials showed approximately the same results. As the final scores of the modified SHAP, the mean of the last three runs was taken. This means that for each task, the mean of the last three obtained transformed time scores was calculated. The mean was calculated as presented in Equation J1.

$$Ts_{mean} = \frac{Ts_{l-2} + Ts_{l-1} + Ts_l}{3} \tag{J1}$$

Here, l stands for the number of the last trial. In most cases, 12 trials were done, so the mean is taken of trial 10, 11 and 12. Ts_{mean} is the transformed time score of each task used for the final scores of the modified SHAP. Naturally, a standard deviation of the mean can be calculated for the final transformed time scores. The standard deviation was calculated using Equation J2.

$$\sigma_{Ts} = \sqrt{\frac{\Sigma(X - Ts_{mean})^2}{3}} \tag{J2}$$

In this equation, X is one of the last three transformed time scores.

From here, the LIFPP and W-LIF scores could be generated using the formulas presented in Appendix I 3 a. The LIFPP scores was just the average of the related transformed time scores. The uncertainty of the LIFPP scores due to error propagation was calculated as presented in Equation J3.

$$\begin{aligned} u_{LIFPP} &= \sqrt{\sum_{i=1}^{k} (u_{LIFPP\ i})^2} \\ u_{LIFPP\ i} &= \frac{dTs_{mean}}{dTs_{l-i}} u_i \\ u_{LIFPP\ i} &= \frac{1}{k} u_i \\ u_{LIFPP} &= \frac{1}{k} \sqrt{\sum_{i=1}^{k} (u_i)^2} \end{aligned} \tag{J3}$$

In these equations, u_{LIFPP} is the uncertainty of the LIFPP score. Furthermore, k is the amount of tasks related to the LIFPP score. u_i is the uncertainty of the transformed time score. As in Equation J1, l is the number of the last trial.

As an example, the completely worked out version for computing the uncertainty of the LIFPP$_{spherical}$ is presented in Equation J4. The LIFPP$_{spherical}$ of the modified SHAP consists of three tasks, namely the light spherical object, heavy spherical object and carton pouring.

$$u_{sphe} = \frac{1}{3} \sqrt{u^2_{Ts_{sp-light}} + u^2_{Ts_{sp-heavy}} + u^2_{Ts_{carton\ pouring}}} \tag{J4}$$

The W-LIF score is not simply the average of the LIFPP scores, but a weighted average. Therefore, the computation of the uncertainty of the W-LIF score is more elaborate. The computation of the uncertainty of the W-LIF score can be found in Equation J5.

$$\begin{aligned} u_{W-LIF} &= \sqrt{\sum_{i=1}^{j} (u_{W-LIF\ i})^2} \\ u_{W-LIF\ i} &= \frac{d(W-LIF)}{d(LIFPP\ i)} u_{LIFPP} \\ u_{W-LIF\ i} &= \frac{k}{j} u_{LIFPP} \\ u_{W-LIF} &= \sqrt{\sum_{i=1}^{k} (u_{W-LIF\ i})^2} \end{aligned} \tag{J5}$$

In this equation, j is the amount of sub-scores. The amount of sub-scores of the modified SHAP is seven. Again, k is the amount of tasks related to the sub-score in question. For the formula for W-LIF to take the derivative of, see Equation I3 in Appendix I 3 a.

For clarification, the completely worked out equation for calculating the uncertainty of the W-LIF score of the modified SHAP is presented in Equation J6.

TABLE XVII: z-scores for the differences in obtained scores for the modified SHAP

	Compared Grippers		
	RPG-4FH	**4FH-4FHi**	**RPG-4FHi**
$z_{spherical}$	-15.5303	3.7443	-11.6701
z_{tripod}	-1.7821	-0.9637	-4.9564
z_{power}	-31.2801	-0.6777	-24.1666
$z_{lateral}$	-16.0466	1.8770	-12.9231
z_{tip}	-4.9415	-2.8623	-6.2014
$z_{extension}$	-9.8875	-1.5214	-12.9034
z_{extra}	-10.0888	-1.4042	-9.3909
z_{W-LIF}	-23.5815	-1.1285	-21.2202

$$u_{W-LIF} = \sqrt{a}$$
$$a = (\frac{3}{28}u_{spe})^2 + (\frac{2}{28}u_{tri})^2 + (\frac{5}{28}u_{pow})^2 + (\frac{5}{28}u_{lat})^2 + (\frac{5}{28}u_{tip})^2 + (\frac{2}{28}u_{ext})^2 + (\frac{6}{28}u_{extra})^2 \tag{J6}$$

2. Statistical significance analysis

The difference in results between the grippers was evaluated, to check whether the results are significant. The significance of the difference between the outcomes was tested as follows. First, the z-score was computed. This z-score was transformed to a p-value. A p-value smaller than 0.05 was considered significant. A p-value larger than 0.05 indicates that it is likely that the difference in results is by chance. The z-score was calculated as presented in Equation J7.

$$z = \frac{score_1 - score_2}{\sqrt{\frac{u^2_{score1}}{n_1} + \frac{u^2_{score2}}{n_2}}} \tag{J7}$$

Here, score1 and score 2 can be any kind of score, LIFPP or W-LIF. Score1 is the outcome of one gripper, score2 is the outcome of another gripper on the same topic. n are the sample sizes. The z-scores are presented in Table XVII.

The z-scores were transformed to p-values. A one-tailed hypothesis needs to be considered in this scenario. The final p-values are presented in Table XVIII. The insignificant differences (p>0.05) are presented in orange. It can be seen that all differences in results between the RPG and the other grippers are significant. The differences in results between the 4FH and 4FH-i are not significant for four of the sub-scores. Also, the difference in W-LIF scores is not significant for these two grippers.

TABLE XVIII: p-values for the differences in obtained scores for the modified SHAP

	Compared Grippers		
	RPG-4FH	**4FH-4FHi**	**RPG-4FHi**
$p_{spherical}$	<0.00001	0.00009	<0.00001
p_{tripod}	0.03738	0.16777	<0.00001
p_{power}	<0.00001	0.24920	<0.00001
$p_{lateral}$	<0.00001	0.03026	<0.00001
p_{tip}	<0.00001	0.00211	<0.00001
$p_{extension}$	<0.00001	0.06413	<0.00001
p_{extra}	<0.00001	0.08016	<0.00001
p_{W-LIF}	<0.00001	0.12966	<0.00001

The uncertainty analysis and statistical significance analysis were done in the same manner for the original SHAP. The outcome of this analysis was that all p-values were smaller than 0.00001. Therefore, all differences in scores are significant.

Appendix K:
Results

1. Modified AHAP

Table XIX shows an overview of the points scored per task of the modified AHAP by each of the three grippers. In the modified AHAP, 0.5 points are scored for each item that is not dropped during the assessment. None of the items were dropped by any of the three grippers, so for each task at least 0.5 point is scored. An additional 0.5 point could be scored for each task, when no relative movement between the object and the gripper could be seen during rotation.

In total, seven objects showed relative movement for at least one of the grippers. For the RPG, the objects that showed movement were the skillet lid, plate, pitcher base, cracker box, coffee can, power drill and skillet. Only the coffee can and skillet showed relative movement for the 4FH. For the 4FH-i, relative movement was only seen for the skillet.

TABLE XIX: Modified AHAP scores achieved by the RPG, 4FH and 4FH-i for each of the tasks

Item	**Object**	**RPG**	**4FH**	**4FH-i**
T01	Skillet lid	0.5	1	1
T02	Apple	1	1	1
T03	Large marker	1	1	1
T04	Plate	0.5	1	1
T05	Chips can	1	1	1
T06	Screwdriver	1	1	1
T07	Bowl	1	1	1
T08	Small marker	1	1	1
T10	Pitcher base	0.5	1	1
T11	Softball	1	1	1
T12	Tuna can	1	1	1
T13	Cracker box	0.5	1	1
T14	Coffee can	0.5	0.5	1
T15	Spatula	1	1	1
T16	XS Clamp	1	1	1
T17	Pear	1	1	1
T20	Mini soccer ball	1	1	1
T21	Golf ball	1	1	1
T22	Chocolate pudding box	1	1	1
T23	Power drill	0.5	1	1
T24	Skillet	0.5	0.5	0.5
T25	Key	1	1	1
T26	Washer 10mm	1	1	1
	Total	**19.5**	**22**	**22.5**

2. Modified SHAP

The modified SHAP was performed 12 times with the RPG, 12 times with the 4FH, and 6 times with the 4FH-i. The outcomes obtained per each trial can be seen in Figure 40. Each sub-score and the overall score are presented in the graphs. Figure 40a presents the scores obtained with the RPG. Figure 40b and Figure 40c show the outcomes of the 4FH and 4FH-i respectively. In the graphs, a learning curve can be seen.

The exact data of the performance of the grippers on the modified SHAP can be found in Table XX to Table XXV. Table XX, Table XXI and Table XXII present all task completion times achieved with the RPG, 4FH and 4FH-i respectively. In Table XXIII, Table XXIV and Table XXV, all transformed time scores are presented for the RPG, 4FH and 4FH-i respectively. In these tables, also the sub-scores, LIFPP, and overall score, W-LIF, are presented. Furthermore, the mean and standard deviation of the last three trials is presented. The mean of the last three trials, namely, was taken as the final achieved score.

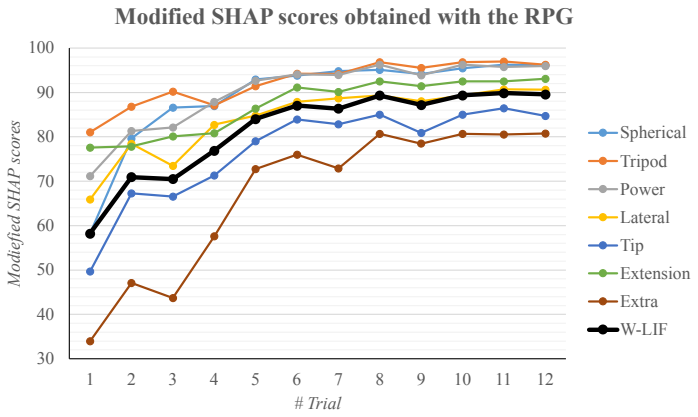

((a)) Scores obtained for the modified SHAP with the RPG

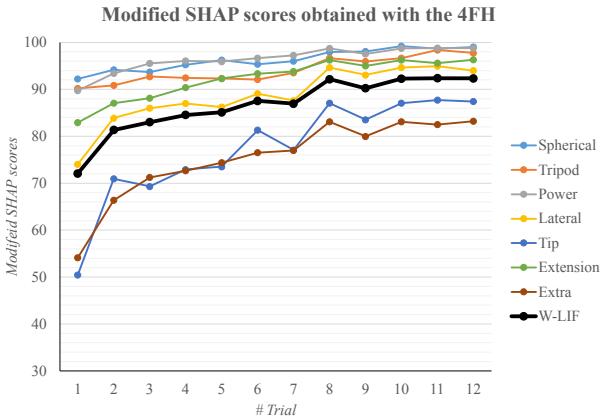

((b)) Scores obtained for the modified SHAP with the 4FH

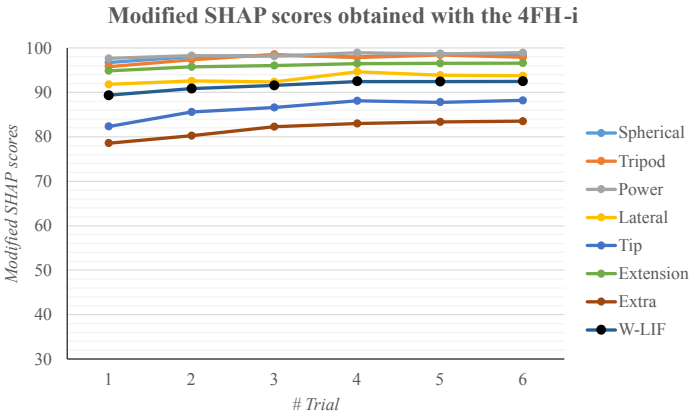

((c)) Scores obtained for the modified SHAP with the 4FH-i

FIG. 40: Presentation of the outcomes achieved by the three the grippers for the modified SHAP, over the complete span of trials performed.

TABLE XX: Completion times obtained with the RPG on each task of the modified SHAP for each of the 12 trials

		RPG											
Task	**Trial**	**1**	**2**	**3**	**4**	**5**	**6**	**7**	**8**	**9**	**10**	**11**	**12**
	Norm [s]	**t [s]**	**t [s]**	**t [s]**	**t [s]**	**t [s]**	**t [s]**	**t [s]**	**t [s]**	**t [s]**	**t [s]**	**t [s]**	**t [s]**
Abstract objects - Lightweight													
Spherical	1.63	4.50	3.25	2.56	2.66	2.03	2.03	1.96	1.90	2.03	1.78	1.72	1.78
Tripod	1.66	3.78	3.03	2.71	2.94	2.72	2.25	2.41	2.19	2.32	2.09	2.03	2.12
Power	1.77	3.78	2.84	2.44	2.53	2.00	1.78	1.97	1.91	1.72	1.72	1.78	1.75
Lateral	1.77	3.62	3.16	3.00	3.06	2.63	2.68	2.38	2.35	2.25	2.03	2.15	2.00
Tip	1.59	5.50	4.34	3.94	3.91	3.60	3.03	2.90	3.09	2.59	2.62	2.53	2.62
Extension	1.78	4.84	4.37	4.15	4.38	3.40	3.13	3.04	3.07	2.88	2.66	2.72	2.59
Abstract objects - Heavyweight													
Spherical	1.84	5.65	4.31	3.90	2.94	2.44	2.28	2.00	2.19	2.25	2.03	1.91	1.94
Tripod	1.58	3.75	3.19	2.75	3.22	2.47	2.29	2.16	2.10	1.94	1.87	1.90	1.97
Power	1.76	4.00	3.10	3.47	2.81	1.93	2.16	2.00	1.94	1.87	1.78	1.85	1.84
Lateral	1.84	4.43	3.56	4.34	3.56	3.22	3.13	2.98	2.97	3.08	2.88	2.59	2.78
Tip	1.61	5.66	4.50	3.94	4.16	3.38	2.68	2.72	2.78	2.78	2.50	2.41	2.66
Extension	1.71	4.13	4.53	4.19	3.81	3.41	2.53	2.87	2.84	2.71	2.66	2.60	2.59
Activities of Daily Living													
Coins	4.41	80.46	22.53	21.15	23.59	14.65	12.75	14.69	14.35	17.12	12.25	12.00	13.97
Jug pouring	4.66	22.50	14.00	15.07	12.69	11.28	8.63	8.53	8.68	8.41	8.23	7.97	8.25
Carton Pouring	5.79	34.34	17.03	12.34	14.53	11.10	10.56	10.41	11.34	10.19	10.19	9.78	9.72
Full Jar	2.1	7.34	4.81	5.10	3.32	2.66	2.50	2.75	3.00	2.72	2.47	2.53	2.62
Empty tin	1.77	3.40	3.38	3.03	2.44	2.59	2.22	2.62	2.25	2.19	1.90	1.96	1.85
Key	1.78	7.72	5.66	7.43	5.09	5.31	4.75	4.78	4.94	5.32	4.85	4.47	4.53
Zip	2.43	8.03	6.41	6.85	4.37	4.09	3.66	3.59	4.25	3.53	3.75	3.44	3.25
Door handle	1.49	7.84	5.90	5.60	4.84	3.91	3.57	3.09	3.41	3.81	3.06	3.16	3.09
Extra tasks													
Credit card	1.32	13.87	6.72	10.97	10.15	3.93	3.84	3.97	3.97	3.66	3.62	3.60	3.58
Plate	1.42	13.05	10.81	9.75	7.35	5.63	5.22	6.18	6.46	4.91	4.13	4.00	4.06
Cloth	1.36	4.97	4.85	4.94	3.63	3.16	3.10	3.59	3.31	3.10	3.13	3.31	3.03
Mug	1.26	4.87	4.06	4.10	3.25	2.94	2.62	2.88	2.78	2.47	2.41	2.50	2.37
Grocery bag	2.67	11.15	11.60	12.38	8.78	7.84	7.94	7.85	6.35	6.69	5.84	5.65	6.00
Drawer	2.18	13.15	9.59	7.08	5.22	6.37	4.75	4.69	5.53	4.53	4.50	4.57	4.69

TABLE XXI: Completion times obtained with the 4FH on each task of the modified SHAP for each of the 12 trials. The gripper mode used for each task is presented as well, being the orientation of the thumb.

			4FH											
Task		**Trial**	**1**	**2**	**3**	**4**	**5**	**6**	**7**	**8**	**9**	**10**	**11**	**12**
	Mode	**Norm [s]**	**t [s]**	**t [s]**	**t [s]**	**t [s]**	**t [s]**	**t [s]**	**t [s]**	**t [s]**	**t [s]**	**t [s]**	**t [s]**	**t [s]**
Abstract objects - Lightweight														
Spherical	Pinch	1.63	2.31	2.28	2.22	2.00	1.97	2.10	1.97	2.06	1.75	1.63	1.72	1.69
Tripod	Pinch	1.66	2.44	2.63	2.25	2.57	2.44	2.50	2.43	2.18	1.97	2.00	1.82	1.93
Power	Pinch	1.77	2.03	2.16	1.65	1.88	1.69	1.84	1.75	1.53	1.41	1.46	1.50	1.53
Lateral	Pinch	1.77	2.78	2.69	2.66	2.65	2.78	2.50	2.16	2.10	2.03	1.94	1.94	2.00
Tip	Pinch	1.59	4.53	3.22	3.03	3.47	3.47	2.81	2.41	2.60	2.50	2.25	2.12	2.04
Extension	Pinch	1.78	3.50	3.47	3.66	3.00	2.97	2.54	2.38	2.32	2.43	2.19	2.25	2.10
Abstract objects - Heavyweight														
Spherical	Pinch	1.84	3.09	2.47	2.78	2.50	2.22	2.00	2.28	2.03	2.03	1.85	1.94	1.88
Tripod	Pinch	1.58	3.00	2.68	2.63	2.38	2.53	2.53	2.28	2.00	2.18	2.00	1.78	1.82
Power	Pinch	1.76	3.16	2.22	2.06	1.97	2.19	1.78	1.88	1.78	1.56	1.65	1.62	1.59
Lateral	Pinch	1.84	3.25	3.18	3.06	2.87	3.12	2.90	2.75	2.53	2.31	2.09	2.10	2.18
Tip	Pinch	1.61	4.82	3.28	4.28	2.59	2.37	2.90	2.82	2.65	2.35	2.13	2.06	2.05
Extension	Pinch	1.71	4.15	3.19	2.75	2.84	2.41	2.57	2.62	2.41	2.28	2.22	2.32	2.28
Activities of Daily Living														
Coins	Grip	4.41	34.47	24.09	25.60	25.34	25.37	17.38	19.47	16.72	17.87	14.53	14.32	14.69
Jug pouring	Pinch	4.66	9.66	8.13	6.38	7.25	7.91	8.40	5.94	5.84	6.25	5.34	5.09	5.87
Carton Pouring	Grip	5.79	8.91	8.62	8.41	8.17	7.94	9.25	8.06	7.94	7.09	6.72	6.75	6.63
Full Jar	Grip	2.1	2.75	2.96	2.50	2.50	2.53	2.59	2.34	2.19	2.50	2.03	2.16	2.12
Empty tin	Grip	1.77	2.66	2.37	2.04	2.32	2.25	2.13	2.10	1.93	1.94	1.66	1.59	1.78
Key	Pinch	1.78	6.37	5.57	5.13	5.50	5.63	4.71	4.47	4.43	4.22	4.03	3.91	3.94
Zip	Pinch	2.43	12.40	6.12	6.06	4.50	4.13	3.37	6.88	3.38	3.19	3.00	3.00	3.18
Door handle	Grip	1.49	4.22	3.09	3.05	2.53	2.55	2.50	2.37	2.19	2.35	2.15	2.07	2.10
Extra tasks														
Credit card	Grip	1.32	8.29	5.75	4.68	4.37	5.50	4.35	4.12	4.66	3.88	3.75	3.78	3.65
Plate	Grip	1.42	9.34	7.94	7.53	7.72	6.31	6.47	5.81	7.18	5.15	4.87	5.00	4.75
Cloth	Pinch	1.36	3.56	3.47	3.52	3.41	3.21	3.31	3.44	3.03	2.84	2.63	2.62	2.60
Mug	Grip	1.26	3.09	2.53	2.22	2.43	2.78	2.44	2.32	2.31	2.28	2.06	2.09	2.09
Grocery bag	Grip	2.67	11.02	6.66	7.25	5.56	4.66	5.03	5.63	5.19	5.38	4.31	4.54	4.23
Drawer	Grip	2.18	7.03	6.81	4.75	4.84	4.00	3.84	4.31	4.72	4.22	3.60	3.69	3.90

TABLE XXII: Completion times obtained with the 4FH-i on each task of the modified SHAP for each of the 6 trials. The gripper mode used for each task is presented as well, being the orientation of the thumb.

			4FH-i					
Task		**Trial**	**1**	**2**	**3**	**4**	**5**	**6**
	Mode	**Norm [s]**	**t [s]**	**t [s]**	**t [s]**	**t [s]**	**t [s]**	**t [s]**
Abstract objects - Lightweight								
Spherical	Pinch	1.63	1.69	1.57	1.50	1.63	1.60	1.56
Tripod	Pinch	1.66	2.19	2.03	1.82	1.88	1.81	1.84
Power	Pinch	1.77	1.47	1.56	1.38	1.47	1.56	1.43
Lateral	Pinch	1.77	2.28	2.47	2.28	1.97	2.19	2.19
Tip	Pinch	1.59	2.37	2.35	2.40	2.10	2.28	2.03
Extension	Pinch	1.78	2.10	2.31	2.29	2.09	2.18	2.10
Abstract objects - Heavyweight								
Spherical	Pinch	1.84	2.25	2.00	1.93	1.97	1.75	1.90
Tripod	Pinch	1.58	2.00	1.81	1.75	1.84	1.78	1.87
Power	Pinch	1.76	1.63	1.62	1.57	1.66	1.62	1.62
Lateral	Pinch	1.84	2.40	2.25	2.37	2.06	2.28	2.25
Tip	Pinch	1.61	2.57	2.22	2.16	2.16	2.16	2.19
Extension	Pinch	1.71	2.63	2.22	2.16	2.25	2.15	2.22
Activities of Daily Living								
Coins	Grip	4.41	18.65	15.22	13.22	13.53	13.06	13.04
Jug pouring	Pinch	4.66	6.50	5.78	5.88	5.69	5.22	5.56
Carton Pouring	Grip	5.79	8.28	7.68	7.47	7.78	7.44	7.56
Full Jar	Grip	2.1	2.50	2.19	2.25	2.19	2.03	2.06
Empty tin	Grip	1.77	1.81	1.65	1.82	1.66	1.66	1.59
Key	Pinch	1.78	4.29	4.19	4.00	3.81	4.12	3.93
Zip	Pinch	2.43	3.56	3.38	3.88	3.12	2.97	3.22
Door handle	Grip	1.49	2.41	2.31	2.31	2.00	2.18	2.04
Extra tasks								
Credit card	Grip	1.32	4.22	4.44	3.79	3.56	3.66	3.63
Plate	Grip	1.42	5.81	4.81	4.62	4.98	4.47	4.62
Cloth	Pinch	1.36	2.81	2.82	2.62	2.69	2.50	2.59
Mug	Grip	1.26	2.47	2.25	2.31	2.13	2.25	2.19
Grocery bag	Grip	2.67	4.93	5.15	4.78	4.34	4.56	4.28
Drawer	Grip	2.18	4.00	3.84	3.87	3.56	3.78	3.65

TABLE XXIII: Transformed time scores, LIFPP and W-LIF obtained with the RPG on each task of the modified SHAP for each of the 12 trials. The mean of the last three trials was taken as final outcome.

	RPG													
Trial	**1**	**2**	**3**	**4**	**5**	**6**	**7**	**8**	**9**	**10**	**11**	**12**	**Last 3 trials**	
Transformed time score	**Ts**	**Ts**	**Ts**	**Ts**	**Ts**	**Ts**	**Ts**	**Ts**	**Ts**	**Ts**	**Ts**	**Ts**	**Mean**	**Std**
Abstract objects - Lightweight														
Spherical	74.85	85.80	91.85	90.97	96.49	96.49	97.11	97.63	96.49	98.69	99.21	98.69	98.86	0.30
Tripod	81.76	88.21	90.96	88.98	90.88	94.92	93.55	96.30	94.32	96.30	96.82	96.04	96.39	0.39
Power	83.78	91.36	94.59	93.87	98.14	99.92	98.39	100.00	100.00	100.00	99.92	100.00	99.97	0.05
Lateral	85.07	88.78	90.07	89.59	93.06	92.66	95.08	97.90	96.13	97.90	96.93	98.14	97.66	0.64
Tip	64.87	75.29	78.89	79.16	81.94	87.06	88.23	90.75	91.02	90.75	91.55	90.75	91.02	0.47
Extension	75.44	79.21	80.98	79.13	87.00	89.17	89.89	92.94	91.17	92.94	92.46	93.50	92.96	0.52
Abstract objects - Heavyweight														
Spherical	70.42	80.82	84.01	91.46	95.34	96.58	98.76	98.52	96.82	98.52	99.46	99.22	99.07	0.48
Tripod	80.38	85.44	89.42	85.17	91.95	93.58	94.76	97.38	96.75	97.38	97.11	96.47	96.99	0.46
Power	81.82	89.12	86.12	91.48	98.62	96.75	98.05	99.84	99.11	99.84	99.27	99.35	99.49	0.31
Lateral	79.89	86.65	80.59	86.65	89.29	89.98	91.15	91.93	90.37	91.93	94.18	92.70	92.93	1.14
Tip	64.06	74.36	79.33	77.37	84.29	90.51	90.15	92.10	89.62	92.10	92.90	90.68	91.90	1.12
Extension	79.78	76.44	79.28	82.46	85.80	93.15	90.31	92.06	91.65	92.06	92.56	92.65	92.43	0.32
Activities of Daily Living														
Coins	0.00	41.30	45.77	37.87	66.83	72.98	66.70	74.60	58.83	74.60	75.41	69.03	73.02	3.47
Jug pouring	45.31	71.37	68.09	75.38	79.71	87.83	88.14	89.06	88.50	89.06	89.85	88.99	89.30	0.48
Carton Pouring	29.56	72.27	83.84	78.44	86.90	88.23	88.60	89.14	89.14	89.14	90.16	90.30	89.87	0.63
Full Jar	64.35	81.56	79.59	91.70	96.19	97.28	95.58	97.48	95.78	97.48	97.07	96.46	97.01	0.51
Empty tin	86.84	87.01	89.83	94.59	93.38	96.37	93.14	98.95	96.61	98.95	98.47	99.35	98.92	0.44
Key	52.33	68.86	54.65	73.43	71.67	76.16	75.92	75.36	71.59	75.36	78.41	77.93	77.23	1.64
Zip	67.08	76.60	74.02	88.59	90.24	92.77	93.18	92.24	93.53	92.24	94.06	95.18	93.83	1.48
Door handle	39.12	57.72	60.59	67.88	76.80	80.06	84.66	84.95	77.76	84.95	83.99	84.66	84.53	0.49
Extra tasks														
Credit card	41.56	0.00	4.44	71.75	72.73	71.32	75.11	74.68	75.11	75.32	75.54	3.58	75.32	0.22
Plate	5.53	16.20	40.34	57.65	61.77	52.11	72.74	64.89	72.74	74.04	73.44	4.06	73.41	0.65
Cloth	63.34	62.39	76.16	81.09	81.72	76.58	81.41	81.72	81.41	79.52	82.46	3.03	81.13	1.49
Mug	68.25	67.80	77.44	80.95	84.58	81.63	86.96	86.28	86.96	85.94	87.41	2.37	86.77	0.75
Grocery bag	52.22	48.05	67.31	72.34	71.80	72.28	83.04	78.49	83.04	84.06	82.18	6.00	83.09	0.94
Drawer	51.44	67.89	80.08	72.54	83.16	83.55	84.80	84.60	84.80	84.34	83.55	4.69	84.23	0.63
													Last 3 trials	
LIFPP **Trial**	**1**	**2**	**3**	**4**	**5**	**6**	**7**	**8**	**9**	**10**	**11**	**12**	**Mean**	**Std**
Spherical	58.27	79.63	86.56	86.96	92.91	93.77	94.82	95.10	94.15	95.45	96.27	96.07	95.93	0.28
Tripod	81.07	86.83	90.19	87.08	91.42	94.25	94.15	96.84	95.53	96.84	96.96	96.26	96.69	0.30
Power	71.18	81.36	82.15	87.90	92.63	94.08	93.96	96.24	93.85	96.24	95.74	95.97	95.98	0.18
Lateral	65.94	78.45	73.48	82.73	84.79	87.88	88.69	89.30	88.02	89.30	90.69	90.59	90.19	0.52
Tip	49.67	67.28	66.53	71.29	78.99	83.90	82.84	85.01	80.92	85.01	86.47	84.71	85.40	0.86
Extension	77.61	77.83	80.13	80.79	86.40	91.16	90.10	92.50	91.41	92.50	92.51	93.07	92.69	0.31
Extra	33.98	47.06	43.72	57.63	72.72	75.96	72.91	80.67	78.44	80.67	80.54	80.76	80.66	0.78
W-LIF	58.21	70.93	70.48	76.86	84.03	87.04	86.35	89.31	87.18	89.35	89.84	89.56	89.58	0.25

TABLE XXIV: Transformed time scores, LIFPP and W-LIF obtained with the 4FH on each task of the modified SHAP for each of the 12 trials. The mean of the last three trials was taken as final outcome.

	4FH													
Trial	**1**	**2**	**3**	**4**	**5**	**6**	**7**	**8**	**9**	**10**	**11**	**12**	**Last 3 trials**	
Transformed time score	**Ts**	**Ts**	**Ts**	**Ts**	**Ts**	**Ts**	**Ts**	**Ts**	**Ts**	**Ts**	**Ts**	**Ts**	**Mean**	**Std**
Abstract objects - Lightweight														
Spherical	94.04	94.30	94.83	96.76	97.02	95.88	97.02	96.23	98.95	100.00	99.21	99.47	99.56	0.40
Tripod	93.29	91.65	94.92	92.17	93.29	92.77	93.37	97.07	97.33	97.07	98.62	97.68	97.79	0.78
Power	97.90	96.85	100.00	99.11	100.00	99.44	100.00	100.00	100.00	100.00	100.00	100.00	100.00	0.00
Lateral	91.85	92.57	92.82	92.90	91.85	94.11	96.85	98.63	97.90	98.63	98.63	98.14	98.47	0.28
Tip	73.58	85.35	87.06	83.11	83.11	89.04	92.63	94.07	91.82	94.07	95.24	95.96	95.09	0.95
Extension	86.20	86.44	84.91	90.21	90.45	93.90	95.18	96.71	94.78	96.71	96.23	97.43	96.79	0.61
Abstract objects - Heavyweight														
Spherical	90.30	95.11	92.70	94.88	97.05	98.76	96.58	99.92	98.52	99.92	99.22	99.69	99.61	0.36
Tripod	87.16	90.05	90.51	92.77	91.41	91.41	93.67	96.20	94.58	96.20	98.19	97.83	97.41	1.06
Power	88.64	96.27	97.56	98.30	96.51	99.84	99.03	100.00	100.00	100.00	100.00	100.00	100.00	0.00
Lateral	89.05	89.60	90.53	92.00	90.06	91.77	92.93	98.06	96.35	98.06	97.98	97.36	97.80	0.38
Tip	71.52	85.18	76.31	91.30	93.26	88.55	89.26	95.39	93.43	95.39	96.01	96.10	95.83	0.39
Extension	79.62	87.64	91.31	90.56	94.15	92.82	92.40	95.74	95.24	95.74	94.90	95.24	95.29	0.42
Activities of Daily Living														
Coins	2.62	36.25	31.36	32.20	32.10	57.99	51.21	67.22	56.40	67.22	67.90	66.70	67.27	0.60
Jug pouring	84.67	89.36	94.73	92.06	90.04	88.53	96.08	97.92	95.13	97.92	98.68	96.29	97.63	1.22
Carton Pouring	92.30	93.02	93.54	94.13	94.70	91.46	94.40	97.71	96.79	97.71	97.63	97.93	97.75	0.15
Full Jar	95.58	94.15	97.28	97.28	97.07	96.67	98.37	100.00	97.28	100.00	99.59	99.86	99.82	0.21
Empty tin	92.82	95.16	97.82	95.56	96.13	97.09	97.34	100.00	98.63	100.00	100.00	99.92	99.97	0.05
Key	63.16	69.58	73.11	70.14	69.10	76.48	78.41	81.94	80.42	81.94	82.91	82.66	82.50	0.50
Zip	41.39	78.31	78.66	87.83	90.01	94.47	73.84	96.65	95.53	96.65	96.65	95.59	96.30	0.61
Door handle	73.83	84.66	85.04	90.03	89.84	90.32	91.56	93.67	91.75	93.67	94.44	94.15	94.09	0.39
Extra tasks														
Credit card	24.57	52.06	63.64	66.99	54.76	67.21	69.70	73.70	72.29	73.70	73.38	74.78	73.95	0.74
Plate	20.32	34.41	38.53	36.62	50.80	49.20	55.84	65.29	62.47	65.29	63.98	66.50	65.26	1.26
Cloth	76.89	77.84	77.31	78.47	80.57	79.52	78.15	86.66	84.45	86.66	86.76	86.97	86.80	0.16
Mug	79.25	85.60	89.12	86.73	82.77	86.62	87.98	90.93	88.44	90.93	90.59	90.59	90.70	0.20
Grocery bag	55.32	78.65	75.49	84.54	89.35	87.37	84.16	91.23	85.50	91.23	89.99	91.65	90.96	0.86
Drawer	68.22	69.66	83.16	82.57	88.07	89.12	86.04	90.69	86.63	90.69	90.10	88.73	89.84	1.01
													Last 3 trials	
LIFPP **Trial**	**1**	**2**	**3**	**4**	**5**	**6**	**7**	**8**	**9**	**10**	**11**	**12**	**Mean**	**Std**
Spherical	92.21	94.14	93.69	95.25	96.26	95.37	96.00	97.95	98.09	99.21	98.69	99.03	98.98	0.19
Tripod	90.22	90.85	92.71	92.47	92.35	92.09	93.52	96.64	95.95	96.64	98.41	97.75	97.60	0.66
Power	89.75	93.42	95.54	96.06	95.91	96.67	97.26	98.73	97.53	98.73	98.81	98.79	98.78	0.09
Lateral	74.02	83.88	85.97	86.99	86.21	89.07	87.62	94.64	93.07	94.64	94.97	94.01	94.54	0.31
Tip	50.46	70.94	69.30	72.92	73.51	81.31	77.07	87.05	83.52	87.05	87.74	87.40	87.40	0.29
Extension	82.91	87.04	88.11	90.38	92.30	93.36	93.79	96.22	95.01	96.22	95.57	96.33	96.04	0.37
Extra	54.10	66.37	71.21	72.65	74.39	76.51	76.98	83.08	79.97	83.08	82.47	83.20	82.92	0.70
W-LIF	72.09	81.34	83.00	84.54	85.09	87.55	86.94	92.15	90.23	92.29	92.37	92.34	92.33	0.18

TABLE XXV: Transformed time scores, LIFPP and W-LIF obtained with the 4FH-i on each task of the modified SHAP for each of the 6 trials. The mean of the last three trials was taken as final outcome.

	4FH-i							
Trial	**1**	**2**	**3**	**4**	**5**	**6**	**Last 3 trials**	
Transformed time score	**Ts**	**Ts**	**Ts**	**Ts**	**Ts**	**Ts**	**Mean**	**Std**
Abstract objects - Lightweight								
Spherical	99.47	100.00	100.00	100.00	100.00	100.00	100.00	0.00
Tripod	95.44	96.82	98.62	98.11	98.71	98.45	98.42	0.30
Power	100.00	100.00	100.00	100.00	100.00	100.00	100.00	0.00
Lateral	95.88	94.35	95.88	98.39	96.61	96.61	97.20	1.03
Tip	92.99	93.17	92.72	95.42	93.80	96.05	95.09	1.16
Extension	97.43	95.75	95.91	97.51	96.79	97.43	97.24	0.40
Abstract objects - Heavyweight								
Spherical	96.82	98.76	99.30	98.99	100.00	99.53	99.51	0.51
Tripod	96.20	97.92	98.46	97.65	98.19	97.38	97.74	0.41
Power	100.00	100.00	100.00	100.00	100.00	100.00	100.00	0.00
Lateral	95.65	96.82	95.89	98.29	96.58	96.82	97.23	0.93
Tip	91.48	94.59	95.12	95.12	95.12	94.85	95.03	0.15
Extension	92.31	95.74	96.24	95.49	96.32	95.74	95.85	0.43
Activities of Daily Living								
Coins	53.87	64.98	71.46	70.46	71.98	72.04	71.49	0.90
Jug pouring	94.36	96.57	96.26	96.84	98.28	97.24	97.46	0.74
Carton Pouring	93.86	95.34	95.85	95.09	95.93	95.63	95.55	0.43
Full Jar	97.28	99.39	98.98	99.39	100.00	100.00	99.80	0.35
Empty tin	99.68	100.00	99.60	100.00	100.00	100.00	100.00	0.00
Key	79.86	80.66	82.18	83.71	81.22	82.74	82.56	1.25
Zip	93.36	94.42	91.48	95.94	96.83	95.36	96.04	0.74
Door handle	91.18	92.14	92.14	95.11	93.38	94.73	94.41	0.91
Extra tasks								
Credit card	68.61	66.23	73.27	75.76	74.68	75.00	75.14	0.56
Plate	55.84	65.90	67.81	64.19	69.32	67.81	67.10	2.64
Cloth	84.77	84.66	86.76	86.03	88.03	87.08	87.04	1.00
Mug	86.28	88.78	88.10	90.14	88.78	89.46	89.46	0.68
Grocery bag	87.91	86.73	88.71	91.06	89.89	91.39	90.78	0.79
Drawer	88.07	89.12	88.93	90.96	89.52	90.37	90.28	0.72
							Last 3 trials	
LIFPP **Trial**	**1**	**2**	**3**	**4**	**5**	**6**	**Mean**	**Std**
Spherical	96.72	98.03	98.39	98.03	98.64	98.39	98.35	0.22
Tripod	95.82	97.37	98.54	97.88	98.45	97.91	98.08	0.26
Power	97.63	98.31	98.14	98.90	98.68	98.95	98.84	0.19
Lateral	91.82	92.56	92.34	94.63	93.90	93.75	94.10	0.43
Tip	82.31	85.56	86.59	88.13	87.79	88.21	88.04	0.41
Extension	94.87	95.74	96.07	96.50	96.56	96.59	96.55	0.29
Extra	78.58	80.24	82.26	83.02	83.37	83.52	83.30	1.06
W-LIF	89.35	90.85	91.55	92.47	92.43	92.49	92.47	0.26

3. SHAP

The original SHAP was also performed with the RPG and 4FH-i. Most of the tasks of the original SHAP were already performed in the modified SHAP. The scores on these tasks can be found in Table XX to Table XXV. Six tasks of the SHAP were not yet covered in the modified SHAP. Therefore, these tasks needed to be performed to generate SHAP scores. The tasks of the SHAP disregarded in the modified SHAP were using a button board, cutting food, page turning, opening a jar, lifting a tray and using a screwdriver. These six tasks were performed 12 times with both the RPG and 4FH-i. The achieved results per trial are presented in Figure 41. Figure 41a shows the outcomes achieved by the RPG. The results obtained with the 4FH-i are presented in Figure 41b.

The outcomes of the SHAP are presented in Figure 42. In Figure 42a, the SHAP sub-scores obtained with the RPG and 4FH-i are presented. Figure 42c shows a zoomed in version, such that differences and error bars are easier to see. The overall SHAP score, the W-LIF, achieved with the RPG and 4FH-i is presented in Figure 42b. Figure 42d again shows a zoomed in version for better readability.

A complete overview of the results obtained by the RPG and 4FH-i on the original SHAP can be found in Table XXVI to Table XXIX. Table XXVI and Table XXVII present the task completion times for each task per trial. In Table XXVIII and Table XXIX, the transformed time scores can be found. Additionally, the LIFPP and W-LIF scores are presented. The mean and standard deviation of the last three trials is presented as well, as this is used as the final score.

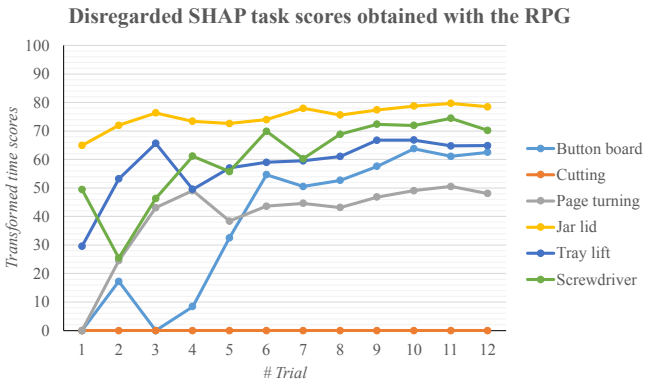

((a)) Scores obtained for the SHAP with the RPG

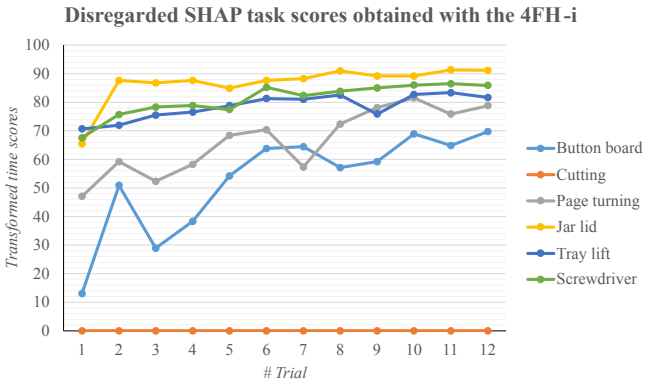

((b)) Scores obtained for the SHAP with the 4FH-i

FIG. 41: Outcomes achieved per trial by the RPG and 4FH-i for the tasks of the SHAP which are disregarded for the modified SHAP.

TABLE XXVI: Completion times obtained with the RPG, on the tasks of the SHAP which were disregarded for the modified SHAP. The completion times for the remainder of the tasks were copied from the results of the modified SHAP.

RPG - SHAP disregarded tasks

Task	**Trial**	**1**	**2**	**3**	**4**	**5**	**6**	**7**	**8**	**9**	**10**	**11**	**12**
	Norm [s]	**t [s]**	**t [s]**	**t [s]**	**t [s]**	**t [s]**	**t [s]**	**t [s]**	**t [s]**	**t [s]**	**t [s]**	**t [s]**	**t [s]**
Button board	6.77	57.41	45.97	54.37	50.18	38.75	28.25	30.22	29.19	26.87	23.94	25.21	24.53
Cutting	3.12	-	-	-	-	-	-	-	-	-	-	-	-
Page turning	1.8	21.46	11.31	8.97	8.22	9.56	8.90	8.78	8.96	8.50	8.22	8.03	8.34
Jar lid	2.26	7.81	6.69	6.00	6.47	6.59	6.38	5.75	6.12	5.84	5.62	5.47	5.66
Tray lift	3.02	17.91	12.91	10.28	13.69	12.10	11.69	11.57	11.25	10.05	10.03	10.47	10.44
Screwdriver	3.9	17.69	24.25	18.55	14.50	15.97	12.12	14.75	12.41	11.44	11.56	10.88	12.03

TABLE XXVII: Completion times obtained with the 4FH-i, on the tasks of the SHAP which were disregarded for the modified SHAP. The completion times for the remainder of the tasks were copied from the results of the modified SHAP.

4FH-i - SHAP disregarded tasks

Task	**Trial**	**1**	**2**	**3**	**4**	**5**	**6**	**7**	**8**	**9**	**10**	**11**	**12**
	Norm [s]	**t [s]**	**t [s]**	**t [s]**	**t [s]**	**t [s]**	**t [s]**	**t [s]**	**t [s]**	**t [s]**	**t [s]**	**t [s]**	**t [s]**
Button board	6.77	48.00	30.03	40.47	36.00	28.47	23.91	23.63	27.10	26.09	21.50	23.43	21.12
Cutting	3.12	-	-	-	-	-	-	-	-	-	-	-	-
Page turning	1.8	8.47	6.94	7.81	7.06	5.78	5.53	7.18	5.28	4.56	4.13	4.84	4.47
Jar lid	2.26	7.72	4.22	4.35	4.22	4.65	4.22	4.12	3.69	3.97	3.97	3.63	3.65
Tray lift	3.02	9.22	8.94	8.19	7.97	7.50	6.97	7.03	6.71	8.12	6.68	6.54	6.90
Screwdriver	3.9	12.75	10.53	9.81	9.68	10.06	7.94	8.72	8.31	8.00	7.72	7.59	7.75

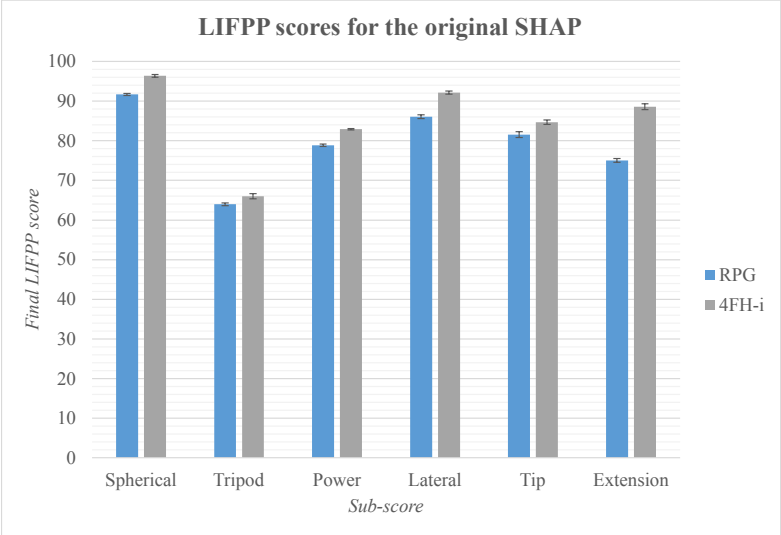

((a)) Sub-scores obtained for the original SHAP

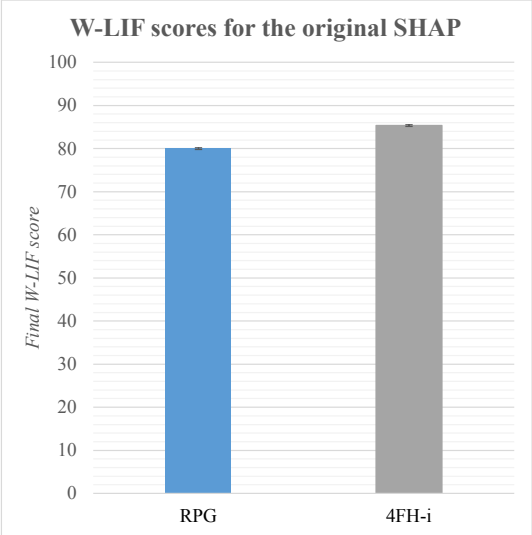

((b)) Overall scores obtained for the original SHAP

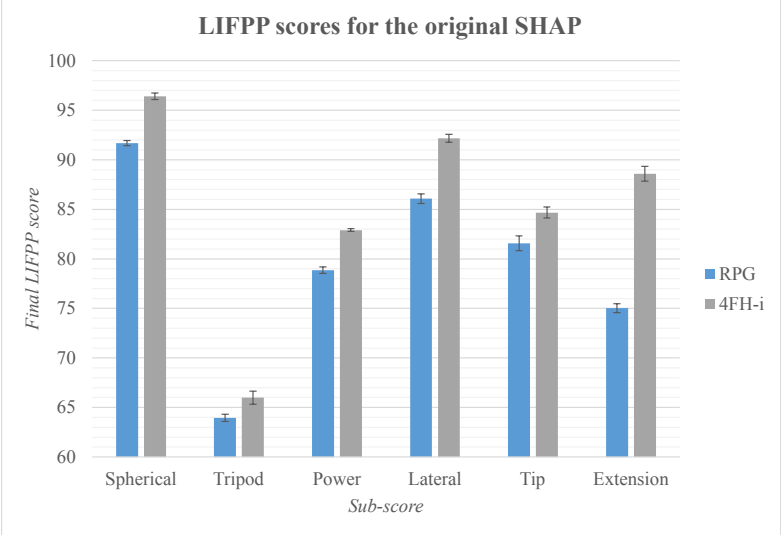

((c)) Zoomed in presentation of the sub-scores

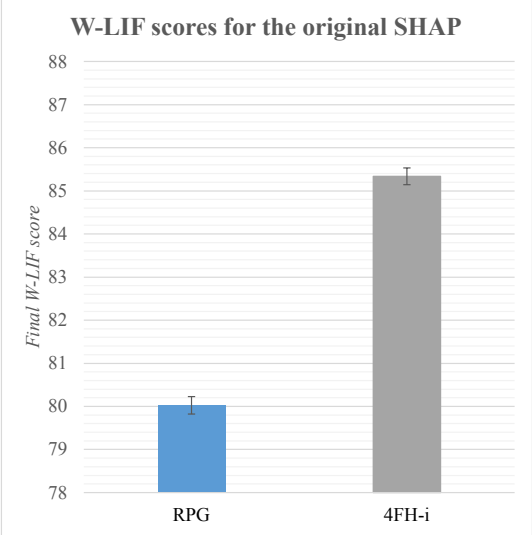

((d)) Zoomed in presentation of the overall scores

FIG. 42: Outcomes achieved by the RPG and 4FH-i for the original SHAP. All differences are significant ($p>0.05$). The error bars show the standard deviation.

TABLE XXVIII: Transformed time scores obtained with the RPG on the SHAP tasks disregarded by the modified SHAP. The outcomes for the remainder of the tasks were copied from the achieved times and scores on the modified SHAP. The LIFPP and W-LIF are presented as well for each trial. The mean of the last three trials was taken as final outcome.

RPG - SHAP disregarded tasks

Trial	**1**	**2**	**3**	**4**	**5**	**6**	**7**	**8**	**9**	**10**	**11**	**12**	**Last 3 trials**	
Transformed time score	**Ts**	**Ts**	**Ts**	**Ts**	**Ts**	**Ts**	**Ts**	**Ts**	**Ts**	**Ts**	**Ts**	**Ts**	**Mean**	**Std**
Button board	0.00	17.28	0.00	8.40	32.52	54.67	50.52	52.69	57.59	63.77	61.09	62.52	62.46	1.34
Cutting	0.00	0.00	0.00	0.00	0.00	0.00	0.00	0.00	0.00	0.00	0.00	0.00	0.00	0.00
Page turning	0.00	24.52	43.10	49.05	38.41	43.65	44.60	43.17	46.83	49.05	50.56	48.10	49.23	1.24
Jar lid	64.92	72.00	76.36	73.39	72.63	73.96	77.94	75.60	77.37	78.76	79.71	78.51	78.99	0.63
Tray lift	29.56	53.22	65.66	49.53	57.05	58.99	59.56	61.07	66.75	66.84	64.76	64.90	65.50	1.16
Screwdriver	49.49	25.46	46.34	61.17	55.79	69.89	60.26	68.83	72.38	71.94	74.43	70.22	72.20	2.12
LIFPP **Trial**	**1**	**2**	**3**	**4**	**5**	**6**	**7**	**8**	**9**	**10**	**11**	**12**	**Mean**	**Std**
Spherical	59.94	77.72	84.01	83.56	87.84	88.82	90.60	89.21	89.96	91.28	92.13	91.68	91.70	0.27
Tripod	40.53	47.73	45.10	45.64	53.84	60.79	59.70	60.86	62.16	64.36	63.75	63.76	63.96	0.37
Power	57.91	61.75	65.30	71.53	74.13	77.18	75.72	76.83	77.38	79.02	79.02	78.58	78.87	0.33
Lateral	59.87	74.25	72.18	77.20	80.17	83.06	83.84	83.21	84.48	85.55	86.37	86.31	86.08	0.48
Tip	41.39	58.95	55.44	60.80	71.25	79.03	77.45	76.76	77.03	81.47	82.24	81.02	81.57	0.75
Extension	46.20	58.35	67.25	65.04	67.06	71.24	71.09	71.11	74.10	75.22	75.08	74.79	75.03	0.45
W-LIF	51.60	63.44	64.78	67.92	72.98	77.30	76.88	76.85	77.92	79.96	80.28	79.84	80.02	0.20

TABLE XXIX: Transformed time scores obtained with the 4FH-i on the SHAP tasks disregarded by the modified SHAP. The outcomes for the remainder of the tasks were copied from the achieved times and scores on the modified SHAP. The LIFPP and W-LIF are presented as well for each trial. The mean of the last three trials was taken as final outcome.

4FH-i - SHAP disregarded tasks

Trial	**1**	**2**	**3**	**4**	**5**	**6**	**7**	**8**	**9**	**10**	**11**	**12**	**Last 3 trials**	
Transformed time score	**Ts**	**Ts**	**Ts**	**Ts**	**Ts**	**Ts**	**Ts**	**Ts**	**Ts**	**Ts**	**Ts**	**Ts**	**Mean**	**Std**
Button board	13.00	50.92	28.89	38.32	54.21	63.83	64.42	57.10	59.23	68.92	64.84	69.72	67.83	2.61
Cutting	0.00	0.00	0.00	0.00	0.00	0.00	0.00	0.00	0.00	0.00	0.00	0.00	0.00	0.00
Page turning	47.06	59.21	52.30	58.25	68.41	70.40	57.30	72.38	78.10	81.51	75.87	78.81	78.73	2.82
Jar lid	65.49	87.61	86.79	87.61	84.89	87.61	88.24	90.96	89.19	89.19	91.34	91.21	90.58	1.21
Tray lift	70.67	72.00	75.54	76.58	78.81	81.32	81.03	82.54	75.88	82.69	83.35	81.65	82.56	0.86
Screwdriver	67.58	75.71	78.35	78.83	77.44	85.20	82.34	83.85	84.98	86.01	86.48	85.90	86.13	0.31
LIFPP **Trial**	**1**	**2**	**3**	**4**	**5**	**6**	**7**	**8**	**9**	**10**	**11**	**12**	**Mean**	**Std**
Spherical	-	-	-	-	-	-	94.60	96.26	96.09	95.82	96.82	96.60	96.41	0.34
Tripod	-	-	-	-	-	-	64.02	62.96	64.08	66.17	65.44	66.39	66.00	0.67
Power	-	-	-	-	-	-	81.50	82.20	82.24	82.93	82.84	82.95	82.90	0.15
Lateral	-	-	-	-	-	-	90.02	90.89	89.59	92.64	92.15	91.74	92.17	0.38
Tip	-	-	-	-	-	-	79.33	80.82	82.03	84.93	83.96	85.13	84.67	0.56
Extension	-	-	-	-	-	-	82.02	86.60	86.53	89.30	88.08	88.41	88.60	0.75
W-LIF	-	-	-	-	-	-	82.23	83.51	83.62	85.52	85.09	85.40	85.34	0.19

Appendix L:
Achievement of requirements

In Table XXX, an overview is presented of which of the requirements were achieved and which were not.

TABLE XXX: Presentation of the achieved and non-achieved requirements

Criteria	Description	Metric	Achieved
R1	**Overall properties**		
R1.1	Cost of the gripper	Max: $8.000,-	✓
R1.2	Volume of the gripper while closed	Max: 15x15x20 cm^3	✓
R1.3	Mass of the gripper needs to be lower than current gripper	Max: 500 g	✓
R2	**Mechanical properties**		
R2.1	Grip and pinch force		N.A.
R2.1.1	Sufficient pinch force for enabling a broad range of activities	Min: 30 N	✓
R2.1.2	Able to pick up items with significant weight	Min: 2 kg	✓
R2.1.3	The force at the contact points must be distributed over a sufficient area to avoid damaging objects	Min: 2 cm^2	✓
R2.2	Gripper stroke width at the tip of the gripper	Min: 85 mm	✓
R2.3	Repeatability of opening and closing the gripper	Max: 1 mm	×
R2.4	Sufficient robustness to complete the functional and mechanical testing procedure without being damaged	Pass/fail	✓
R2.5	Time between fully open and fully closed gripper position	Max: 0.7 s ±10	✓
R3	**Functional properties**		
R3.1	Able to pick up essential items, namely a pill box, credit card, keys, wallet, cloth, mug, plastic bottle, TV-remote and bowl from different heights: floor level and table height	Pass/fail	✓
R3.2	Able to perform a self-modified version of the SHAP, specifically designed for applications of robot Rose, with an overall score higher than the RPG	Pass/fail	✓
R3.3	Able to perform a self-modified version of the AHAP, with an overall score higher than the RPG	Pass/fail	✓
R4	**Actuation and control**		
R4.1	Electrically powered, with a power supply of 12 V or 24 V	12 V or 24 V	✓
R4.2	Simplicity of the control system	Pass/fail	✓
R4.3	Application of force sensor(s) to allow for force feedback	Pass/fail	✓
R4.4	The actuation mechanism may not overheat	Max: 80° C	✓
R5	**Safety**		
R5.1	No sharp points or edges on the outer surface of the gripper	Pass/fail	✓
R5.2	Outer surface of the fingers and palm of the gripper may not exceed temperatures safe for continuously holding	Max: 43° C	✓
R5.3	Outer surface of the gripper, except the fingers and palm, may not exceed temperatures safe to touch for short periods (up to 10 seconds)	Max metallic: 55° C Max non-metalic: 65 °C	✓
R6	**Build up and casing**		
R6.1	Short manufacturing time	Max: 1 w	✓
R6.2	Short time needed for maintenance and replacement of parts	Max: 1 h	✓
R6.3	Modular design		N.A.
R6.3.1	All functional components contained inside the gripper	Pass/fail	✓
R6.3.2	No exposed electrical wires	Pass/fail	✓
R6.3.3	Integrate camera on the gripper for visual inspection	Pass/fail	✓
R6.4	Function in wet and dirty conditions		N.A.
R6.4.1	Water resistant	Pass/fail	✓
R6.4.2	No possibility for dirt accumulation	Pass/fail	✓
R6.4.3	Corrosion resistant materials for outer surface of the gripper	Pass/fail	✓
R6.5	Allow for disinfection after each use	Pass/fail	✓
R6.6	Pleasant aesthetic, which will not frighten clients	Pass/fail	✓
R7	**Interfacing**		
R7.1	Bayonet-fitting for mounting the gripper on the robot arm	Pass/fail	✓
R7.2	Bayonet-fitting bolted to the gripper, to allow for simple interface change for application on a different robot	Pass/fail	✓